

E. WOLF, PROGRESS IN OPTICS XXI
© ELSEVIER SCIENCE PUBLISHERS B.V. 1984

II

THEORY OF OPTICAL BISTABILITY

BY

LUIGI A. LUGIATO

*Istituto di Fisica dell' Università,
Milan, Italy*

CONTENTS

	PAGE
§ 1. INTRODUCTION	71
§ 2. SEMICLASSICAL TREATMENT	78
§ 3. QUANTUM STATISTICAL TREATMENT	158
CONCLUDING NOTE	204
ACKNOWLEDGEMENTS	204
APPENDIX A	205
APPENDIX B	207
APPENDIX C	208
APPENDIX D	209
REFERENCES	211

This paper is dedicated to the memory of Mario Gronchi, beloved friend and respected collaborator whose outstanding contributions to the theory of optical bistability are well known in the field. An absurd destiny has prevented us from enjoying further his humanity and intelligence.

§ 1. Introduction

Bistable operation in optical systems has been theoretically predicted and sometimes experimentally observed in several situations, for instance with two-mode lasers (LAMB [1965]), Zeeman lasers (HEER and GRAFT [1965], SARGENT, LAMB and FORK [1967]), lasers with a saturable absorber (KAZANTSEV, RAUTIAN and SURDUTOVICH [1968], LUGIATO, MANDEL, DEMBINSKI and KOSSAKOWSKI [1978], RUSHIN and BAUER [1979]), parametric oscillators (WOO and LANDAUER [1971], LUGOVOI [1979], DRUMMOND, MCNEIL and WALLS [1980a]), dye lasers (BACZYNISKI, KOSSAKOWSKI and MARSZALEK [1976], SCHAEFER and WILLIS [1976], HAAG, MUNZ and MAROWSKY [1981]), reflection by a nonlinear interface (KAPLAN [1977], SMITH, TOMLINSON, MALONEY and HERMANN [1981]), and bidirectional ring cavity (L. MANDEL, ROY and SINGH [1981]). However, the name “optical bistability” has been given specifically to the bistable behavior which arises in the class of systems described below.

1.1. WHAT IS OPTICAL BISTABILITY

Let us consider a cw laser beam injected into an optical cavity (for instance a Fabry–Perot or a ring cavity), tuned or nearly tuned to the incident light. In general, the incident field is partially transmitted, partially reflected and partially absorbed. When the cavity is empty, the transmitted power P_T is proportional to the incident power P_I , and the proportionality constant depends on the cavity detuning and on the finesse of the cavity. The interesting case is when the cavity is filled with absorbing material resonant or nearly resonant with the incident field. In this case, P_T becomes a nonlinear function of P_I . The behavior of the system is determined by the ratio of the absorption parameter αL and the mirror transmissivity T , where α is the unsaturated absorption coefficient per unit length on resonance and L the length of the sample. Increasing $\alpha L/T$, one finds that the steady state curve of transmitted versus incident power develops first a portion with differential gain dP_T/dP_I larger than unity. In this

condition, if one slowly modulates the incident intensity, the modulation is transferred to the transmitted field via the nonlinear steady state relation $P_T = P_T(P_I)$ and turns out to be *amplified*. Thus, the system works as an *optical transistor*. If one further increases the ratio $\alpha L/T$ the steady state curve $P_T = P_T(P_I)$ becomes S-shaped. The segment with negative slope is unstable; hence, there is a definite range of values of P_I in correspondence with which the system is *bistable*. If we slowly sweep the incident power from zero to a value beyond the bistable region, and then sweep it back, we obtain a hysteresis cycle with a low and a high transmission branch. The bistable behavior arises from the interplay of the nonlinearity of the atom-field interaction with the feedback action of the mirrors. The threshold value of $\alpha L/T$ for which one yields bistability, depends on several parameters such as the cavity mistuning, the atomic detuning, the inhomogeneous linewidth, the type of cavity and so on. When the incident field is in perfect resonance with the atomic line, dispersion does not play any role, so that one has *purely absorptive bistability*. Otherwise, one has the general mixed absorptive and dispersive case. When the atomic detuning is so large that absorption becomes negligible one has *purely dispersive bistability*.

The systems which show this behavior are usually called *all-optical (or intrinsic) bistable systems*. We also consider the so-called *hybrid electro-optical systems*, which have been devised in many variants. A typical device of this type is obtained by replacing the absorber by an electro-optic crystal, which is monitored by the output field and produces changes in the refraction index proportional to the output power.

Already from this brief description it is evident that these systems (both all-optical and electro-optical) have great potential as devices, because they can work as optical transistors, memory elements, or pulse shapers, which eliminate the noisy parts of the input light (clippers, discriminators and limiters). Also, we shall see later, they can work as converters of cw light into pulsed light. Therefore, there is presently a big effort towards the construction of practical, miniaturized and fast operating optical devices of this kind.

Optical bistability has also aroused a wide theoretical interest, renewing in part the enthusiasms that in the sixties were devoted to the laser. In fact, optical bistability is a remarkable example of cooperative behavior in an open system far from thermal equilibrium, and therefore is naturally a chapter of Haken's *Synergetics* (HAKEN [1977]) and of Prigogine's *theory of dissipative structures* (NICOLIS and PRIGOGINE [1977]). First of all, it is immediately evident that optical bistability is an example of *non-equilibrium steady state behavior*, analogous to first-order phase transitions in equilibrium systems. Furthermore,

as we shall see later, by controlling the external parameters one can induce either the emergence of *spontaneous pulsations* in the system (self-pulsing behavior) or the appearance of *chaotic* (turbulent) behavior. Clearly, the theoretical interest of hybrid systems is reduced with respect to all-optical systems.

1.2. A HISTORICAL SKETCH

Let us give a brief description of the history of optical bistability, concerning the intrinsic bistability in all-optical systems and the theoretical aspects. Absorptive optical bistability was theoretically predicted by SZÖKE, DANEU, GOLDHAR and KURNIT [1969]. The same problem was considered also by SEIDEL [1971], AUSTIN and DESHAZER [1971] and SPILLER [1972]. Some years later McCALL [1974] proved that under suitable conditions the same system can show differential gain with transistor action, and also treated absorptive optical bistability in a Fabry-Perot cavity by numerical analysis of the Maxwell-Bloch equations. This work led to the experiments of GIBBS, McCALL and VENKATESAN (1976) in sodium, in which both transistor operation and bistability were observed. The analysis of the data showed that the observed bistability was of the dispersive type, with few exceptions. The mechanism which produces dispersive optical bistability was explained with the help of a simple phenomenological cubic model.

These results stimulated theoretical and experimental activity; in particular, three papers that were crucial for the following developments are those of FELBER and MARBURGER [1976], BONIFACIO and LUGIATO [1976] and SMITH and TURNER [1977]. Successively, other experiments on optical bistability have been performed by VENKATESAN and McCALL [1977], BISCHOFBERGER and SHEN [1978, 1979], GRISCHKOWSKI [1978], McCALL and GIBBS [1978], GARMIRE, MARBURGER, ALLEN and WINFUL [1979], GIBBS, McCALL, VENKATESAN, GOSSARD, PASSNER and WIEGMANN [1979], MILLER, SMITH and JOHNSTON [1979], MILLER and SMITH [1979], MILLER, SMITH and SEATON [1981], GRYNBERG, GIACOBINO, DEVAUD and BIRABEN [1980], SANDLE and GALLAGHER [1981], ARIMONDO, GOZZINI, LOVITCH and PISTELLI [1981], WEYER, WIEDENMANN, RATEIKE, MCGILLIVRAY, MEYSTRE and WALther [1981], ARECCHI, GIUSFREDI, PETRIELLA and SALIERI [1982], GRANT and KIMBLE [1982] and MEIER, HOLZNER, DERIGHETTI and BRUN [1982].

The first *exact analytical* theory of optical bistability, fully including propaga-

tion effects and saturation, was given by BONIFACIO and LUGIATO [1978a], in the case of a unidirectional ring cavity in the purely absorptive situation. In particular, this paper showed the crucial importance of the double limit $\alpha L \rightarrow 0$, $T \rightarrow 0$, with $\alpha L/T$ constant (mean-field limit) to obtain a simplified theory. In fact, in this limit one recovers exactly the previously formulated "mean field theory" (BONIFACIO and LUGIATO [1976, 1977]), which produced quite a number of predictions also concerning transient behavior and quantum statistical effects. The exact analytical solution of BONIFACIO and LUGIATO [1978a] was extended to the mixed absorptive-dispersive case independently by IKEDA [1979], BONIFACIO, LUGIATO and GRONCHI [1979] and ROY and ZUBAIRY [1980a]. The generalization to the case of the bidirectional ring cavity has been given in AGRAWAL [1981], ASQUINI and CASAGRANDE [1981] and KAPLAN and MEYSTRE [1982].

The mean field model for a ring cavity has been generalized, both at semiclassical and quantum statistical level, to the case of mixed absorptive and dispersive bistability by BONIFACIO and LUGIATO [1978c]. The general bistability conditions have been worked out in HASSAN, DRUMMOND and WALLS [1978], BONIFACIO, GRONCHI and LUGIATO [1979a] and AGRAWAL and CARMICHAEL [1979]. Further analyses of dispersive bistability are given in SCHWENDIMANN [1979], BOWDEN and SUNG [1979], WILLIS and DAY [1979], TEWARI [1979], MILLER [1981], GRAHAM and SCHENZLE [1981] and BOWDEN [1981].

At the semiclassical level, the mean field model has been used to investigate various aspects of the transient behavior, in particular with regard to switching characteristics (BONIFACIO and LUGIATO [1978d], BONIFACIO and MEYSTRE [1978, 1979], MEYSTRE and HOPF [1979], BENZA and LUGIATO [1979a], HOPF, MEYSTRE, DRUMMOND and WALLS [1979], LUGIATO, MILANI and MEYSTRE [1982]).

At the quantum statistical level, the mean field model was used to describe the spectrum of transmitted and fluorescent light (AGARWAL, NARDUCCI, FENG and GILMORE [1977], AGARWAL, NARDUCCI, GILMORE and FENG [1978a,b, 1979], CARMICHAEL and WALLS [1977], BONIFACIO and LUGIATO [1978d,e], LUGIATO [1979], CASAGRANDE and LUGIATO [1980]) and the photon statistics of the transmitted light in the good cavity case. In BONIFACIO, GRONCHI and LUGIATO [1978] the bimodal character of the distribution function in the bistability region was discussed describing the behavior of the mean value and the fluctuations of the transmitted light. This behavior completes the analogy between optical bistability and first-order phase transitions, showing, on the other hand, the nonthermodynamic character of the transition,

which stems from the fact that the diffusion coefficient of the Fokker–Planck equation is intensity-dependent. These results have been further developed in WILLIS [1978, 1981], SCHENZLE and BRAND [1978, 1979], GRAGG, SCHIEVE and BULSARA [1978, 1979], ARECCHI and POLITI [1979], DRUMMOND and WALLS [1980, 1981], ZARDECKI [1980], HANGGI, BULSARA and JANDA [1980], LUGIATO, FARINA and NARDUCCI [1980], LUGIATO, CASAGRANDE and PIZZUTO [1982], BONIFACIO, LUGIATO, FARINA and NARDUCCI [1981] and ENGLUND, SCHIEVE, ZUREK and GRAGG [1981].

The stability analysis of the exact stationary solution in a ring cavity showed that, under suitable conditions, a part of the high transmission branch becomes unstable (BONIFACIO and LUGIATO [1978b], LUGIATO [1980a]). In this situation, the system works as a converter of cw into pulsed light (BONIFACIO, GRONCHI and LUGIATO [1979b], GRONCHI, BENZA, LUGIATO, MEYSTRE and SARGENT [1981]). For proper values of the parameters the sequence of pulses is chaotic (IKEDA [1979], IKEDA, DAIDO and AKIMOTO [1980]). An analytical treatment of self-pulsing has been given in BENZA and LUGIATO [1979b, 1981, 1982], BENZA, LUGIATO and MEYSTRE [1980] and LUGIATO, BENZA, NARDUCCI and FARINA [1981, 1982]. Self-pulsing and chaotic behavior have been observed in hybrid systems (MC CALL [1978] and GIBBS, HOPF, KAPLAN and SHOEMAKER [1981], respectively).

The analysis of BONIFACIO and LUGIATO [1978a] has also been generalized to the case of a Fabry–Perot cavity. MEYSTRE [1978] first analyzed the mean field limit in this framework and the deviations from the mean field theory that one finds when T is not small enough. To treat this problem he used some equations obtained in BONIFACIO and LUGIATO [1978d] by suitably truncating the infinite hierarchy of equations derived by FLECK [1968]. The analysis of MEYSTRE [1978] has been extended by ABRAHAM, BULLOUGH and HASSAN [1979], ABRAHAM, HASSAN and BULLOUGH [1980], ABRAHAM and HASSAN [1980] and by ROY and ZUBAIRY [1980b]. In particular, ABRAHAM, BULLOUGH and HASSAN [1979] analyzed the generation of hysteresis cycles by pulses. On the other hand, CARMICHAEL [1980] and HERMANN [1980] solved both numerically and analytically the steady state Maxwell–Bloch equations derived by MC CALL [1974]. These equations include the standing wave effects more completely than the truncated hierarchy equations, producing corrections on the order of 15%. This analysis was extended to the mixed absorptive–dispersive case in CARMICHAEL and HERMANN [1980], who have shown that in the mean field limit one obtains for a Fabry–Perot a state equation which differs from that valid for a ring cavity (again quantitatively the difference is on the order of 15%). The state equation for a Fabry–Perot

coincides, apart from a change of sign to convert the absorber into an amplifier, with that previously obtained by SPENCER and LAMB [1972] for a laser with injected signal. MCCALL and GIBBS [1980] derived from this state equation the general bistability conditions for a Fabry-Perot.

The effects of the radial shape of the electric field injected into the cavity have been analyzed in MARBURGER and FELBER [1978], BALLAGH, COOPER, HAMILTON, SANDLE and WARRINGTON [1981], ARIMONDO, GOZZINI, LOVITCH and PISTELLI [1981], DRUMMOND [1981], ROSANOV and SEMENOV [1981], FIRTH and WRIGHT [1982] and MOLONEY, BELIC and GIBBS [1982].

Considerable attention has been devoted also to two-photon bistability or multistability (ARECCHI and POLITI [1978], AGRAWAL and FLYTZANIS [1980], HERMANN and THOMPSON [1980, 1981]) which has been also experimentally observed (GRYNBERG, GIACOBINO, DEVAUD and BIRABEN [1980]).

Recently, the possibility of bistable or multistable operation with three-level atoms (WALLS, ZOLLER and STEYN-ROSS [1981]), degenerate two-level atoms (KITANO, YABUZAKI and OGAWA [1981], HAMILTON, BALLAGH and SANDLE [1982]), or optical pumping (ARECCHI, GIUSFREDI, PETRIELLA and SALIERI [1982], GOZZINI [1982]) has been pointed out.

Another problem to which a remarkable theoretical interest is presently devoted is the description of bistability in semiconductors. This interest is stimulated by the recent progress in constructing miniaturized all-optical bistable devices using GaAs (GIBBS, MCCALL, VENKATESAN, GOSSARD, PASSNER and WIEGMANN [1979]), InSb (MILLER, SMITH and JOHNSTON [1979]) or tellurium (STAUPENDAHL and SCHINDLER [1980]). The first approaches have been made by the experimentalists themselves in order to obtain an overall picture of the phenomenon (GIBBS, MCCALL, VENKATESAN, GOSSARD, PASSNER and WIEGMANN [1979], MILLER, SMITH and SEATON [1981], MILLER [1981]). These authors essentially adapt the two-level description to the situation in semiconductors. First-principle approaches, including the details of the dynamics in semiconductors, have been developed recently (GOLL and HAKEN [1980], STEYN-ROSS and GARDINER [1983]).

1.3. AIM OF THE ARTICLE

Let us now outline the scope of this chapter. In recent years, a huge amount of literature on optical bistability has accumulated. A large number of variants has been considered; see for instance the recent works of AGRAWAL and FLYTZANIS [1981], LUGOVOI [1981], BJORKHOLM, SMITH and TOMLINSON

[1981] and SARID [1981]. The aim of this article is not to give a review of all the papers on optical bistability, but to select a few topics which illustrate in the simplest way the main physical principles of optical bistability and related phenomena. The treatment is theoretical, but we systematically discuss many of the points which are relevant for the experiments. Furthermore, the analysis is restricted to intrinsic all-optical systems.

For all the points which are not discussed in this paper, we advise the reader to consult one of the following general references: the Proceedings of the Asheville Conference, edited by BOWDEN, CIFTAN and ROBL [1981], the special issue of the IEEE Journal of Quantum Electronics edited by SMITH [1981], the book on Dissipative Systems in Quantum Optics, edited by BONIFACIO [1982], and the recent review by ABRAHAM and SMITH [1982b]. In particular, the last article complements the present paper. Other, shorter reviews can be found in GIBBS, MCCALL and VENKATESAN [1979], GIBBS, MCCALL and VENKATESAN [1980], COLLINS and WASMUNDT [1980] and ABRAHAM and SMITH [1982a].

Our selection is dictated by the general criterium of maximum simplicity. Thus, we restrict ourselves to the case of unidirectional ring cavity, plane wave approximation, two-level atoms, homogeneous broadening, and one-photon transitions. Both the absorptive and the dispersive cases will be treated. The starting point of our analysis is the set of coupled Maxwell–Bloch equations, obtained in the slowly varying envelope and rotating wave approximations. The connections of this treatment with the mode description of optical bistability are studied in detail. At a quantum statistical level, we base ourselves on a suitable many-mode master equation, which allows a deep analysis of the fluctuations in the system. Starting from a comprehensive description of the steady state behavior, the treatment will be developed with particular emphasis on the cooperative effects, on the nonstationary behavior (transient effects and self-pulsing) and on the quantum effects.

Section 2 is devoted to the semiclassical treatment, and § 3 to the quantum statistical theory. In particular, § 2.1 concerns the steady state behavior, §§ 2.2 and 2.3 the transient effects, and §§ 2.4 and 2.5 the self pulsing behavior. In the quantum statistical part, §§ 3.1 and 3.2 discuss the basic equations, §§ 3.3 and 3.4 analyze the spectrum of transmitted and fluorescent light, while § 3.5 describes the photon statistics of the transmitted light. Section 3.6 studies the transient behavior in its quantum statistical aspects, and finally, § 3.7 gives a brief discussion on the observability of the quantum effects.

§ 2. Semiclassical treatment

In order to describe theoretically the phenomenon of optical bistability, it is easier to consider a unidirectional *ring cavity* (Fig. 1) than a Fabry–Perot, because in this cavity one has to deal with propagation only in one direction, thus avoiding standing wave difficulties. For simplicity we assume that mirrors 3 and 4 have 100% reflectivity. We call R and T (with $R + T = 1$) the reflection and transmission coefficients of mirrors 1 and 2. We describe the dynamics of the coupled system atoms plus radiation field by the well known, one-sided Maxwell–Bloch equations, which incorporate the *plane wave approximation*.

In the case of a *homogeneously broadened system of N two level atoms*, the Maxwell–Bloch equations read (ARECCHI and BONIFACIO [1965], HAKEN [1970], SARGENT, SCULLY and LAMB [1974], ALLEN and EBERLY [1975])

$$\frac{\partial E}{\partial t} + c \frac{\partial E}{\partial z} = -gP, \quad (1a)$$

$$\frac{\partial P}{\partial t} = \frac{\mu}{\hbar} ED - [\gamma_{\perp} + i(\omega_a - \omega_0)]P, \quad (1b)$$

$$\frac{\partial D}{\partial t} = -\frac{\mu}{2\hbar} (EP^* + E^*P) - \gamma_{\parallel}(D - N/2). \quad (1c)$$

E is the slowly varying envelope of the electric field, P is the macroscopic atomic polarization and D is one half the difference between the populations of the lower and of the upper level. The equations for E^* and P^* are the complex conjugates of eqs. (1a) and (1b) respectively. μ is the modulus of the dipole

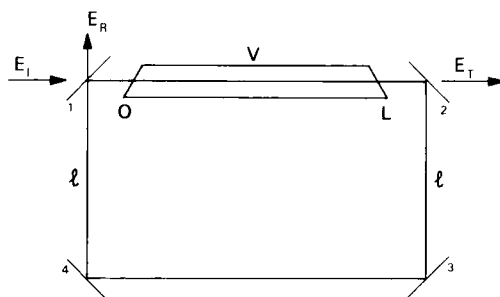


Fig. 1. Ring Cavity. E_I , E_T and E_R are the incident, transmitted and reflected fields respectively.

moment of the atoms and g is a coupling constant given by

$$g = \frac{4\pi\omega_0\mu}{V}, \quad (2)$$

where ω_0 is the frequency of the incident field, and V the volume of the atomic sample. γ_{\parallel} and γ_{\perp} are the inverse of the atomic relaxation times T_1 and T_2 respectively, and ω_a is the transition frequency of the atoms.

The coherent cw field E_I enters into the cavity from the left (Fig. 1) and drives the atoms. E_I is taken as real and positive for definiteness. The cavity imposes two relations between E_I , the transmitted field amplitude E_T , and the fields $E(0, t)$ and $E(L, t)$ (BONIFACIO and LUGIATO [1978a])

$$E_T(t) = \sqrt{T} E(L, t), \quad (3a)$$

$$E(0, t) = \sqrt{T} E_I + R \exp(-i\delta_0) E(L, t - \Delta t), \quad (3b)$$

where L is the length of the atomic sample and $\Delta t = (2l + L)/c$ is the time the light takes to travel from mirror 2 to mirror 1. δ_0 is the cavity detuning:

$$\delta_0 = \frac{\omega_c - \omega_0}{c/\mathcal{L}}, \quad (3c)$$

where ω_c is the frequency of the cavity that is nearest to resonance with the incident field, and $\mathcal{L} = 2(L + l)$ is the total length of the cavity. In particular, eq. (3b) is a boundary condition characteristic of the ring cavity. The second contribution on the right hand side describes a feedback mechanism due to the mirrors, which is essential to give rise to bistability.

2.1. STEADY STATE BEHAVIOR

Let us first consider the steady state ($\partial E / \partial t = \partial P / \partial t = \partial D / \partial t = 0$). The stationary equation for the field in general has the form

$$\frac{dE}{dz} = -\chi(|E|^2)E, \quad (4)$$

where

$$\chi = \chi_a + i\chi_d \quad (5)$$

is the complex dielectric susceptibility, with an absorptive (dispersive) com-

ponent $\chi_a(\chi_d)$. In the particular case of eqs. (1), χ has the expression

$$\chi = \alpha(1 - i\Delta)[1 + \Delta^2 + |E|^2/I_s]^{-1}, \quad (6)$$

where α is the unsaturated absorption coefficient on resonance,

$$\alpha = \frac{\mu g N}{2\hbar c \gamma_{\perp}}, \quad (7a)$$

Δ is the atomic detuning parameter

$$\Delta = (\omega_a - \omega_0)/\gamma_{\perp} \quad (7b)$$

and I_s is the saturation intensity

$$I_s = \frac{\hbar^2 \gamma_{\perp} \gamma_{\parallel}}{\mu^2}. \quad (7c)$$

However, eq. (4) is more general than eqs. (1); for instance it holds for inhomogeneously broadened systems or for Kerr media, with suitable expressions of the susceptibility χ .

2.1.1. The case of perfect resonance

Let us consider first the case in which the incident field, the atoms and the cavity are perfectly in resonance; i.e. $\omega_0 = \omega_a = \omega_c$. This is a particular case of purely absorptive bistability. From eqs. (4) and (6) we have

$$\frac{dF}{dz} = -\alpha \frac{F}{1 + F^2}, \quad (8)$$

where F is the normalized adimensional electric field

$$F = \frac{E}{\sqrt{I_s}} = \frac{\mu E}{\hbar(\gamma_{\perp} \gamma_{\parallel})^{1/2}} \quad (9)$$

and the field has been taken as real. Together with F , it is suitable to consider the normalized incident and transmitted amplitudes

$$y = \frac{\mu E_I}{\hbar(\gamma_{\perp} \gamma_{\parallel} T)^{1/2}} = \frac{E_I}{(I_s T)^{1/2}}, \quad x = \frac{\mu E_T}{\hbar(\gamma_{\perp} \gamma_{\parallel} T)^{1/2}} = \frac{E_T}{(I_s T)^{1/2}}, \quad (10)$$

so that eqs. (3) become, at steady state,

$$x = F(L), \quad (11a)$$

$$F(0) = Ty + Rx. \quad (11b)$$

Equation (8) can be solved immediately and gives

$$\ln \frac{F(0)}{x} + \frac{1}{2}[F^2(0) - x^2] = \alpha L. \quad (12)$$

By combining eqs. (11b) and (12) we finally obtain (BONIFACIO and LUGIATO [1978a])

$$\ln \left[1 + T \left(\frac{y}{x} - 1 \right) \right] + \frac{x^2}{2} \left\{ \left[1 + T \left(\frac{y}{x} - 1 \right) \right]^2 - 1 \right\} = \alpha L. \quad (13)$$

This equation gives an exact relation between the transmitted field x and the incident field y . It depends on the two parameters αL and T . The structure of eq. (13) can be intuitively understood by a graphical representation of eqs. (11b) and (12) as shown in Fig. 2. The steady state values of x are the intersections

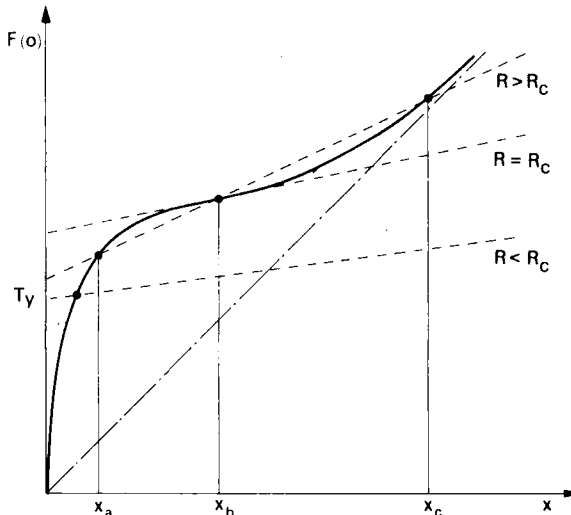


Fig. 2. Qualitative graph of the normalized field $F(0)$ at $z = 0$ as a function of the field $F(L) \equiv x$ at $z = L$ (transfer function of the atomic medium at steady state). For $R = 0$ one has $F(0) = y$. Quantities x and y are proportional to the transmitted and incident fields E_T and E_I respectively (see eq. (10)). For a generic R , the function $x = x(y)$ is obtained by intersecting the curve with the straight line $F(0) = RF(L) + Ty$.

of the straight line (11b) with the curve (12). The first one is the boundary condition of the cavity. The second is the transfer function of the medium, which expresses the field at $z = 0$ as a function of the field at $z = L$ (and vice versa). It has neither maxima nor minima (see Fig. 2), but it has an inflection point. The angular coefficient R_c of the tangent at the inflection point is such that $0 < R_c < 1$. R_c depends only on αL . For $R < R_c$ there is only one intersection point for all values of y . For $R > R_c$ there is a range of values of y in correspondence with which one finds three intersection points $x_a < x_b < x_c$. Points x_b are unstable, hence, this is a bistable situation. If we plot the steady state solutions x as a function of the incident field y , we obtain an S-shaped curve (Fig. 3) which leads to a hysteresis cycle.

From this analysis we see that bistability arises from the combined action of the *nonlinear* transfer of the medium (eq. (12)) and of the feedback from the mirrors (eq. (11b)). This feedback action is essential, because as one sees from Figs. 2 and 3 there is no bistability for $R = 0$.

If we add a linear loss term (representing, for example, diffraction) $-\zeta E$ to the right hand side of eq. (1a), it is easy to verify that it reduces the bistable region. This effect was first pointed out by SPILLER [1972].

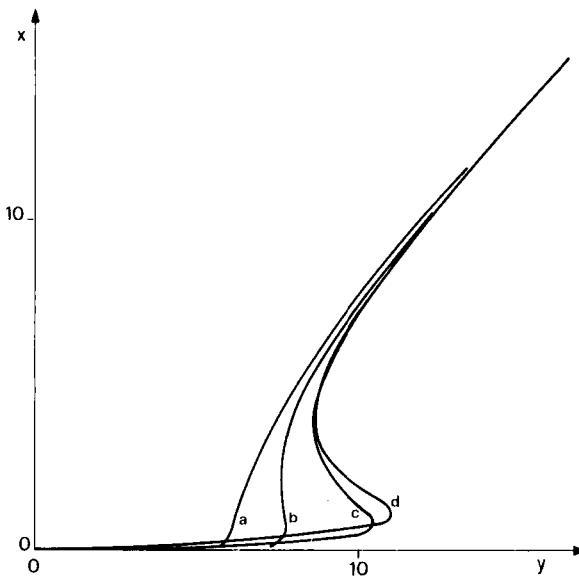


Fig. 3. Plot of transmitted light versus incident light at steady state for $C = \alpha L / 2T$ fixed equal to 10, and different values of αL and T . For $\alpha L \rightarrow 0$ one approaches the behavior predicted by the mean field theory (see eq. (32)): (a) $\alpha L = 20$, $T = 1$; (b) $\alpha L = 10$, $T = 0.5$; (c) $\alpha L = 2$, $T = 0.1$; (d) mean field, $C = 10$.

2.1.2. The general case

Let us now consider the general case, in which E is complex at steady state. By writing

$$E(z) = \rho(z) \exp[i\varphi(z)], \quad (14)$$

we obtain from eq. (4)

$$\frac{d\rho}{dz} = -\chi_a(\rho^2)\rho, \quad (15a)$$

$$\frac{d\varphi}{dz} = -\chi_d(\rho^2). \quad (15b)$$

On the other hand, indicating by $P_I = E_I^2$ and $P_T = |E_T|^2$ the incident and transmitted intensities respectively, using eqs. (3a) and (3b) we obtain, for the transmissivity of the cavity,

$$\mathcal{T} = \frac{P_T}{P_I} = \frac{T^2}{(\eta - R)^2 + 4R\eta \sin^2\{\frac{1}{2}[\varphi(L) - \varphi(0) - \delta_0]\}}, \quad (16)$$

with

$$\eta = \frac{\rho(0)}{\rho(L)} \quad \Rightarrow \quad \eta \geq 1. \quad (17)$$

Let us now consider a few cases separately.

a) *Empty cavity.* In this case $\chi_a = \chi_b = 0$, so that $\eta = 1$, and $\varphi(L) = \varphi(0)$. Hence, eq. (16) reduces to the usual expression of the transmissivity as a function of the cavity detuning (BORN and WOLF [1970])

$$\mathcal{T} = \frac{1}{1 + 4R \sin^2 \frac{\delta_0}{2} / T^2}. \quad (18)$$

b) *Kerr medium.* (FELBER and MARBURGER [1976], MARBURGER and FELBER [1978].) In this case one has

$$\chi_a = 0, \quad \chi_d = c_1 + c_2\rho^2, \quad (19)$$

where c_1 and c_2 are constants. Hence, $\eta = 1$ and

$$\varphi(L) - \varphi(0) = -L(c_1 + c_2 P_T/T)$$

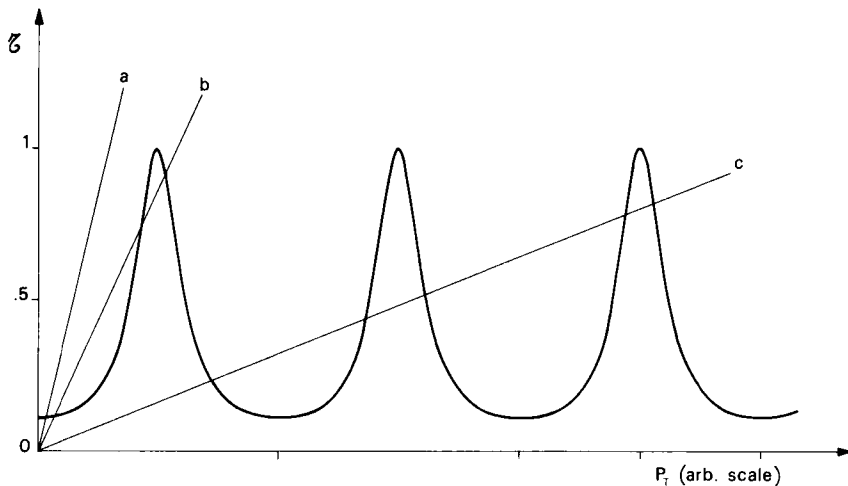


Fig. 4. The steady state transmission \mathcal{T} of the cavity, filled with a Kerr medium, is graphed as a function of the transmitted power P_T . **a**, **b** and **c**, show the straight line $\mathcal{T} = P_T/P_1$ for different values of the incident power P_1 . The intersections with the curve correspond to the (stable or unstable) stationary states of the system for a fixed value of P_1 .

so that eq. (16) becomes

$$\mathcal{T} = \frac{1}{1 + 4R \sin^2 \left\{ \frac{1}{2}(\delta + \beta P_T) \right\} / T^2}, \quad (20)$$

with $\delta = \delta_0 + Lc_1$, $\beta = Lc_2/T$. Therefore the plot of \mathcal{T} versus P_T has the same shape as the usual graph of transmissivity as a function of detuning (FELBER and MARBURGER [1976]) (Fig. 4). Using the procedure of FELBER and MARBURGER, the steady state solutions can be found by intersecting the line (20) with the straight line $\mathcal{T} = P_T/P_1$ in the plane (\mathcal{T}, P_T) . The value of P_1 controls the angular coefficient of the straight line. For small P_1 one has only one intersection (line a). By increasing P_1 , the intersections become three (line b), with the middle one being unstable. Thus, we obtain bistability and the plot of P_T versus P_1 shows a hysteresis cycle. This bistability is of a purely dispersive type. For larger values of P_1 one obtains multiple solutions (line c), which leads to multistability and multiple hysteresis cycles. When T approaches unity, the curve (20) flattens and bistability disappears as usual.

c) *Two-level, homogeneously broadened atomic system in the general absorptive plus dispersive case* (BONIFACIO, LUGIATO and GRONCHI [1979]). Let us

introduce the normalized incident and transmitted intensities

$$\begin{aligned} Y &= \left(\frac{\mu E_I}{\hbar} \right)^2 \frac{1}{\gamma_{\perp} \gamma_{\parallel} T} = y^2 = \frac{P_I}{I_s T}, \\ X &= \left(\frac{\mu |E_T|}{\hbar} \right)^2 \frac{1}{\gamma_{\perp} \gamma_{\parallel} T} = |x|^2 = |F(L)|^2 = \frac{P_T}{I_s T}, \end{aligned} \quad (21)$$

From eqs. (15) with eqs. (3a), (5), (6) and (9) we obtain

$$X = \frac{2}{\eta^2 - 1} [\alpha L - (1 + \Delta^2) \ln \eta], \quad (22)$$

$$\varphi(L) - \varphi(0) = \Delta \ln \eta. \quad (23)$$

By solving eq. (22) with respect to η , we obtain the function $\eta = \eta(X)$. Hence, by inserting eq. (22) into eq. (16) we find the expression of the transmissivity as a function of the normalized transmitted intensity X :

$$\mathcal{T} = \frac{X}{Y} = \frac{T^2}{[\eta(X) - R]^2 + 4R\eta(X) \sin^2 \{ \frac{1}{2}[\Delta \ln \eta(X) - \delta_0] \}} \quad (24)$$

Therefore in this case the shape of the function $\mathcal{T}(X)$ is governed by the dependence of η on X . In particular, for large X η approaches unity, so that the transmissivity becomes constant and equal to the empty cavity value (18). In general, the curve $\mathcal{T}(X)$ is quite different from the Kerr medium curve (20). However, when dispersion is dominant, under suitable conditions one or a few resonances survive (see Fig. 5).

The possibility of multistability (Fig. 6) depends on the number of oscillations that the function $\sin \{ \frac{1}{2}[\Delta \ln \eta(X) - \delta_0] \}$ undergoes (IKEDA [1979]). As one sees from eq. (22), η is a monotonically decreasing function of X which varies from unity to $\exp[\alpha L/(1 + \Delta^2)]$. Hence, the quantity $\Delta \ln \eta - \delta_0$ varies from $-\delta_0$ to $\alpha L \Delta/(1 + \Delta^2) - \delta_0$. Therefore the number of oscillations of the sine function is determined by the parameter $\alpha L \Delta/(1 + \Delta^2)$.

Equation (24) can be rephrased as follows:

$$Y = X(\eta) \frac{1}{T^2} \{ (\eta - R)^2 + 4R\eta \sin^2 \{ \frac{1}{2}(\Delta \ln \eta - \delta_0) \} \}. \quad (25)$$

Equations (22) and (25) together give a parametric representation $X = X(\eta)$, $Y = Y(\eta)$ of the function $X(Y)$ of transmitted versus incident intensity.

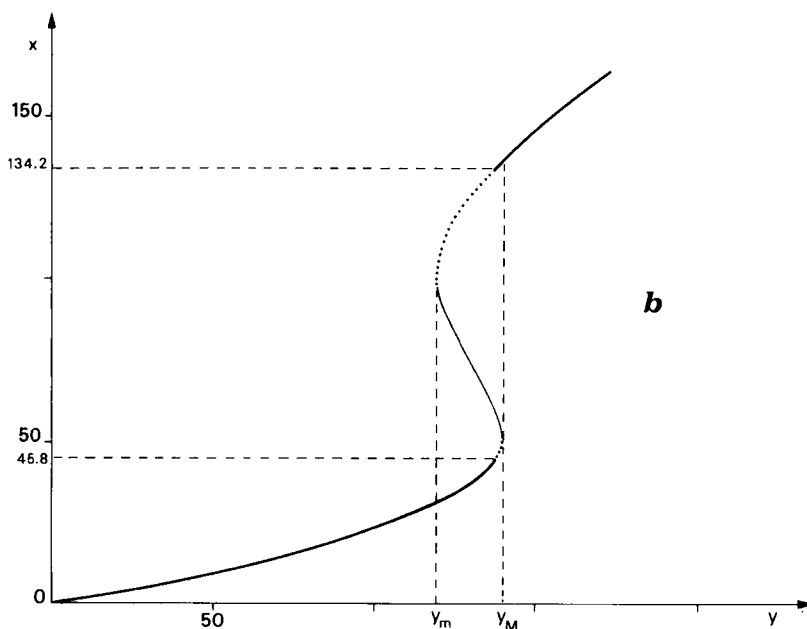
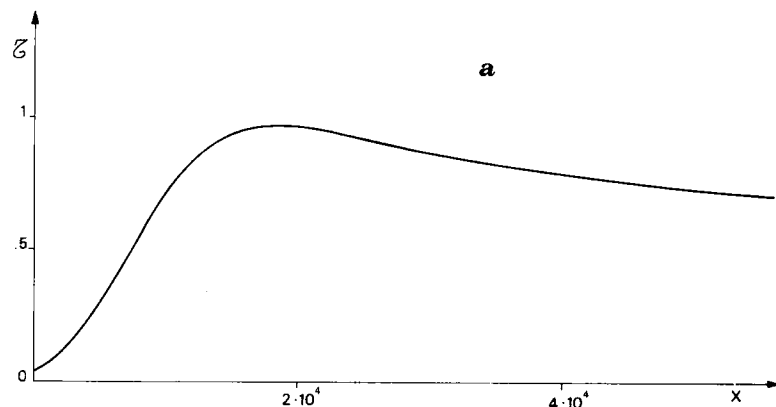


Fig. 5. (a) Same as Fig. 4, but for a cavity filled with a two-level medium; X is the normalized transmitted intensity. $\alpha L = 3.6$, $T = 0.1$ (hence $C = 180$), $\Delta = 60$, $\theta = \delta_0/T = 1$. (b) Plot of transmitted field x ($= \sqrt{X}$) versus incident field y for the same values of the parameters of Fig. 5a. The part of the curve with negative slope is unstable. The approach to the states in the solid positive slope part of the curve is oscillatory, and that in the dotted part is monotonic.

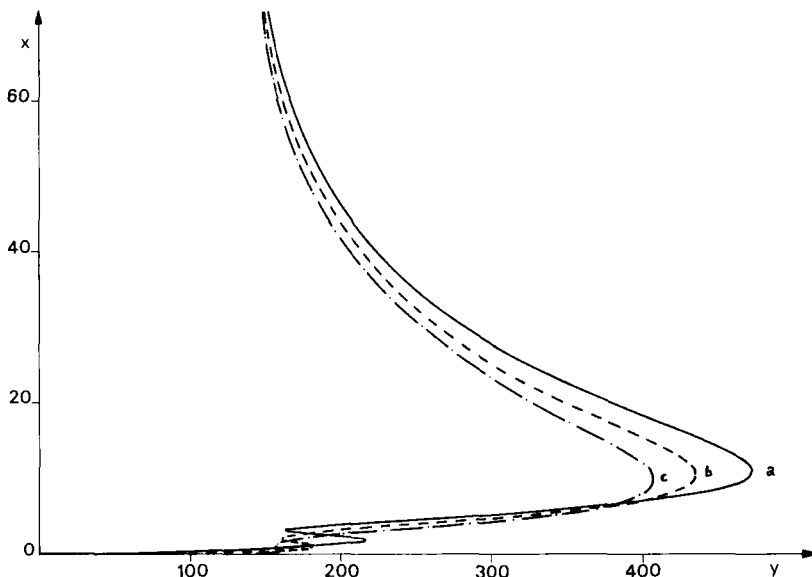


Fig. 6. Optical multistability. $x = \sqrt{X}$ is the normalized transmitted field. In all curves $C = 900$, $\Delta = 5$, $\theta = 0.05$. Curve **a** corresponds to the case of homogeneous broadening ($T_2^* = \infty$). In **b**, $\gamma_\perp T_2^* = 1$; in **c**, $\gamma_\perp T_2^* = 0.5$. Clearly, multistability disappears with increased inhomogeneous broadening.

Examples of this curve are given in Fig. 7. The generalization of eqs. (22) and (25) to the case of Lorentzian inhomogeneous broadening has been given in GRONCHI and LUGIATO [1980]; for the Fabry–Perot case see CARMICHAEL and AGRAWAL [1980].

2.1.3. The stationary solution in the mean field limit

From now on, we consider exclusively the case of a two-level atomic system. In general, the susceptibility has the structure

$$\chi(|E|^2) = \alpha \tilde{\chi}(|F|^2), \quad (26)$$

where α and F are defined in eqs. (7a) and (9) respectively. Therefore the steady state solution becomes particularly simple in the case $\alpha L \ll 1$, because, as one sees from eqs. (15), the field becomes practically uniform in space. More precisely, we shall perform the multiple limit (BONIFACIO and LUGIATO [1978a,c])

$$\alpha L \rightarrow 0, \quad T \rightarrow 0, \quad \delta_0 \rightarrow 0$$

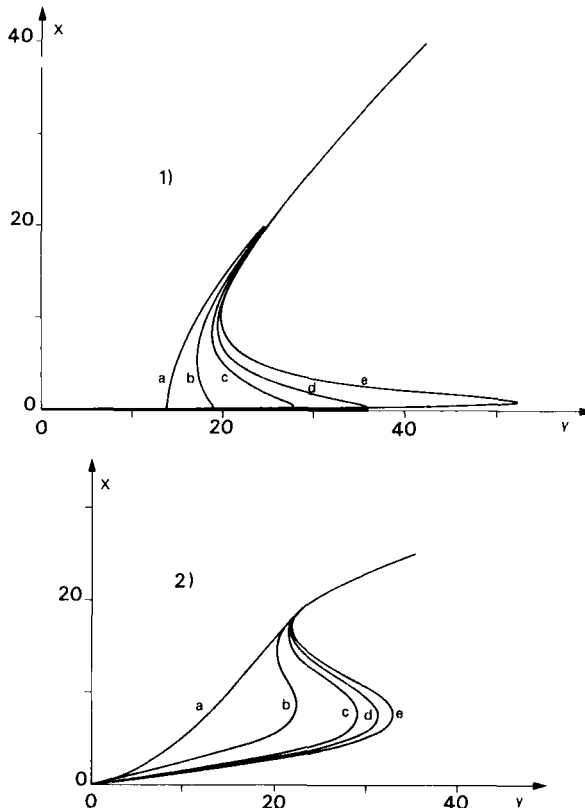


Fig. 7. Plot of the transmitted amplitude $x = \sqrt{X}$ as a function of the incident amplitude y in the homogeneously broadened case. In both Figs. 7.1 and 7.2 curves **a**, **b**, **c** and **d** show the exact stationary solution (eqs. (22) and (25)); curve **e** is the mean field result (eq. (31)). In Fig. 7.1 $C = 50$, $\Delta = \theta = 0$; in Fig. 7.2 $C = 50$, $\Delta = 10$, $\theta = 2.25$. Curves **a**: $\alpha L = 100$, $T = 1$; curves **b**: $\alpha L = 50$, $T = 0.5$; curves **c**: $\alpha L = 20$, $T = 0.2$; curves **d**: $\alpha L = 10$, $T = 0.1$.

with

$$C \equiv \frac{\alpha L}{2T} \equiv \text{constant}$$

$$\theta \equiv \frac{\delta_0}{T} = \frac{\omega_c - \omega_0}{cT/\mathcal{L}} \equiv \text{constant}. \quad (27)$$

It is easy to derive the steady state solution in the limit (27). In fact, from eqs. (15a,b) and (17), (27) we have to first order in αL

$$\begin{aligned} \eta &= 1 + \alpha L \tilde{\chi}_a(|F(L)|^2 = 1 + \alpha L \tilde{\chi}_a(X), \\ \varphi(L) - \varphi(0) &= \alpha L \tilde{\chi}_d(X). \end{aligned} \quad (28)$$

By inserting eq. (28) into eq. (16) we obtain, in the limit (27),

$$\mathcal{T} = \{[1 + 2C\tilde{\chi}_a(X)]^2 + [\theta - 2C\tilde{\chi}_d(X)]^2\}^{-1} \quad (29)$$

and because $\mathcal{T} = Y/X$ we have

$$Y = X\{[1 + 2C\tilde{\chi}_a(X)]^2 + [\theta - 2C\tilde{\chi}_d(X)]^2\}. \quad (30)$$

Equation (30) coincides with the state equation of optical bistability in a ring cavity, derived from the mean field model of optical bistability (see § 2.2.1). For this reason, the limit (27) is called “mean field limit”.

The explicit expression of eq. (30), in the case of Lorentzian inhomogeneous broadening, is given in BONIFACIO and LUGIATO [1978c]. For a homogeneously broadened system, from eq. (6) we have (BONIFACIO and LUGIATO [1978c], HASSAN, DRUMMOND and WALLS [1978])

$$Y = X \left\{ \left(1 + \frac{2C}{1 + \Delta^2 + X} \right)^2 + \left(\theta - \frac{2C\Delta}{1 + \Delta^2 + X} \right)^2 \right\}. \quad (31)$$

In the particular case $\Delta = \theta = 0$, eq. (31) can be written in terms of amplitudes instead of intensities as follows (BONIFACIO and LUGIATO [1976]):

$$y = x + \frac{2Cx}{1 + x^2}. \quad (32)$$

Equations (31) and (32) can be also recovered directly from the exact solutions (22) + (25) and (13), respectively, by performing the limit (27).

Relations of the type (31) between incident and transmitted intensity were given in SZÖKE, DANEU, GOLDHAR and KURNIT [1969] and GIBBS, McCALL and VENKATESAN [1976] on the basis of phenomenological arguments. Our approach derives this formula from first principles as an analytical solution of the Maxwell–Bloch equations with boundary condition, pointing out its limit of validity, which is $\alpha L \ll 1$, $T \ll 1$, $\delta_0 \ll 1$.

Let us now briefly comment on the physical meaning of the limit (27). First, $\alpha L \rightarrow 0$ (i.e. $\alpha \rightarrow 0$) is the weak coupling limit in the interaction between the electric field and the atoms. However, if we only let $\alpha L \rightarrow 0$ but keep T finite, C vanishes and therefore we obtain the empty cavity solution $Y = X(1 + \theta^2)$. On the contrary, if we also let $T \rightarrow 0$, the parameter C is arbitrary and we obtain the nonlinear terms in eq. (30), which produce all the interesting phenomena. The physical meaning of the limit $T \rightarrow 0$ is that the mean lifetime \mathcal{L}/cT of the

photons in the cavity becomes infinite, so that the photons can experience the interaction with the atoms even when this becomes vanishingly small. Finally, the limit

$$\delta_0 = \frac{\omega_c - \omega_0}{c/\mathcal{L}} \rightarrow 0, \quad \theta = \frac{\omega_c - \omega_0}{cT/\mathcal{L}} \quad \text{finite}$$

means that the cavity detuning must be smaller than the free spectral range, but of the same order of magnitude as the cavity linewidth k , given by

$$k = cT/\mathcal{L}. \quad (33)$$

This limit implies that the system operates only with the cavity mode resonant with the incident field.

Note that, despite the limit $\alpha L \rightarrow 0$, eqs. (30) and (31) do not give a weak coupling theory. In fact, the limit (27) is peculiar because the internal field E becomes infinite, in such a way that the normalized variables F , X and Y remain finite in the limit. Since X is proportional to μ^2 , one sees that the coupling constant appears in eq. (31) at all orders.

Figure 7 shows how the curve (31) is approached in the limit (27) (see also Fig. 3). The parts of the curves with negative slope are unstable, as we shall see later, so that one finds a hysteresis cycle. Curve (e) in Fig. 7.1 is obtained from eq. (31) for $C = 50$, $\Delta = \theta = 0$ (purely absorptive case); curve (e) in Fig. 7.2 comes from eq. (31) for $C = 50$, $\Delta = 10$, and $\theta = 2.25$ (dispersive case). In both Figs. 7.1 and 7.2 the curves a, b, c and d show the exact solution (22) and (25) for different values of αL and of the transmissivity, chosen in such a way that $C = \alpha L/2T$ is a constant, equal to 50. For large values of αL and T , as in curve (a), there is no bistability whereas the bistable behavior increases by decreasing αL and T . In this way one approaches the mean field result (31) which is already a good approximation for $\alpha L \approx 1$. With C and T fixed the mean field curve is a better approximation in the dispersive case (Fig. 7.2) than in the absorptive one (Fig. 7.1). This is due to the fact that absorption is reduced in the dispersive case so that the variation of the field in space is not strong even when αL is large. This can be understood on the basis of the fact that in the dispersive case the mean field condition $\alpha L \ll 1$ can be replaced by $\bar{\alpha}L \ll 1$, where $\bar{\alpha}$ is the unsaturated absorption coefficient off resonance $\bar{\alpha} = \alpha/(1 + \Delta^2)$.

In the following two subsections we shall analyze the mean field state equation (31), which expresses the incident intensity as a function of the transmitted intensity. It depends on three parameters, the cooperativity parameter C , the atomic detuning Δ and the cavity mistuning θ . In comparing

eq. (31) with experimental data, the definition (27) of C must be changed into

$$C = \alpha L \mathcal{F} / 2\pi, \quad (34)$$

where \mathcal{F} is the effective finesse of the cavity.

A general property of eq. (31) is that, contrary to eqs. (22) and (25), it can never produce multistability, but at most can lead to bistability.

2.1.4. *Bistability conditions in the resonant case (mean field limit) (BONIFACIO and LUGIATO [1976])*

The field internal to the cavity is in general quite different from the incident field, because there is a reaction field, cooperatively produced by the atoms, which counteracts the incident one.

In the purely absorptive, resonant case $\Delta = \theta = 0$, the steady state behavior is described by eq. (32). The nonlinear term $2Cx/(1 + x^2)$ arises from the reaction field and hence, from atomic cooperation, which is “measured” by the parameter C . For very large x eq. (32) reduces to the empty cavity solution $x = y$ (i.e. $E_T = E_I$). The atomic system is saturated, so that the medium is bleached. In this situation each atom interacts with the incident field as if the other atoms were not there: this is the noncooperative situation, and in fact the quantum statistical treatment shows that atom–atom correlations are negligible. On the other hand, for small X eq. (32) reduces to $y = (2C + 1)x$. Here the linearity arises simply from the fact that, for a small external field, the response of the system is linear. In this situation the atomic system is unsaturated; for large C the atomic cooperation is dominant and one has strong atom–atom correlations (LUGIATO [1979]).

The curves $y(x)$, obtained by varying C , are analogous to the Van der Waals curves for the liquid–vapor phase transition, with y , x and C playing the role of pressure, volume and temperature respectively. For $C < 4$, y is a monotonic function of x , so that one has no bistability (Fig. 8). However, in part of the curve the differential gain dx/dy is larger than unity, so that in this situation one has the possibility of transistor operation. In fact, if the incident intensity is adiabatically modulated around a value of P_I , such that $dP_T/dP_I = (x/y)dx/dy > 1$, the modulation is amplified in the transmitted light (MC CALL [1974]).

For $C = 4$ (critical curve) the graph has an inflection point with horizontal tangent. Finally for $C > 4$ the curve develops a maximum and a minimum, which for $C \gg 1$ correspond to $(x_M \approx 1, y_M \approx C)$ and $(x_m \approx \sqrt{2C},$

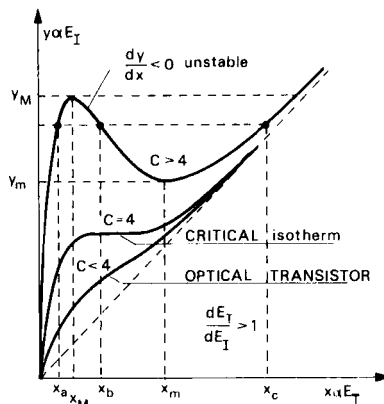


Fig. 8. Plot of the mean field state equation (32) for purely absorptive bistability with $\theta = 0$, for different values of the bistability parameter C .

$y_m \approx \sqrt{8C}$). Hence, for $y_m < y < y_M$ one finds three stationary solutions $x_a < x_b < x_c$. As we shall show in § 2.4.2, solutions x_b on the part of the curve with negative slope are unstable. Therefore we have a bistable situation, and by exchanging the axes x and y we immediately obtain the hysteresis cycle of transmitted versus incident light. Since atomic cooperation is dominant in the states x_a , and negligible in the states x_c , we shall call x_a “cooperative stationary state” and x_c “one-atom stationary state”.

2.1.5. Bistability conditions in the general case (mean field limit)

Let us now consider eq. (31) for general values of Δ and θ (HASSAN, DRUMMOND and WALLS [1978], BONIFACIO, GRONCHI and LUGIATO [1979a], AGRAWAL and CARMICHAEL [1979]). We assume that $\Delta\theta > 0$, because for $\Delta\theta < 0$ it is more difficult to obtain bistability. For definiteness, we take $\Delta, \theta \geq 0$; however the situation is symmetrical with respect to a simultaneous sign change in Δ and θ . The function $Y(X)$, defined by eq. (31) always has a single inflection point at

$$X_{\text{inf}} = \frac{2C - \Delta\theta + 1}{C + \Delta\theta - 1} (\Delta^2 + 1). \quad (35)$$

In order to have bistability the obvious conditions are

$$X_{\text{inf}} > 0, \quad \left. \frac{dY}{dX} \right|_{X_{\text{inf}}} < 0. \quad (36)$$

The first condition guarantees that the inflection point is within the physical region $X > 0$, while the second one identifies the values of the parameters for which the curve $Y(X)$ has a maximum and a minimum. For $\Delta\theta > 0$, the first condition in eq. (36) reads

$$2C > \Delta\theta - 1. \quad (37)$$

The second condition gives

$$(2C - \Delta\theta + 1)^2(C + 4\Delta\theta - 4) > 27C(\Delta + \theta)^2. \quad (38)$$

The analysis of eqs. (37) and (38) leads us (BONIFACIO, GRONCHI and LUGIATO [1979a]) to conclude that

- (i) bistability is impossible for $C < 4$.
- (ii) for a fixed value of $C > 4$, the largest hysteresis cycle is obtained for $\Delta = \theta = 0$ and bistability exists only in a finite domain of the plane $\{\Delta, \theta\}$ around the origin.
- (iii) if we keep C and Δ fixed and C satisfies condition (38) for $\theta = 0$, by increasing θ the size of the hysteresis cycle increases until it reaches a maximum and then decreases. Finally the cycle vanishes in correspondence to a value of θ smaller than $(2C + 1)/\Delta$ (see eq. (37)).
- (iv) if we keep $C > 4$ fixed and increase Δ and θ , simultaneously from zero, with the ratio Δ/θ kept fixed, the hysteresis cycle of the curve $X(Y)$ shifts to the left and decreases in size, until it disappears.

Therefore in homogeneously broadened, two-level systems, when absorptive bistability for $\theta = 0$ is not possible, dispersive bistability for general values of Δ and θ is also impossible. This is no longer true in the case of inhomogeneously broadened systems ($T_2^* < \infty$). For fixed Δ , θ and T_2^* , one obtains bistability, provided that C is larger than a suitable value C_{\min} , which depends on Δ , θ , T_2^* . C_{\min} increases rapidly with $(T_2^*)^{-1}$. The important point is that, for $(\gamma_\perp T_2^*)^{-1} \gg 1$, one finds values of C such that the system is not bistable for $\Delta = \theta = 0$, but becomes bistable when Δ and θ are large enough. In other words, for these values of T_2^* and C one does not find absorptive bistability, but only dispersive bistability. (BONIFACIO and LUGIATO [1978c], HASSAN, DRUMMOND and WALLS [1978]).

So far, we have only considered hysteresis cycles obtained by varying the

incident field intensity and keeping the parameters C , Δ , θ fixed. Of course one can also consider cycles obtained by keeping Y fixed and varying C , Δ , or θ , or some of these parameters simultaneously (AGRAWAL and CARMICHAEL [1979]). For instance, one can perform an experiment in which one adiabatically sweeps the incident field frequency, thereby varying Δ and θ together. This procedure is followed in SANDLE and GALLAGHER [1981], and ARIMONDO, GOZZINI, LOVITCH and PISTELLI [1981].

By exploiting optical pumping one can reduce the switching power and obtain a wide tuning range (ARECCHI, GIUSFREDI, PETRIELLA and SALIERI [1982], GOZZINI [1982]).

In the case of Fabry–Perot, the bistability threshold C_{\min} is somewhat higher than for a ring cavity. For example, in the purely absorptive case with homogeneous broadening the bistability condition is $C > 4.96$ (CARMICHAEL [1980], HERMANN [1980], MCCALL and GIBBS [1980]).

The effects of the radial shape of the electric field have been studied in BALLAGH, COOPER, HAMILTON, SANDLE and WARRINGTON [1981], ARIMONDO, GOZZINI, LOVITCH and PISTELLI [1981], DRUMMOND [1981], ROSANOV and SEMENOV [1981], FIRTH and WRIGHT [1982] and MOLONEY, BELIC and GIBBS [1982]. These treatments predict that the bistability threshold C_{\min} and the switching intensity are raised by the Gaussian profile of the incident field. This effect, which is found both for a ring cavity and for a Fabry–Perot, is largest in the purely absorptive case (in which C_{\min} increases by more than a factor two), whereas it is small in the purely dispersive case. With the exception of ROSANOV and SEMENOV [1981], FIRTH and WRIGHT [1982] and MOLONEY, BELIC and GIBBS [1982], these treatments introduce ab initio the hypothesis that when the incident field corresponds to a TEM_{00} mode of the cavity the internal field also has the same radial shape. This assumption remains to be substantiated by further analysis.

MARBURGER and FELBER [1978] predicted that under proper conditions the self-focusing can lower the threshold.

2.1.6. *Absorptive versus dispersive bistability*

As we have said, we have purely absorptive optical bistability when the atomic detuning Δ vanishes. On the contrary, we have purely dispersive optical bistability when Δ is so large that the absorptive part of the nonlinear susceptibility is negligible; hence, the state equation (30) reduces to

$$Y = X \{ 1 + [\theta - 2C\tilde{\chi}_d(X)]^2 \}. \quad (39)$$

In the case of a homogeneously broadened, two-level system eq. (39) is a good approximation of eq. (30) when (BONIFACIO, GRONCHI and LUGIATO [1979a]

$$\Delta^2 \gg 1, \quad \Delta\theta \gg 1, \quad \Delta \gg \theta. \quad (40)$$

Moreover, if the condition

$$\frac{2C}{\Delta\theta} - 1 \ll 1 \quad (41)$$

is also satisfied, eq. (39) reduces in turn to the relation

$$Y = X \left\{ 1 + \left[\theta - \frac{2C}{\Delta} + \frac{2C}{\Delta^3} X \right]^2 \right\}. \quad (42)$$

Equation (42) predicts bistability for $(2C/\Delta) - \theta > \sqrt{3}$. The condition (41) guarantees that $X \ll \Delta^2$ along the hysteresis cycle, which in turn implies that the atoms remain in the ground state (i.e., no absorption) in the whole bistable domain (see eq. (50), below).

Equation (42) is a particular example of the cubic model of purely dispersive optical bistability, that was first considered by GIBBS, McCALL and VENKATESAN [1976]:

$$Y = X \{ 1 + [B - AX]^2 \}, \quad (43)$$

which gives bistability for $B > \sqrt{3}$. Equation (43) describes optical bistability in several materials, for instance in a Kerr medium in the limit of small $\delta + \beta P_T$ (see eq. (20)).

Let us now describe the physical mechanisms that give rise to hysteresis in absorptive and dispersive optical bistability. In the absorptive case, let us consider for simplicity the resonant situation $\theta = 0$. In the cooperative (i.e. lower transmission) branch the transmission is small, because the presence of the saturable absorber drastically decreases the quality factor Q of the cavity. Most of the incident light is reflected from the cavity. Increasing the incident field causes the absorber to saturate, which allows the Q to increase. This in turn increases the internal field which again increases the saturation and so on, until the absorber is bleached, so that $P_T \approx P_1$. On the other hand, when the system is in the one-atom (i.e. higher transmission) branch and the incident intensity is decreased, the field internal to the cavity is already strong enough to maintain the absorber saturated, and therefore the transmitted light switches “off” at an incident power lower than that necessary to switch “on”, thereby producing hysteresis.

In the case of purely dispersive optical bistability the mechanism is quite

different, and was first pointed out in GIBBS, MCCALL and VENKATESAN [1976]. In the lower branch the transmission is low because the empty cavity frequency ω_c is detuned from the incident frequency ω_0 . If the atomic and cavity detunings have the same sign, by increasing the incident field the nonlinear refractive index changes the effective optical length of the cavity towards resonance. This in turn increases the internal field, which further drives the effective cavity frequency $\omega'_c = \omega_c - k\chi_d(X)$ towards the incident field frequency and so on, until resonance is reached, so that $P_T \approx P_I$. On the other hand, when the system is in the higher transmission branch and the incident intensity is decreased, the internal field is already strong enough to maintain resonance, which again produces hysteresis.

In order to complete the discussion of the steady state behavior, let us illustrate the relative advantages of absorptive and dispersive optical bistability. First of all, it is clear that dispersive optical bistability is “easier” mainly for two reasons:

a) it does not require saturation of the medium as it appears from the cubic model (43);

b) in absorptive optical bistability the resonance condition between the incident field and the atoms cannot be easily maintained for a time long enough to allow the system to reach steady state, owing to the jitter in laser frequency. This problem emerges from the experiment of WEYER, WIEDENMANN, RATEIKE, MCGILLIVRAY, MEYSTRE and WALther [1981].

As we have seen in the previous section, in the case of homogeneous broadening absorptive optical bistability has the advantage of exhibiting the largest hysteresis cycle for fixed C , when $\Delta = \theta = 0$. However, this is no longer true in the case of inhomogeneous broadening. Furthermore, even in the case of homogeneous broadening, the switching from the low transmission to the high transmission branch occurs for lower values of the input field when Δ and θ are different from zero (see § 2.1.5, point (iv)). This is an important advantage, also because the presence of too intense a field in the absorber might produce undesirable effects, for instance heating of the medium.

For these reasons most experiments on optical bistability are in dispersive conditions. Absorptive optical bistability has been first observed by GIBBS, MCCALL and VENKATESAN [1976] and SANDLE, BALLAGH and GALLAGHER [1981], and later in greater detail by WEYER, WIEDENMANN, RATEIKE, MCGILLIVRAY, MEYSTRE and WALther [1981] and GRANT and KIMBLE [1982] (see Fig. 32, below) at optical frequencies, by GOZZINI, LONGO and MACCARRONE [1982] at microwave frequencies, and by MEIER, HOLZNER, DERIGHETTI and BRUN [1982] at radio frequencies.

On the other hand, from the viewpoint of theory and hence, of the comparison between experiment and theory, absorptive optical bistability with $\theta = 0$ is certainly much easier to deal with, because in the Maxwell–Bloch equations (1) all the fields can be safely assumed as real. This is the reason why most theoretical papers treat the absorptive case, and this also explains why some parts of this article are exclusively devoted to the problem of absorptive optical bistability. This occurs especially in the treatment of the most sophisticated problems, such as self-pulsing or quantum effects. The generalization to the case $\Delta, \theta \neq 0$ involves quite cumbersome calculations and would reduce the pedagogical impact of this paper.

A final remark concerns the nomenclature. We called the bistability absorptive or dispersive according to whether it is produced by the absorptive or by the dispersive part of the susceptibility. This, however, does not mean that absorption is dominant in the purely absorptive case and necessarily absent in purely dispersive optical bistability. In general, the incident energy is in part transmitted, in part reflected, and in part absorbed by the atomic sample. By “absorbed” we mean both the energy diffused as fluorescent light and the energy dissipated in the medium. The absorbed energy is proportional to the population of the upper level. In the case of purely absorptive optical bistability, when the system is in the higher transmission branch most energy is transmitted, except in a neighborhood of the lower bistability threshold x_m (Fig. 8), where the absorbed and the transmitted energies have the same order of magnitude (see § 3.4.2). In the lower transmission branch absorption is dominated by reflection. On the other hand, in the two-level system there are situations that fulfil conditions (40) of purely dispersive optical bistability, in which, however, the population of the upper level is not negligible in the bistable region. An example is $C = 180$, $\Delta = 60$, and $\theta = 1$ (BONIFACIO, GRONCHI and LUGIATO [1979a]); see also Fig. 5. Only when condition (41) is satisfied is absorption really absent in the range of values of the incident field for which the system is bistable.

2.1.7. *The cooperation parameter C*

We stress that the parameter C is crucial not only in optical bistability, but also in many other cooperative phenomena in quantum optics. For instance, in superfluorescence (see the book edited by BONIFACIO [1982]), that is, in cooperative emission from a pencilshaped, mirrorless sample of two-level atoms prepared in a state of complete inversion, the necessary condition for the rise of cooperativity is $\alpha L \gg 1$, i.e. (since $T = 1$) $C \gg 1$.

Another interesting example is that of the laser with injected signal (DEGIORGIO and SCULLY [1970], SPENCER and LAMB [1972], CHOW, SCULLY and VAN STRYLAND [1975] and LUGIATO [1978]). The configuration of this system is the same as for optical bistability, but with an amplifier instead of an absorber. That is, the atoms are continuously pumped to yield a positive unsaturated inversion per atom σ . The Maxwell-Bloch equations for this system are identical to eqs. (1), with N replaced by $-\sigma N$. Hence, all the formulas derived up to now remain valid for the laser with injected signal, provided that one replaces α by $-\sigma\alpha$ and therefore defines C as:

$$C = -\frac{\sigma\alpha L}{2T}.$$

With this definition, the state equation for the laser with injected signal in the perfect resonant case is still eq. (32), but now C is negative.

For $y = 0$, eq. (32) reduces to the steady state equation of the normal laser (i.e., without injected signal), which has the two solutions $x = 0$ (nonlasing system) and $x = (2|C| - 1)^{1/2}$ (oscillating laser). Since the trivial solution is unstable for $|C| > 1/2$, the graph of the stationary solution x versus the pump parameter C shows a second-order phase transition in correspondence to the threshold $|C| = 1/2$ (DEGIORGIO and SCULLY [1970], GRAHAM and HAKEN [1970]).

In the case $y \neq 0$, for $|C| > 1/2$ the plot of transmitted light versus incident light obtained from eq. (32) shows multiple solutions (LUGIATO [1978]) (Fig. 9). However, one does not have a bistable situation, because all the part of the curve where $x < 0$ is unstable due to phase fluctuations. However, using the procedure of BÖSIGER, BRUN and MEIER [1981] one can maintain a fixed difference of 180° between the phases of the transmitted and incident fields, so that the system actually becomes bistable. In such a way bistability was observed in a laser with injected signal based on the dynamics of nuclear spin systems. These experiments correspond to "bad cavity" conditions with $\gamma_{\parallel} \ll \gamma_{\perp}$ (MEIER, HOLZNER, DERIGHETTI and BRUN [1982]).

2.2. SIMPLIFIED TREATMENT OF OPTICAL BISTABILITY IN THE LIMIT OF SMALL ABSORPTION, TRANSMISSION AND DETUNING

As we have seen in § 2.1, the simplest situation corresponds to (see eq. (27))

$$\alpha L \ll 1, \quad T \ll 1, \quad \delta_0 \ll 1 \tag{44}$$

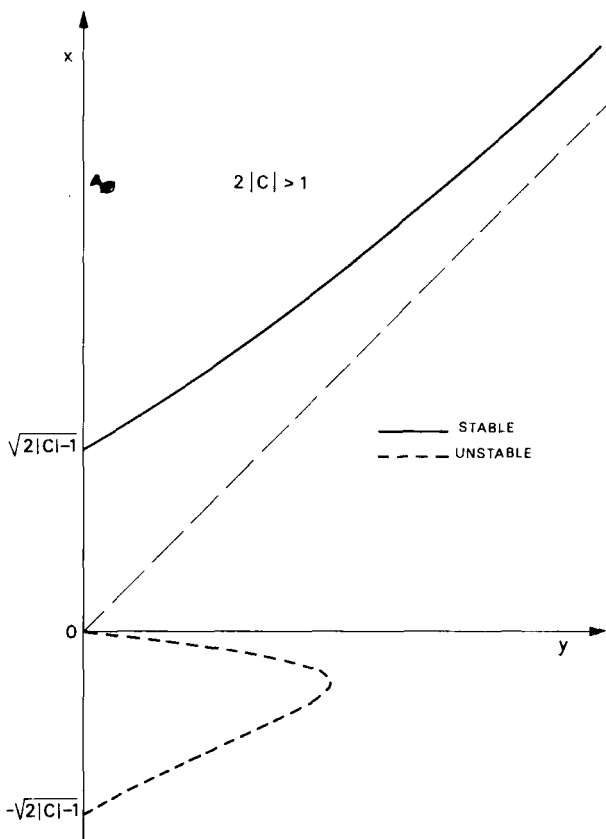


Fig. 9. Laser with injected signal. The output field x is plotted as a function of the incident field y for $|C| > 1/2$.

with $C = \alpha L/2T$ arbitrary, and $\theta = \delta_0/T$ arbitrary. For this reason, most of the following treatment is limited to the case (44), in which we can obtain the maximum physical insight and the maximal amount of analytical results. However, it is important to stress that conditions (44) may not be ideal from a practical viewpoint. In fact, a very small transmissivity renders the empty cavity response time \mathcal{L}/cT long, and this is opposite to the requirement of a fast operating device.

2.2.1. The Maxwell–Bloch equations in the limit $\alpha L \ll 1$, $T \ll 1$, $\delta_0 \ll 1$

As shown in Appendix A, in the limit (44) the Maxwell equation (1a) and the boundary condition (3b) can be reformulated as (LUGIATO [1981])

$$\frac{\partial E}{\partial t'} + c \frac{L}{\mathcal{L}} \frac{\partial E}{\partial z} = -i k \theta E - k \left(E - \frac{E_1}{\sqrt{T}} \right) - g \frac{L}{\mathcal{L}} P, \quad (45)$$

$$E(0, t') = E(L, t'), \quad (46)$$

where the variable t' is defined by

$$t' = t + \Delta t \frac{z}{L}. \quad (47)$$

The time t' is introduced in order to eliminate the retardation Δt from the boundary condition (3b), which then becomes the standard periodicity condition in space (46). In a sense, the transformation (47) has the effect of “bending” the atomic sample onto itself, transforming it into a ring. Note that t' can be replaced by the real time t whenever the evolution occurs on a time scale much longer than the cavity transit time \mathcal{L}/c . This is generally true in the limit (44) for a wide class of initial conditions, except when self-pulsing behavior arises.

Equation (45) describes propagation with velocity $c' = cL/\mathcal{L}$. The factor L/\mathcal{L} arises from the geometry of the cavity (Fig. 1).

The difference between eq. (45) and the original Maxwell–Bloch equation (1a) arises from the fact that most of the information contained in the boundary condition (3b) has been transferred into the time evolution equation for the field (45). Namely, the external field E_1 , the transmissivity coefficient, and the cavity mistuning parameter appear now in eq. (45), which also incorporates the retardation Δt via the time t' .

From now on, it is suitable to express the time evolution equations in terms of the normalized quantities F defined by eq. (9) and

$$\tilde{P} = \left[\frac{N}{2} \left(\frac{\gamma_{\perp}}{\gamma_{\parallel}} \right)^{1/2} \right]^{-1} P, \quad \tilde{D} = \left(\frac{N}{2} \right)^{-1} D. \quad (48)$$

Thus, eqs. (45) and (1b,c) become

$$\frac{\partial F}{\partial t'} + c \frac{L}{\mathcal{L}} \frac{\partial F}{\partial z} = k[-i\theta F - (F - y) - 2C\tilde{P}], \quad (49a)$$

$$\frac{\partial \tilde{P}}{\partial t'} = \gamma_{\perp} [F\tilde{D} - (1 + i\Delta)\tilde{P}], \quad (49b)$$

$$\frac{\partial \tilde{D}}{\partial t'} = -\gamma_{\parallel} [\frac{1}{2}(F\tilde{P}^* + F^*\tilde{P}) + \tilde{D} - 1]. \quad (49c)$$

It is straightforward to calculate the stationary solutions from eqs. (49). In fact, in the limit (44) the steady state fields are uniform in space, so that one must set not only $\partial F/\partial t' = \partial \tilde{P}/\partial t' = \partial \tilde{D}/\partial t' = 0$ but also $\partial F/\partial z = 0$. In such a way, using eqs. (10), (11b), and (21), one obtains

$$\tilde{P}_{st} = \frac{(1 - i\Delta)x_{st}}{1 + \Delta^2 + X_{st}}, \quad \tilde{D}_{st} = \frac{1 + \Delta^2}{1 + \Delta^2 + X_{st}} \quad (50)$$

and the mean field state equation (31) for X_{st} .

2.2.2. Formulation in terms of equations for the modes. The mean field model of optical bistability

It may be suitable to re-express eqs. (49) in terms of mode variables for the field and the atomic system. This procedure is quite common in quantum optics (HAKEN [1970], SARGENT, SCULLY and LAMB [1974]). The cavity frequencies are $\omega_c + \alpha_n$, where ω_c is the frequency that is nearest to the incident frequency, and

$$\alpha_n = \frac{2\pi c}{\mathcal{L}} n, \quad n = 0, \pm 1, \dots \quad (51)$$

Let us consider the following expansions

$$\begin{Bmatrix} F(z, t') \\ \tilde{P}(z, t') \\ \tilde{D}(z, t') \end{Bmatrix} = \sum_n e^{ik_n z} \begin{Bmatrix} f_n(t') \\ p_n(t') \\ d_n(t') \end{Bmatrix}, \quad (52)$$

with

$$k_n = \frac{\alpha_n}{cL/\mathcal{L}} = \frac{2\pi}{L} n, \quad n = 0, \pm 1, \dots \quad (53)$$

The functions $\exp(ik_n z)$ obey the periodicity boundary condition (46). By substituting eqs. (52) into eqs. (49), and taking into account the orthogonality

of the functions $\exp(ik_n z)$ in the internal $0 \leq z \leq L$, one finds the following equations for the mode amplitudes f_n , p_n and d_n :

$$f_n = -i\alpha_n f_n + k[-i\theta f_n - (f_n - y\delta_{n,0}) - 2Cp_n], \quad (54a)$$

$$\dot{p}_n = \gamma_{\perp} \left[\sum_{n'} f_{n'} d_{n-n'} - (1 + i\Delta)p_n \right], \quad (54b)$$

$$\dot{d}_n = -\gamma_{\parallel} \left[\frac{1}{2} \sum_{n'} (f_{n'} p_{n'-n}^* + f_{n'}^* p_{n'+n}) + d_n - \delta_{n,0} \right]. \quad (54c)$$

where the dot means derivative with respect to time t' . When the fields F , \tilde{P} and \tilde{D} are uniform in space only the amplitudes f_0 , p_0 , d_0 , corresponding to the resonant mode, are different from zero. Note from eqs. (54) that if the fields are initially (i.e. at $t' = 0$) uniform, they remain uniform during the whole evolution. This is a consequence of the assumption (44). Hence, in this case, eqs. (54) reduce to

$$k^{-1} \dot{x} = -i\theta x - (x - y) - 2Cp_0, \quad (55a)$$

$$\gamma_{\perp}^{-1} \dot{p}_0 = x d_0 - (1 + i\Delta)p_0, \quad (55b)$$

$$\gamma_{\parallel}^{-1} \dot{d}_0 = -\frac{1}{2}(xp_0^* + x^*p_0) - d_0 + 1, \quad (55c)$$

where we have taken into account that in this case $x = f_0$. Equations (55) were first introduced in BONIFACIO and LUGIATO [1976, 1978d], and are usually called the “mean field model” of optical bistability. Here the words “mean field” refer to the fact that the fields are uniform in space. Therefore, they have quite a different meaning, for instance, from the one used in the theory of equilibrium phase transitions. The mean field model (55) holds in the limit (44), provided that the initial condition is perfectly uniform. As we shall see in § 2.4.3, in order to describe self-pulsing we shall have to consider initial conditions that are at least slightly nonuniform in space.

Hence, the mean-field theory of optical bistability is a *one-mode theory*. As one immediately verifies, at steady state ($\dot{f}_0 = \dot{p}_0 = \dot{d}_0 = 0$) one obtains, for p_0 and d_0 , the expressions (50), and one immediately derives the state equation (31). In fact, at steady state, only the resonant mode has a nonvanishing amplitude in the limit (44).

2.3. TRANSIENT BEHAVIOR

For the sake of simplicity, we shall describe the transient behavior in the framework of the mean field model (55). However, most of these results also remain valid out of the range of parameters specified by (44).

We shall first analyze the regression of the system to steady state, after it has been slightly displaced from it. In §§ 2.3.3 and 2.3.4 we shall describe the complete transient approach to steady state, emphasizing a few points that are relevant for the switching properties of the system.

2.3.1. Regression to steady state and critical slowing down

Let us consider a stable stationary state of the system. If the system is slightly shifted from this stationary state, the regression to the steady state is ruled by the set of equations obtained by linearizing eqs. (55) around steady state. By calling $\delta x = x - x_{\text{st}}$ etc. one obtains

$$k^{-1} \delta \dot{x} = -(1 + i\theta)x - 2C\delta p_0, \quad (56a)$$

$$\gamma_{\perp}^{-1} \delta \dot{p}_0 = x_{\text{st}} \delta d_0 + d_{0,\text{st}} \delta x - (1 + iA)\delta p_0, \quad (56b)$$

$$\gamma_{\parallel}^{-1} \delta \dot{d}_0 = \frac{1}{2}(x_{\text{st}} \delta p_0^* + p_{0,\text{st}}^* \delta x + x_{\text{st}}^* \delta p_0 + p_{0,\text{st}} \delta x^*) - \delta d_0. \quad (56c)$$

The equations for δx^* and δp_0^* are the complex conjugates of eqs. (56a) and (56b) respectively. $p_{0,\text{st}}$ and $d_{0,\text{st}}$ are given by eq. (50). To be more specific, we consider the following experiment. Let us assume that the system is initially in a steady state corresponding to some value E_1 of the incident field. If E_1 is rapidly changed into $E_1 + \delta E_1$ ($|\delta E_1| \ll E_1$) the system approaches the new, slightly different, steady state corresponding to $E_1 + \delta E_1$. This approach is described by a solution of the linearized equations (56) and can be experimentally observed by looking at the transient behavior of the transmitted light. The solutions of the linearized equations are linear combinations of five exponentials $\exp(\lambda_i t)$, $i = 1, \dots, 5$. When the decay constants $-\text{Re } \lambda_i$ are well separated, the approach to the stationary situation is mainly characterized by the decay constant $\bar{\lambda}$, which is equal to the smallest among the quantities $-\text{Re } \lambda_i$. We prove in general the following results:

- 1) Let us consider a point (x, y) on the cooperative branch, very near to the upper discontinuity point $(x = x_M, y = y_M)$ (see Fig. 8). The approach to the steady state (x, y) is very slow, and becomes slower the nearer y is to y_M . Hence, there is a *critical slowing down* in correspondence to the discontinuity point y_M .

This critical slowing down is similar to that which one finds in tunnel diodes; see LANDAUER and Woo [1973]. More specifically, one finds that $\bar{\lambda} \rightarrow 0$ as $(y_M - y)^{1/2}$ when y approaches y_M from below. Hence, $\bar{\lambda}$ corresponds with a *soft mode* of the system.

2) A similar critical slowing down is found in correspondence to the lower discontinuity point ($x = x_m$, $y = y_m$). In fact, let us consider a point (x, y) on the one-atom branch, very near to $(x = x_m, y = y_m)$. The damping constant $\bar{\lambda}$, which characterizes the approach to (x, y) , tends to zero as $(y - y_m)^{1/2}$ when y approaches y_m from above.

This critical slowing down at the boundaries of the steady state hysteresis cycle was first pointed out in BONIFACIO and LUGIATO [1976], and is an absolutely general feature of optical bistability, that is, it holds for whatever values of the important parameters in play, including αL , T and δ_θ , for any kind of cavity and absorbing material.

The other features of the behavior of $\bar{\lambda}$ when y is varied depend on whether Δ and θ vanish or not, and on the relative order of magnitude of the constants k , γ_\perp , γ_\parallel . Two typical situations, which we shall consider in the following, are (BONIFACIO and LUGIATO [1978d]):

a) $k \ll \gamma_\perp, \gamma_\parallel$. In this situation, which is usual in laser amplifiers, the empty cavity width is much smaller than the atomic linewidth. We shall call this case “good (quality) cavity case”.

b) $k \gg \gamma_\perp, \gamma_\parallel$. We shall call this situation “bad (quality) cavity case” even if this name is somewhat improper when $T \ll 1$, because in this case the finesse of the cavity is large.

For $T \ll 1$ the condition $k \gg \gamma_\perp, \gamma_\parallel$ can be achieved only with a very short cavity or with an atomic material with long relaxation times.

In case a), two of the roots λ_i have a much smaller (in modulus) real part than all the others. They are the solution of the equation

$$\lambda^2 + 2k \left[1 + \frac{2C(1 + \Delta^2)}{(1 + \Delta^2 + X_{st})^2} \right] \lambda + k^2 \frac{dY}{dX} \Big|_{X_{st}} = 0, \quad (57)$$

where the function $Y(X)$ is defined by eq. (31). When Δ and θ are different from zero, the solutions of eq. (57) are complex conjugate over a large part of the steady state curve, with the exception of two segments including the boundaries of the cycle (see Fig. 5b). For instance, for $X_{st} \ll 1$ the solutions are

$$\lambda = -k \{ [1 + 2C/(1 + \Delta^2)] \pm i[\theta - 2CA/(1 + \Delta^2)] \}$$

and for $X_{st} \rightarrow \infty$ they are $\lambda = -k(1 \pm i\theta)$. Hence, in these cases the approach to steady state is oscillatory.

For $\Delta = \theta = 0$ the solutions are always real:

$$\begin{aligned}\lambda_1 &= -k \frac{dy}{dx} \Big|_{x_{st}} = -k \left(1 + 2C \frac{1 - x_{st}^2}{(1 + x_{st}^2)^2} \right), \\ \lambda_2 &= -k \frac{y}{x_{st}} = -k \left(1 + \frac{2C}{1 + x_{st}^2} \right),\end{aligned}\quad (58)$$

where the function $y(x)$ is defined in eq. (32). Hence, in this case the approach to steady state is always monotonic.

In case b), we limit ourselves to considering the situation $\Delta = \theta = 0$. When (x, y) lies on the cooperative branch the approach is monotonic. For $C \gg 1$ one has approximately

$$\bar{\lambda} = 2\gamma_{\parallel} \left(1 - \frac{y^2}{C^2} \right)^{1/2} / \left[1 + \left(1 - \frac{y^2}{C^2} \right)^{1/2} \right]. \quad (59)$$

When (x, y) lies on the one-atom branch the approach is oscillatory except when (x, y) is very near to the lower discontinuity point (x_m, y_m) or when the ratio $\gamma_{\parallel}/\gamma_{\perp}$ is too small. In particular, for $y \gtrsim y_M$ (BONIFACIO and LUGIATO [1976])

$$\bar{\lambda} \approx (\gamma_{\perp} + \gamma_{\parallel})/2 \quad (60)$$

and the oscillation frequency is the Rabi frequency of the incident field,

$$\Omega_1 = \mu E_1/\hbar \sqrt{T}. \quad (61)$$

Rabi oscillations in the bad cavity case have been reported in ROHART and MACKE [1980]. Observation of transients in optical bistability was reported in GRYNBERG, BIRABEN and GIACOBINO [1981].

Of course, situations different from $k \ll \gamma_{\perp}, \gamma_{\parallel}$ or $k \gg \gamma_{\perp}, \gamma_{\parallel}$ can be considered. For instance, DRUMMOND [1982] studied the case $\gamma_{\parallel} \ll k, \gamma_{\perp}$ which is close to the situation one finds in GaAs (GIBBS, McCALL and VENKATESAN [1979]). A general study of the mean field model for absorptive optical bistability in the limit of very large C has been done by MANDEL and ERNEUX [1982].

2.3.2. Adiabatic elimination of the atomic variables in the good cavity case

Let us now consider in detail the good cavity case $k \ll \gamma_{\perp}, \gamma_{\parallel}$. In this situation, the atomic variables vary in time much more rapidly than the field

variables. After a short transient of the order of T_1, T_2 , the atomic variables attain a stationary situation, i.e. we can put $\dot{p}_0 = \dot{d}_0 = 0$ in eqs. (55). Hence, the atomic variables p_0 and d_0 follow without retardation the motion of the field variable x , or using Haken's language are *slaved* by the field variable. In fact, the expressions for $p_0(t)$ and $d_0(t)$ for times much larger than T_1, T_2 are given by eq. (50) with x_{st} replaced by $x(t)$ and X_{st} by $|x|^2(t)$. By substituting the expression for p_0 into eq. (55a) one obtains a closed equation for the field variable which reads (BONIFACIO and LUGIATO [1978c])

$$k^{-1} \dot{x} = y - x \left[\left(1 + \frac{2C}{1 + \Delta^2 + |x|^2} \right) + i \left(\theta - \frac{2C\Delta}{1 + \Delta^2 + |x|^2} \right) \right]. \quad (62)$$

This procedure is called *adiabatic elimination of the atomic variables* (HAKEN [1977]).

The following two subsections illustrate some properties of the transient that are relevant for the switching behavior of the system.

2.3.3. Good cavity, case of perfect resonance: complete transient approach to steady state

Let us first consider the simplest setting, that is the case of perfect resonance $\Delta = \theta = 0$. In this situation, by writing $x = x_1 + ix_2$ eq. (62) becomes

$$k^{-1} \dot{x}_1 = -\frac{\partial \tilde{V}_y}{\partial x_1}, \quad k^{-1} \dot{x}_2 = -\frac{\partial \tilde{V}_y}{\partial x_2},$$

$$\tilde{V}_y(x_1, x_2) = -yx_1 + \frac{1}{2}(x_1^2 + x_2^2) + C \ln(1 + x_1^2 + x_2^2), \quad (63)$$

where \tilde{V}_y plays the role of a mechanical potential in the overdamped motion of a particle. Hence, if $x_2(0) = 0$, the imaginary part vanishes at all times. In this case, the dynamics are ruled by the equation

$$k^{-1} \dot{x} = -\frac{\partial V_y}{\partial x} = y - x - \frac{2Cx}{1 + x^2}, \quad V_y(x) = \tilde{V}_y(x, 0), \quad (64)$$

where we have written x instead of x_1 . We shall use eq. (64) to discuss the following problem. Let us assume that initially the system is at steady state, with a vanishingly small external field ($y \approx 0$), so that $x(0) \equiv x_0 \approx 0$. At this point, we abruptly switch the incident light on to some operating value y_{op} , larger than the upper bistability threshold y_M (Fig. 8). Hence, the transmitted light

approaches the stationary value \bar{x} in the high transmission branch corresponding to the value y_{op} of the incident field, that is the solution of eq. (32) for $y = y_{op}$. Equation (64), which describes the transient approach to the steady state \bar{x} , can be easily solved. For $y = y_{op} > y_M$, $x(0) = x_0$ we obtain (BENZA and LUGIATO [1979a])

$$\begin{aligned}
 k t' &= f(x) - f(x_0), \\
 f(x) &= A_1 \ln|x - \bar{x}| + \frac{1}{2} A_2 \ln \left[x^2 + (\bar{x} - y_{op})x + \frac{y_{op}}{\bar{x}} \right] \\
 &\quad + \frac{1}{\sqrt{A_3}} [2A_4 - A_2(\bar{x} - y_{op})] \tan^{-1} \frac{2x + \bar{x} - y_{op}}{\sqrt{A_3}}, \\
 A_1 &= \frac{1 + \bar{x}^2}{\bar{x}y_{op} - 2\bar{x}^2 - y_{op}/\bar{x}}, \quad A_2 = \frac{\bar{x}^2 - 1 - \bar{x}y_{op} + y_{op}/\bar{x}}{\bar{x}y_{op} - 2\bar{x}^2 - y_{op}/\bar{x}}, \\
 A_3 &= 4 \frac{y_{op}}{\bar{x}} - (\bar{x} - y_{op})^2 > 0, \quad A_4 = \frac{2(y_{op} - \bar{x})}{\bar{x}y_{op} - 2\bar{x}^2 - y_{op}/\bar{x}}. \quad (65)
 \end{aligned}$$

The plot of x versus $\tau \equiv kt'$ is obtained from the graph of τ versus x by simply exchanging the axes. Figure 10a shows several plots of x versus τ for $C = 20$ and different values of y_{op} . Clearly, the approach shows a kind of “lethargy”, and the time the system takes to reach steady state becomes longer and longer as y_{op} approaches y_M from above (BONIFACIO and MEYSTRE [1979], BENZA and LUGIATO [1979a]). This behavior is another facet of the *critical slowing down* mentioned in § 2.3.1. Let us consider eq. (64). The potential $V_y(x)$ has two minima in correspondence with the two stable stationary solutions $x = x_a$ and $x = x_c$ (Fig. 8), and one maximum in correspondence to the unstable state $x = x_b$. For $y_M - \varepsilon < y < y_M$, with $\varepsilon \ll y_M$, the left minimum is very shallow (Fig. 11a); hence, if we slightly displace the system from the minimum the system takes a long time to return to the steady state x_a . This lengthening is the critical slowing down discussed in § 2.3.1. For $y = y_M$ the left minimum becomes an inflection point with horizontal tangent (Fig. 11b). Finally for $y_M < y < y_M + \varepsilon$ there is only one stationary state \bar{x} , but the potential has a very flat part, hence, the system takes a long time to reach the steady state \bar{x} (Fig. 11c).

This critical slowing down behavior in the approach to the steady state in the high transmission branch has been experimentally confirmed by GARMIRE, MARBURGER, ALLEN and WINFUL [1979] in a hybrid system, and by

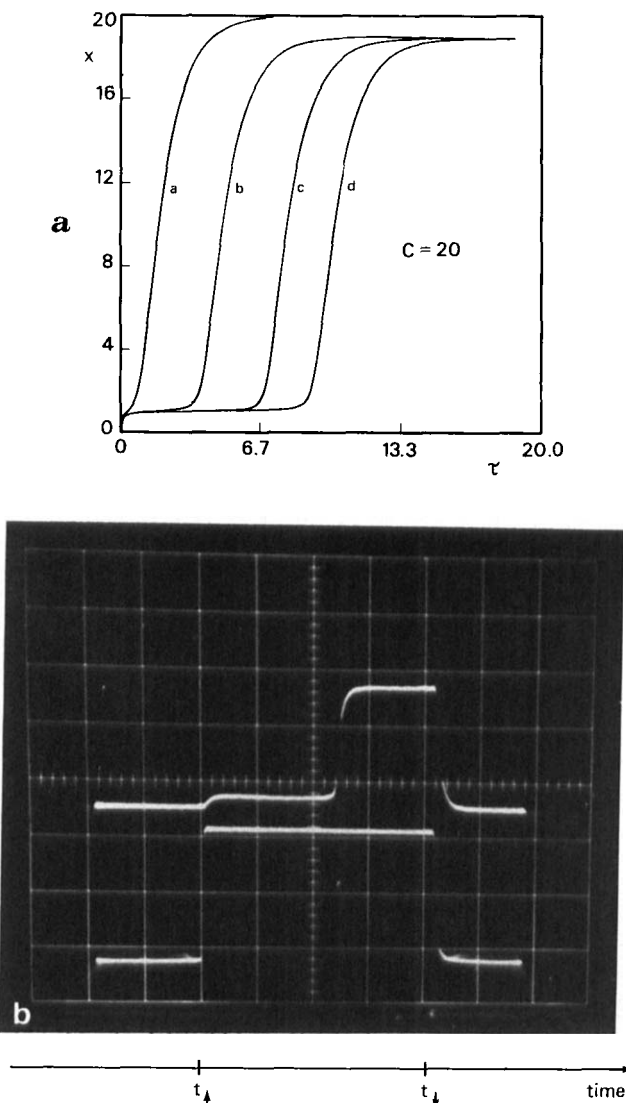


Fig. 10. (a) Time evolution of the transmitted field in the good cavity case for $C = 20$ and: **a**, $y_{op} = 22$; **b**, $y_{op} = 21.1$; **c**, $y_{op} = 21.05$; **d**, $y_{op} = 21.04$. Time is in units of k^{-1} . One has $y_M = 21.0264$ (see Fig. 8). (b) Observation of critical slowing down in microwave absorptive bistability in ammonia (from BARBARINO, GOZZINI, LONGO, MACCARONE and STAMPACCHIA [1982]). Upper trace: transmitted power, lower trace: incident power. At $t = t_1$, the incident power is switched on to a value slightly larger than the bistability threshold y_M (see Fig. 8). At $t = t_2$, the incident power is switched off. The time scale is 10 ms/div. In this experiment T_1 and T_2 are of the order of a microsecond, and the cavity buildup time is ≈ 60 ns. The gas pressure is on the order of a millitorr and the mirror transmissivity is 0.01.

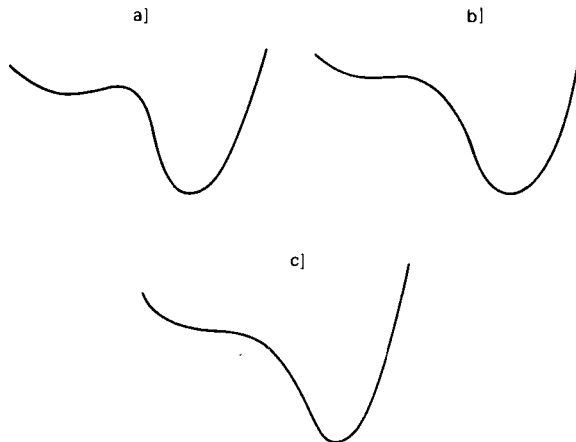


Fig. 11. Qualitative shape of the potential $V_y(x)$ (see eqs. (63) and (64)), when (a) y is slightly smaller than y_M , (b) $y = y_M$, and (c) y is slightly larger than y_M .

BARBARINO, GOZZINI, LONGO, MACCARRONE and STAMPACCHIA [1982] in an all-optical system (Fig. 10b). Needless to say, a similar behavior arises if we start with the system at steady state for $y \gg y_M$ and abruptly decrease the incident field to a value y_{op} smaller than y_m (see Fig. 8).

Coming back now to Fig. 10a, we can easily explain the main features of the time evolution for $C \gg 1$, $y_{op} = y_M + \epsilon$, which are the following: (i) the curve $x(\tau)$ exhibits a plateau with a very slow evolution, followed by a steep rise to the stationary value, and (ii) as y_{op} becomes nearer and nearer to y_M , the length of the plateau increases very rapidly, whereas the slope of the steep part remains practically unchanged.

In order to understand these points, let us consider the inflection points of the curve $\tau = \tau(x)$. From eq. (64) one finds easily that this curve has two inflection points which correspond with the maximum and minimum x_M and x_m (Fig. 8), of the function $y = y(x)$, defined by eq. (32), that are given by

$$x_{\frac{M}{m}} = [C - 1 \mp (C^2 - 4C)^{1/2}]^{1/2}. \quad (66)$$

Precisely, the point $x = x_M$, $\tau = \tau(x_M)$ lies in the plateau of the curve $x = x(\tau)$, whereas the point $x = x_m$, $\tau = \tau(x_m)$ lies in the steep part. Taking into account that

$$x_{\frac{M}{m}} - \frac{2Cx_{\frac{M}{m}}}{1 + x_{\frac{M}{m}}^2} = y_{\frac{M}{m}}$$

we obtain, from eq. (64),

$$\left(\frac{d\tau}{dx} \right)_{x_m^M} = (y_{op} - y_M)^{-1}. \quad (67)$$

Hence, the slope of the curve $x = x(\tau)$ for $x = x_M$, which characterizes the plateau, is equal to $y_{op} - y_M$. When y_{op} is near to y_M this slope becomes very small. On the other hand the slope of the curve $x = x(\tau)$ for $x = x_m$, which characterizes the steep part, is equal to $y_{op} - y_m$. For $C \gg 1$ one has $y_{op} - y_m \approx C \gg 1$, so that the slope is very large. When y_{op} becomes nearer and nearer to y_M , the slope $y_{op} - y_m \approx y_M - y_m$ remains practically unchanged. On the contrary, the time of approach to steady state $\bar{\tau}$ is very sensitive to the difference between y_{op} and y_M . Since the last stage of the evolution is fast, we identify $\bar{\tau}$ as the time for which $x = x_m$, i.e. $\bar{\tau} = \tau(x_m)$, which is given by eq. (65) with $x_0 = 0$. One sees that $\bar{\tau}$ diverges for $y_{op} \rightarrow y_M$ from above, because $A_3 \rightarrow 0$. The plot of $\bar{\tau}$ as a function of y_{op} is shown in Fig. 12.

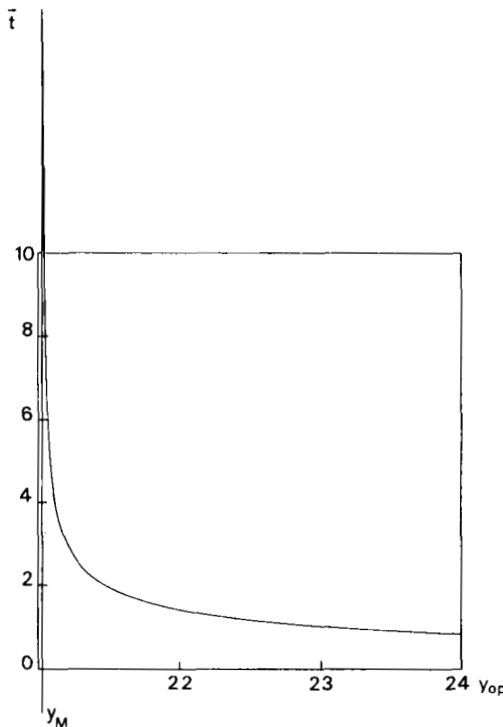


Fig. 12. Plot of the switching time $\bar{\tau}$ (in units of k^{-1}) as a function of the operating value y_{op} of the incident field for $C = 20$ and good cavity limit. $\bar{\tau}$ diverges for $y_{op} \rightarrow y_M$.

The critical slowing down is also important in connection with the following question. In order to obtain the hysteresis cycle of transmitted versus incident light, we must sweep the incident intensity back and forth. What is the maximum sweeping velocity such that the cycle is practically identical to the steady state cycle? A naïve answer is that in the good cavity case the sweeping time must be much larger than the buildup time of the field in the empty cavity. That is, in the resonant case $\theta = 0$, much larger than k^{-1} . Actually, the non-linearity of the dynamics gives a much more stringent condition. This feature emerges clearly from the experiment by WEYER, WIEDENMANN, RATEIKE, MCGILLIVRAY, MEYSTRE and WALther [1981]. In fact when the incident field y is varied, the potential V_y gets continuously deformed. In particular, when y is near to y_M , the potential changes from the configuration of Fig. 11a to that of Figs. 11b and 11c. During this stage, the system lies in a flat part of the potential, so that the time evolution is quite slow. For this reason the switching time from the low to the high transmission branch is on the order of $10^2\text{--}10^3 k^{-1}$ and the sweeping time must be larger than this lower bound in order to obtain a static hysteresis cycle. Otherwise, the hysteresis cycle is rounded by transient effects. The generation of hysteresis cycles by pulses was first analyzed by BISHOFBERGER and SHEN [1978] and ABRAHAM, BULLOUGH and HASSAN [1979].

2.3.4. Good cavity, purely dispersive case: anomalous switching

Let us come back to eq. (62) with $\Delta, \theta \neq 0$, and consider the following problem. As in § 2.3.3, we start with the system initially at steady state, with a vanishingly small external field $y \approx 0$. Abruptly, we change the incident field to a value y_{op} in the bistability region, that is $y_m < y_{op} < y_M$ (Fig. 8). In the absorptive case, the system always approaches the lower transmission steady state corresponding to the value y_{op} of the incident field, and only when y_{op} is made larger than y_M can the high transmission branch be reached. In the dispersive case this is no longer true in general. One achieves switching as soon as y_{op} exceeds a threshold value y_{th} which lies between y_m and y_M and whose value depends on the parameters in play. This phenomenon, which was first pointed out in the framework of a cubic model of dispersive optical bistability by HOPF, MEYSTRE, DRUMMOND and WALLS [1979], is called *anomalous switching*, and has been experimentally observed in hybrid systems (GOLDSTONE, HO and GARMIRE [1981]).

The difference in the switching behavior between the cases $\Delta = \theta = 0$ and $\Delta, \theta \neq 0$ arises from the fact that in the first one the electric field can be treated

as a real variable, whereas in dispersive optical bistability it is necessarily a complex quantity which evolves in a two-dimensional phase space. Furthermore, the approach to the steady state for $k \ll \gamma_{\perp}, \gamma_{\parallel}$ is always monotonic for $\Delta = \theta = 0$, whereas it can be oscillatory for $\Delta, \theta \neq 0$ (see Fig. 5b). This fact can explain the overshoot found in Kerr media when the system switches from the low to the high transmission branch (BISHOFBERGER and SHEN [1979]).

In order to obtain physical insight into the phenomenon of anomalous switching we follow the procedure of LUGIATO, MILANI and MEYSTRE [1982]. Together with eq. (62) let us consider the equation obtained by dropping the damping terms:

$$\dot{x} = y - ix \left(\theta - \frac{2C\Delta}{1 + \Delta^2 + |x|^2} \right). \quad (68)$$

The advantage of eq. (68) with respect to eq. (62) is that eq. (68) is analytically soluble. We note that eqs. (62) and (68) describe systems which are not only quantitatively but also qualitatively different, since in the case of eq. (62) the system approaches one of the two stationary solutions, whereas in the case of eq. (68), and due to the lack of dissipation, the motion is periodic in time. That is, the trajectory is a *closed* curve in the phase plane. However, our aim is only to determine the threshold of anomalous switching. For this purpose, it is enough to ensure that the solution of eq. (68), which starts from the origin, is a good approximation to the exact trajectory during that part of the time evolution which is relevant for the onset of anomalous switching. The relevant part of the trajectory involves only values of x smaller than (or at most on the order of) Δ .

For the sake of argument, let us consider the conditions (40) of purely dispersive optical bistability. Furthermore, we want the dispersive terms to be dominant during the relevant stage of the time evolution, so that eq. (62) is well approximated by eq. (68). This is achieved by imposing the condition

$$2C/\Delta \gg 1. \quad (69)$$

Let us consider the solutions of eq. (68). The trajectories in the phase plane $x_1 = \text{Re } x, x_2 = \text{Im } x$ are ruled by the equation

$$\frac{dx_1}{dx_2} = -\frac{y + x_2 f(x_1, x_2)}{x_1 f(x_1, x_2)}, \quad (70)$$

where

$$f(x_1, x_2) = \theta - \frac{2CA}{1 + A^2 + x_1^2 + x_2^2}.$$

The solution of eq. (70) that starts from the origin obeys the equation

$$\frac{1}{2}\theta(x_1^2 + x_2^2) + yx_2 - CA \ln \frac{1 + A^2 + x_1^2 + x_2^2}{1 + A^2} = 0. \quad (71)$$

The behavior of the trajectory (71) as a function of y is illustrated in Fig. 13. For y smaller than a critical value \bar{y} , the curve (71) is disconnected into two circle-like parts. The inner part, that includes the origin, has a small radius, so that the intensity (proportional to $|x|^2$) remains small during the whole time evolution. The outer part, which corresponds to a large intensity, cannot be

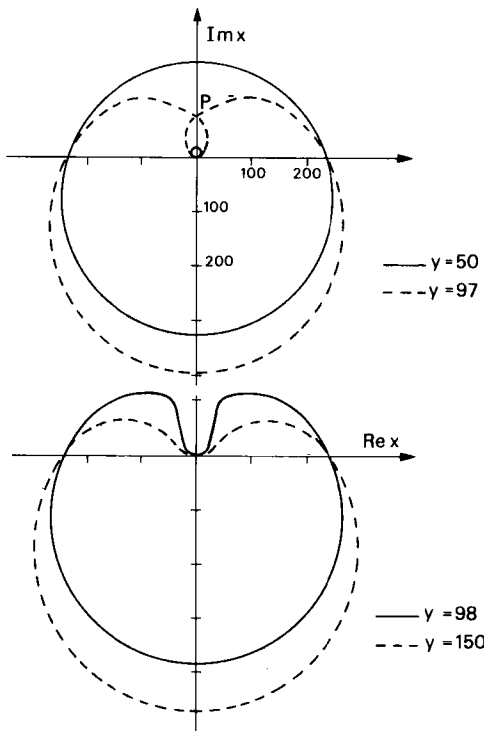


Fig. 13. The curve given by eq. (71) is shown for $C = 180$, $A = 60$, $\theta = 1$ and four different values of y . For $y < \bar{y}$ the curve is disconnected. For $y = \bar{y} = 97$ the two parts of the curve coalesce at their north poles. For $y > \bar{y}$ the curve is connected.

TABLE 1
Threshold of anomalous switching

C	\bar{y}	y_{th}	$ y - y_{\text{th}} /y_{\text{th}}$
1000	748	790	5.3×10^{-2}
2000	1551	1610	3.6×10^{-2}
4000	3219	3250	9.5×10^{-3}

reached for $x(0) = 0$. For $y = \bar{y}$ the two parts touch each other, so that the curve becomes connected (and remains connected for $y > \bar{y}$). This means that for $y \geq \bar{y}$ the intensity can reach large values even though it vanishes initially.

We now argue that the transition point \bar{y} , obtained from eq. (68), can be substantially identified with the anomalous threshold y_{th} of eq. (62). For definiteness, let us take $\Delta = 60$ and $\theta = 1$. In table 1 we compare for various values of C the value \bar{y} , for which the curve (71) becomes connected, to the threshold y_{th} of anomalous switching obtained by numerically solving eq. (62). Clearly the agreement between \bar{y} and y_{th} is excellent for $C \gtrsim 500$. In LUGIATO, MILANI and MEYSTRE [1982] one finds a simple graphical procedure to determine \bar{y} , and hence, y_{th} .

The anomalous switching is caused by the fact that for $y = y_{\text{th}}$ the trajectory in the phase plane, which starts from the origin, "hits" the unstable stationary solution of eq. (62). Hence, the trajectory is "scattered" by the unstable state, which is a repeller, towards larger intensity regions. The orbit for $y = y_{\text{th}}$, which starts from the origin, is covered in an infinite time because it contains a stationary state. Hence, when approaching the anomalous threshold one again finds a "critical slowing down" effect, similar to that found in the previous subsection. The same behavior occurs in eq. (68) for $y = \bar{y}$. In fact, the point P , in correspondence to which the two parts of the orbit touch each other (Fig. 13), is just the unstable stationary solution of eq. (68).

Finally, it is interesting to observe that if we perform the cubic approximation

$$\frac{1}{1 + \Delta^2 + |x|^2} \approx \frac{1}{1 + \Delta^2} \left(1 - \frac{|x|^2}{1 + \Delta^2} \right)$$

eq. (68) becomes formally identical to the time evolution equation discussed in the context of the one-electron theory of the free electron laser formulated in BONIFACIO, CASAGRANDE and LUGIATO [1981].

2.4. INSTABILITIES IN OPTICAL BISTABILITY

The search for instabilities is the crucial point in the study of cooperative phenomena in an open system far from thermodynamic equilibrium (HAKEN [1977], NICOLIS and PRIGOGINE [1977]). In fact, let us consider in general a parameter γ that measures the strength of the interaction of an open system with the external world (in our case γ is the incident field amplitude). When γ is small, the system is in a steady state which is the direct continuation of the thermodynamic equilibrium state (quasi-equilibrium state). On the other hand, when γ increases, the system becomes more and more unbalanced. In correspondence to a suitable threshold value γ_c (in our case γ_M in Fig. 8), the quasi-equilibrium state becomes unstable, and the system can show, roughly speaking, three different types of behavior:

- a) It can perform a transition to a new steady state (in our case, the higher transmission branch). If this new state arises in a continuous way (or, as one usually says in the jargon of instability theory, “bifurcates”) from the quasi-equilibrium state, the behavior is analogous to second-order phase transitions in equilibrium systems. Otherwise one has an analogy with first-order phase transitions, and one usually finds bistability and hysteresis.
- b) It can approach a nonstationary situation, that is, one which is periodic in time. In other words, the state of the system in the long time limit is not represented by a fixed point in the phase space (steady state), but by a limit cycle. In this case the system shows a pulsing behavior, or more precisely a “self-pulsing” behavior, because it does not arise from external manipulation but is spontaneously generated by the self-organization of the system.
- c) It can approach a nonperiodic behavior that does not exhibit any kind of regularity in time, so that it is called *chaotic*.

These three types of transition can also appear in succession when γ is varied, as a result of successive bifurcations.

In the following subsections we shall show that in optical bistability we find not only a behavior of type a), but also self-pulsing and chaotic behavior.

With the exception of § 2.4.4, we shall always consider the situation (44), and furthermore we shall assume the good quality cavity condition $k \ll \gamma_{\perp}, \gamma_{\parallel}$. Therefore, we start from eqs. (49). First, we consider a stationary solution $F_{st} = x_{st}, \tilde{P}_{st}, \tilde{D}_{st}$, and introduce the deviations from steady state

$$\begin{aligned} F(z, t') &= x_{st} + \delta F(z, t'), \\ \tilde{P}(z, t') &= \tilde{P}_{st} + \delta P(z, t'), \\ \tilde{D}(z, t') &= \tilde{D}_{st} + \delta D(z, t'). \end{aligned} \tag{72}$$

In the following analysis of instabilities in optical bistability, we shall always write x instead of x_{st} . By inserting eqs. (72) into (49) we obtain the following equations for the deviations

$$\frac{\partial \delta F}{\partial t'} + c \frac{L}{\mathcal{L}} \frac{\partial \delta F}{\partial z} = -k[(1 + i\theta)\delta F + 2C\delta P], \quad (73a)$$

$$\frac{\partial \delta P}{\partial t'} = \gamma_{\perp}[x\delta D + \tilde{D}_{\text{st}}\delta F - (1 + iA)\delta P] + \gamma_{\perp}\delta F \cdot \delta D, \quad (73b)$$

$$\frac{\partial \delta D}{\partial t'} = -\gamma_{\parallel}[\frac{1}{2}(x\delta P^* + x^*\delta P + \tilde{P}_{\text{st}}^*\delta F + \tilde{P}_{\text{st}}\delta F^*) + \delta D]$$

$$-\frac{\gamma_{\parallel}}{2}(\delta F\delta P^* + \delta F^*\delta P). \quad (73c)$$

The equations for δF and δP^* are the complex conjugates of eqs. (73a) and (73b), respectively.

2.4.1. Linear stability analysis: eigenvalues of the linearized problem

When the deviations δF , etc., are small, we can neglect the nonlinear terms in eqs. (73). Thus we obtain a linear set of equations, which are the basis of the stability analysis of the system. We recall that this linear stability analysis has a local character. A global type of stability analysis will be considered in the quantum statistical treatment (see § 3.5).

Let us now consider the five-component vector

$$\mathbf{q}(z, t') = \begin{pmatrix} \delta F(z, t') \\ \delta F^*(z, t') \\ \delta P(z, t') \\ \delta P^*(z, t') \\ \delta D(z, t') \end{pmatrix}. \quad (74)$$

Next, we introduce the ansatz

$$\mathbf{q}(z, t') = \exp(\lambda t' + ik_n z) \mathbf{q}^0, \quad (75)$$

where λ is a complex number and k_n is defined by eq. (53), and we insert eq. (75) into the linearized equations. We obtain the eigenvalue equation

$$\hat{\mathcal{L}}_n \mathbf{q}^0 = \lambda \mathbf{q}^0, \quad (76)$$

where $\hat{\mathcal{L}}_n$ is the matrix

$$\hat{\mathcal{L}}_n = \begin{pmatrix} -k(1 + i\theta + i\alpha_n) & 0 & -2Ck & 0 & 0 \\ 0 & -k(1 - i\theta + i\alpha_n) & 0 & -2Ck & 0 \\ \gamma_{\perp} \tilde{D}_{st} & 0 & -\gamma_{\perp}(1 + i\Delta) & 0 & \gamma_{\perp}x \\ 0 & \gamma_{\perp} \tilde{P}_{st} & 0 & -\gamma_{\perp}(1 - i\Delta) & \gamma_{\perp}x^* \\ -\frac{\gamma_{\parallel}}{2} \tilde{P}_{st}^* & -\frac{\gamma_{\parallel}}{2} \tilde{P}_{st} & -\frac{\gamma_{\parallel}}{2} x^* & -\frac{\gamma_{\parallel}}{2} x & -\gamma_{\parallel} \end{pmatrix}, \quad (77)$$

and α_n is defined by eq. (51). The characteristic equation $\det(\hat{\mathcal{L}}_n - \lambda) = 0$ has five roots. Hence, the eigenvalues λ_{nj} are labeled by two indices, the frequency index $n = 0, \pm 1, \dots$ and the index $j = 1, \dots, 5$. In particular, $n = 0$ corresponds to the resonant frequency. The steady state is stable if, and only if, $\operatorname{Re} \lambda_{nj} \leq 0$ for all n and j . It is easy to solve the characteristic equation to lowest order in the ratios k/γ_{\perp} , k/γ_{\parallel} . After substituting the expressions (50) of \tilde{P}_{st} and \tilde{D}_{st} , one obtains (LUGIATO [1980a])

$$\begin{aligned} \lambda_{n1} &= -i\alpha_n + k \left\{ \lambda_n^{(+)} + O\left(\frac{k}{\gamma_{\perp}}, \frac{k}{\gamma_{\parallel}}\right) \right\}, \\ \lambda_{n4} &= -i\alpha_n + k \left\{ \lambda_n^{(-)} + O\left(\frac{k}{\gamma_{\perp}}, \frac{k}{\gamma_{\parallel}}\right) \right\}, \end{aligned} \quad (78)$$

where

$$\lambda_n^{(\pm)} = -1 - \{[(1 - i\tilde{\alpha}_n)^2 + \Delta^2](\bar{d} - i\tilde{\alpha}_n) + \bar{d}X(1 - i\tilde{\alpha}_n)\}^{-1}$$

$$\times \frac{2C(1 + \Delta^2)}{1 + \Delta^2 + X} \left[-\tilde{\alpha}_n^2 - i\tilde{\alpha}_n \left(1 + \bar{d} - \frac{1}{2} \frac{\bar{d}X}{1 + \Delta^2} \right) + \bar{d} \right] \pm \mathcal{H}^{1/2}, \quad (79)$$

with

$$\tilde{\alpha}_n = \alpha_n/\gamma_{\perp}, \quad \bar{d} = \gamma_{\parallel}/\gamma_{\perp}, \quad (80)$$

$$\begin{aligned}
\mathcal{H} = & -\theta^2 + \{(1 - i\tilde{\alpha}_n)^2 + \Delta^2](\bar{d} - i\tilde{\alpha}_n) + \bar{d}X(1 - i\tilde{\alpha}_n)\}^{-2} \\
& \times \left\{ \left[\frac{2C(1 + \Delta^2)}{1 + \Delta^2 + X} \right]^2 \left\{ \tilde{\alpha}_n^2 \left[\Delta^2 \left(1 + \frac{\bar{d}X}{1 + \Delta^2} \right) - \left(\frac{1}{2} \frac{\bar{d}X}{1 + \Delta^2} \right)^2 \right] \right. \right. \\
& + i\bar{d}\tilde{\alpha}_n \left(2\Delta^2 + \bar{d}X \frac{\Delta^2 - X}{1 + \Delta^2} \right) + \bar{d}^2\Delta^2 \left(\frac{X}{1 + \Delta^2} - 1 \right) + \bar{d}^2 \frac{X(X - \Delta^2)}{1 + \Delta^2} \Big\} \\
& + 2C\theta\Delta \frac{1 + \Delta^2}{1 + \Delta^2 + X} \left\{ \tilde{\alpha}_n^4 \left(2 + \frac{\bar{d}X}{1 + \Delta^2} \right) \right. \\
& + i\tilde{\alpha}_n^3 \left[2\bar{d} + \left(2 + \frac{\bar{d}X}{1 + \Delta^2} \right) (\bar{d} + 2) \right] \\
& - \tilde{\alpha}_n^2 \left[2\bar{d}(\bar{d} + 2) + \left(2 + \frac{\bar{d}X}{1 + \Delta^2} \right) (2\bar{d} + 1 + \Delta^2 + \bar{d}X) \right] \\
& - i\tilde{\alpha}_n \left[4\bar{d}^2 + 2\bar{d}(1 + \Delta^2) + 2\bar{d}^2X + \bar{d} \left(2 + \frac{\bar{d}X}{1 + \Delta^2} \right) (1 + \Delta^2 + X) \right] \\
& \left. \left. + 2\bar{d}^2(1 + \Delta^2 + X) \right\} . \right. \tag{81}
\end{aligned}$$

On the other hand, for $j = 2, 3$, and 5 we have

$$\lambda_{nj} = \lambda_{nj}^{(0)} \left[1 + O \left(\frac{k}{\gamma_{\perp}}, \frac{k}{\gamma_{\parallel}} \right) \right], \tag{78'}$$

where $\lambda_{nj}^{(0)}$ are the solutions of the cubic equation

$$[(\lambda + \gamma_{\perp})^2 + \gamma_{\perp}^2 \Delta^2](\lambda + \gamma_{\parallel}) + \gamma_{\perp} \gamma_{\parallel} X(\lambda + \gamma_{\perp}) = 0, \tag{82}$$

such that, for $\Delta = 0$,

$$\begin{aligned}
\lambda_{n3}^{(0)} = & -\frac{1}{2} \{ \gamma_{\perp} + \gamma_{\parallel} \pm [(\gamma_{\perp} - \gamma_{\parallel})^{1/2} - 4\gamma_{\perp}\gamma_{\parallel}X]^{1/2} \}, \\
\lambda_{n5}^{(0)} = & -\gamma_{\perp}. \tag{83}
\end{aligned}$$

For $\Delta = \theta = 0$ the expression for $\lambda_n^{(\pm)}$ simplifies as follows

$$\lambda_n^{(+)} = -1 - \frac{2C}{1 + x^2} \frac{\bar{d}(1 - x^2) - i\tilde{\alpha}_n}{(1 - i\tilde{\alpha}_n)(\bar{d} - i\tilde{\alpha}_n) + \bar{d}x^2}, \tag{84a}$$

$$\lambda_n^{(-)} = -1 - \frac{2C}{1 + x^2} \frac{1}{1 - i\tilde{\alpha}_n}. \tag{84b}$$

2.4.2. Instability conditions

Clearly, the real part of λ_{n2} , λ_{n3} and λ_{n5} is always negative. On the contrary, under suitable conditions one finds that $\operatorname{Re} \lambda_{n1} > 0$ or $\operatorname{Re} \lambda_{n4} > 0$, or both for some n , so that the steady state is unstable. Hence, the *instability condition* is

$$\operatorname{Re} \lambda_{n1}^{(+)} > 0 \quad \text{and/or} \quad \operatorname{Re} \lambda_{n4}^{(-)} > 0. \quad (85)$$

Let us first consider the case $n = 0$, that is the resonant mode. The eigenvalues λ_{0j} coincide with the constants λ_i discussed in § 2.3.1. In fact, in the mean field theory, we consider only the resonant mode. Using eqs. (79–81) we can easily verify that λ_{01} and λ_{04} coincide with the two solutions of eq. (57), which was derived in the good cavity limit. For $dY/dX > 0$ both solutions of eq. (57) have negative real part. Instead, when $dY/dX < 0$, the eigenvalue λ_{01} has positive real part. This proves what we anticipated, that is, that the part of the curve $X(Y)$ with negative slope is unstable. In fact, in correspondence to these stationary solutions the resonant frequency is unstable.

Next, let us consider the off-resonant frequencies $n \neq 0$. First, we analyze the case $\Delta = \theta = 0$ in which $\lambda_n^{(\pm)}$ are given by eq. (84). From eq. (84b) we see that, in this situation, $\operatorname{Re} \lambda_n^{(-)} < 0$ for all n . On the other hand, the analysis of the instability condition $\operatorname{Re} \lambda_n^{(+)} > 0$ leads to a biquadratic equation, the discussion of which yields the following conclusions (BONIFACIO and LUGIATO (1978b]): The stationary state is unstable when the following two conditions are simultaneously satisfied:

$$\begin{aligned} \bar{R} &\geq 0, \quad \bar{S} + \bar{R}^{1/2} \geq 0, \\ \bar{R} &= \gamma_\perp^2 \gamma_\parallel^2 x^4 \left(1 - \frac{y}{x}\right)^2 + \left(\gamma_\parallel^2 - \gamma_\perp^2 \frac{y}{x}\right)^2 \\ &\quad - 2\gamma_\perp \gamma_\parallel x^2 \left[3\gamma_\parallel^2 + 4\gamma_\perp \gamma_\parallel + \frac{y}{x}(3\gamma_\perp^2 - \gamma_\parallel^2) + \gamma_\perp^2 \frac{y^2}{x^2}\right], \\ \bar{S} &= \gamma_\parallel(3\gamma_\perp x^2 - \gamma_\parallel) - \frac{y}{x} \gamma_\perp (\gamma_\perp + \gamma_\parallel x^2), \end{aligned} \quad (86)$$

provided that at least one of the discrete values α_n lies in the interval $\alpha_{\min} < \alpha_n < \alpha_{\max}$, where

$$\alpha_{\frac{\max}{\min}} = \frac{1}{\sqrt{2}} (\bar{S} \pm \sqrt{\bar{R}})^{1/2}. \quad (87)$$

Under suitable conditions it happens that, in correspondence to a part of the plot $x(y)$ with positive slope, some off-resonance frequencies are unstable. The unstable frequencies are those such that $\alpha_{\min} < |\alpha_n| < \alpha_{\max}$. As $\lambda_{-n}^{(+)} = (\lambda_n^{(+)})^*$, the frequencies become unstable in pairs, symmetrically with respect to the resonant frequency.

For the sake of definiteness, let us analyze the case $\gamma_{\perp} = \gamma_{\parallel} \equiv \gamma$. The resulting picture is as follows:

1) For $C < 2(1 + \sqrt{2})$ all the points of the plot $x = x(y)$, which lie on the part with positive slope, are stable.

2) For $C > 2(1 + \sqrt{2})$ the points in the one-atom branch (high transmission branch), such that $x < C/2$ (see Fig. 14), are unstable provided that at least one of the discrete values α_n lies in the range $\alpha_{\min}(x) < \alpha_n < \alpha_{\max}(x)$, where (see Fig. 15)

$$\alpha_{\max_{\min}}(x) = \gamma[x^2 - C - 1 \pm (C^2 - 4x^2)^{1/2}]^{1/2}. \quad (88)$$

On the contrary, for $\gamma_{\parallel} \ll \gamma_{\perp}$ (strong elastic collisions) no positive slope instability arises.

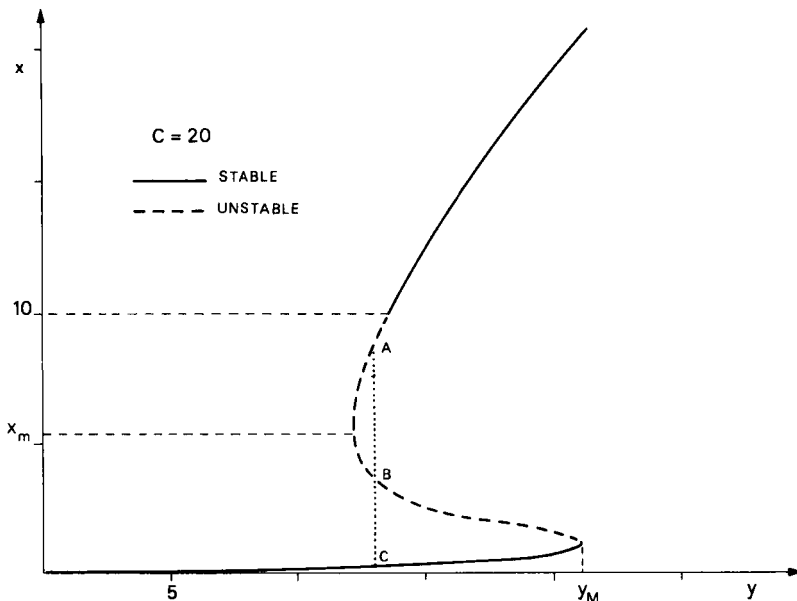


Fig. 14. Purely absorptive bistability S-curve with indication of the stable and unstable states for $\alpha L \rightarrow 0, T \rightarrow 0, C = \alpha L/2T = 20, \gamma_{\perp} = \gamma_{\parallel} = \gamma$. In the broken-line segment of the part with positive slope, the points are unstable, provided that at least one cavity frequency α_n lies in the range $\alpha_{\min}(x) < \alpha_n < \alpha_{\max}(x)$, where $\alpha_{\min}(x)$ and $\alpha_{\max}(x)$ are shown in Fig. 15.

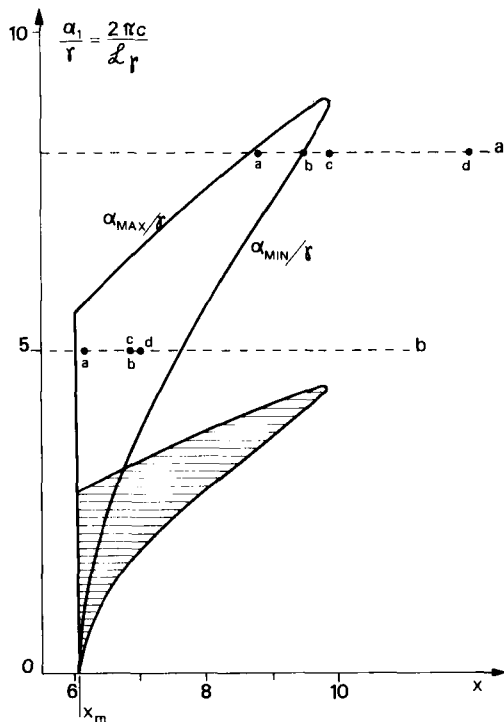


Fig. 15. Instability region in the plane of the variables x and α_1/γ for $\alpha L \rightarrow 0$, $T \rightarrow 0$, $C = \alpha L/2T = 20$, $\gamma_{\perp} = \gamma_{\parallel} = \gamma$. x is the normalized transmitted field in the high transmission branch, $\alpha_1 = 2\pi c/\mathcal{L}$ is the difference between the frequencies of the adjacent mode and of the resonant mode. The curves $\alpha_{\max}(x)$, $\alpha_{\min}(x)$ obey eq. (88). The shaded region indicates the points in correspondence to which the frequencies $n = \pm 2$ are unstable. The points on the lines a and b indicate the values of α_1/γ and x in correspondence to Figs. 19a-d and 21a-d respectively.

Let us now consider the general case $\Delta, \theta \neq 0$. In this case, both $\operatorname{Re} \lambda_n^{(+)}$ and $\operatorname{Re} \lambda_n^{(-)}$ can become positive. For $\gamma_{\perp} = \gamma_{\parallel} = \gamma$ (i.e. $\bar{d} = 1$), we draw the following conclusions (LUGIATO [1980a]):

- When θ is at most of order unity and $\Delta \gg 1$, the instability domain in the part of the curve $X = X(y)$ with positive slope practically vanishes. Note from eq. (40) that this is precisely the situation of purely dispersive optical bistability. This might explain why self-pulsing instabilities have never been observed in the experiments on dispersive optical bistability.
- When $\Delta \lesssim 1$, $\theta > 1$ and C is large enough, part of the high transmission branch is unstable. The interesting feature is that the instability domain can be much larger than the bistability domain, or even can exist in the absence of

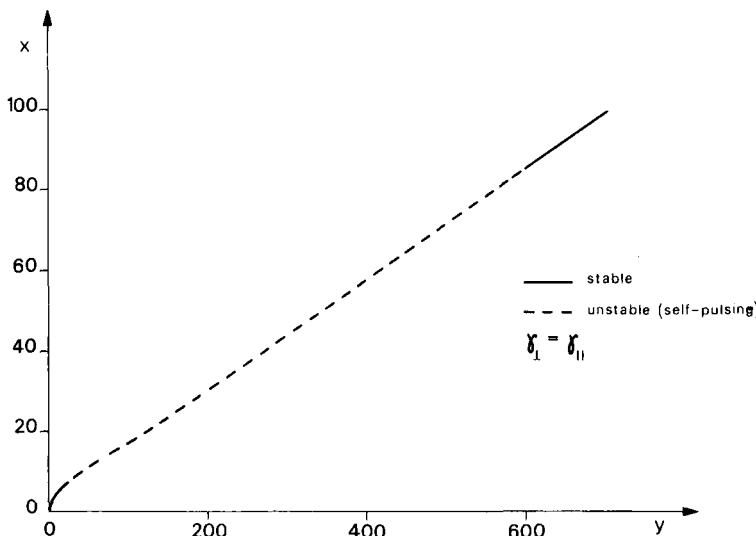


Fig. 16. Dispersive case. Stable and unstable stationary states in the limit $\alpha L \rightarrow 0, T \rightarrow 0$, with $C = \alpha L/2T = 30$, $\gamma_{\perp} = \gamma_{\parallel} = \gamma$. One has $\Delta = \theta = 7$. $x = \sqrt{X}$ and $y = \sqrt{Y}$ are the normalized transmitted and incident field amplitudes respectively.

bistability. Note that this instability occurs also for $\Delta = 0$ but $\theta \neq 0$. In this case the situation is purely absorptive.

c) For $\theta \approx \Delta > 1$ and C large enough, the instability domain turns out to be quite extended (Fig. 16).

The stability analysis in the case of a Fabry-Pérot cavity has been performed in CASAGRANDE, LUGIATO and ASQUINI [1980]. (See also SARGENT [1980]).

2.4.3. Self-pulsing and precipitation

At this point, one asks what happens when the stationary state in the higher transmission branch becomes unstable. The most straightforward procedure to answer this question is offered by computer solutions of the Maxwell-Bloch equations (1) (BONIFACIO, GRONCHI and LUGIATO [1979b], GRONCHI, BENZA, LUGIATO, MEYSTRE and SARGENT [1981]). One finds that the system either precipitates to the lower transmission state, which corresponds to the same value of the incident field, or approaches a self-pulsing behavior. These two types of behavior are shown in Fig. 17, which exhibits the envelope of the time evolution of the transmitted field, that oscillates between the upper and the lower envelope. The initial condition of the evolution shown in Fig. 17 is such that the system is slightly displaced from the unstable steady state in the

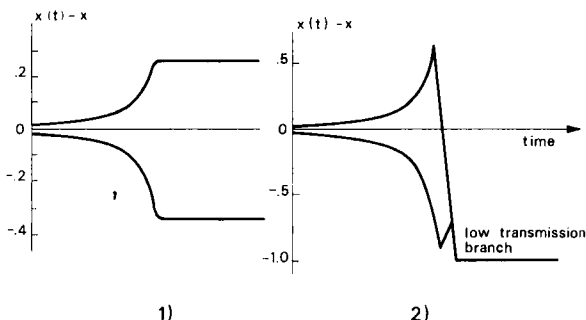


Fig. 17. Envelope of the time evolution of the transmitted field for $C = 20$, $\gamma_{\perp} = \gamma_{\parallel} = \gamma$, $\mathcal{L} = 5L$, $T = 0.1$, obtained by numerically solving the Maxwell-Bloch equations. The transmitted field oscillates between the upper and the lower envelope with a period roughly equal to the cavity transit time \mathcal{L}/c . (1) $x = 9$, $\alpha_1/\gamma = 8$. In the long-time limit, the system approaches a steady self-pulsing regime in which the envelope is perfectly flat. (2) $x = 6.15$, $\alpha_1/\gamma = 3.6$. For long times, the oscillations vanish and the system precipitates to the low transmission branch.

higher transmission branch. The oscillations are first exponentially amplified, during the stage of the time evolution that is governed by the linearized equations. In the case of Fig. 17.2, the oscillations finally vanish because the system precipitates to the lower transmission branch. In the case of Fig. 17.1, in due time the system approaches a regular self-pulsing regime, in which the transmitted light is given by a periodic sequence of short pulses, with a period on the order of the cavity transit time \mathcal{L}/c . The shape of the pulses depends on the number of unstable modes. When only the two modes adjacent to the resonant one are unstable the pulses are sinusoidal. This behavior is interesting also from the practical viewpoint, because it suggests an *all-optical device to convert cw light into pulsed light*.

Another type of converter, based on a completely different mechanism, was suggested by MCCALL [1978], who showed that a bistable device can pulsate when the nonlinearity has two contributions of opposite sign and different time constants. In the same paper the author reports the observation of this behavior in a hybrid electro-optical device, and suggests that the same phenomenon can be observed in an intrinsic all-optical bistable system in which switching is due to a fast electronic effect, but a slower thermal effect prevents either state from being stable. Observation of this behavior in a micron-sized GaAs etalon at 80 K has been recently reported (JEWELL, GIBBS, TARNG, GOSSARD and WIEGMANN [1982]). In this system, the period of the pulsations is of the order of several microseconds, whereas in the self-pulsing behavior we described before the period is of the order of nanoseconds.

Note that the self-pulsing behavior that we find in optical bistability has a completely different character from the so-called passive Q -switching that one finds in lasers with saturable absorbers (see for instance POWELL and WOLGA [1971]). In fact, passive Q -switching is a single-mode phenomenon, in which the field remains uniform in the cavity. On the contrary, self-pulsing in optical bistability is a many-mode phenomenon, because the frequencies which become unstable are different from the resonant frequency. In this case, there is a pulse which propagates in the cavity. On the other hand, the pulsed behavior in optical bistability is quite analogous to the self-pulsing in ring lasers beyond the so-called second threshold, predicted by RISKEN and NUMMEDAL [1968], and GRAHAM and HAKEN [1968].

In order to understand the mechanism which underlies the self-pulsing behavior, let us come back to the equations for the mode amplitudes (54) and let us make the following steps:

- We consider the case $\theta = \Delta = 0$.
- We perform the transformation of variables

$$\bar{f}_n(t') = \exp(i\alpha_n t') f_n(t'), \quad \bar{p}_n(t') = \exp(i\alpha_n t') p_n(t'), \quad (89)$$

- We take into account that $\gamma_{\perp}, \gamma_{\parallel} \gg k$, and therefore we adiabatically eliminate (see § 2.3.2) the atomic variables, by setting $\dot{\bar{p}}_n = \dot{\bar{d}}_n = 0$.
- We subdivide \bar{f}_0 into steady value and deviation: $\bar{f}_0 = x + \delta f_0$. Remember in this connection that for $n \neq 0$ the amplitudes f_n vanish at steady state.
- We subdivide \bar{f}_n for $n \neq 0$ into real and imaginary parts:

$$\bar{f}_n(t') = f'_n(t') + i f''_n(t'). \quad (90)$$

As a consequence, we obtain the following equations for the *off-resonant* modes $n \neq 0$:

$$\begin{aligned} \dot{f}'_n &= k \lambda_n^{(+)} f'_n + \text{nonlinear terms}, \\ \dot{f}''_n &= k \lambda_n^{(-)} f''_n + \text{nonlinear terms}. \end{aligned} \quad (91)$$

When $\operatorname{Re} \lambda_n^{(+)} > 0$ the n th mode experiences amplification and the steady state is unstable. Now, using eq. (84a), $k \operatorname{Re} \lambda_n^{(+)}$ can be rewritten as

$$\begin{aligned} k \operatorname{Re} \lambda_n^{(+)} &= \mathcal{G}_n - k, \\ \mathcal{G}_n &= \frac{2Ck}{1+x^2} \frac{\bar{d}(1-x^2)[\bar{d}(1+x^2) - \tilde{\alpha}_n^2] + \tilde{\alpha}_n^2(1+\bar{d})}{[\bar{d}(1+x^2) - \tilde{\alpha}_n^2]^2 + \tilde{\alpha}_n^2(1+\bar{d})^2}. \end{aligned} \quad (92)$$

When \mathcal{G}_n is positive, eq. (92) is a gain-minus-loss form. The instability arises when, for at least one off-resonant mode, the gain exceeds the loss k . Note that,

contrary to the loss term which is the same as for the usual laser, the gain which produces the off-resonance frequency buildup is quite different from the gain of the laser. In fact, in the laser the gain arises from population inversion. In the case of optical bistability, we deal with a purely passive system with negative population inversion. The gain in optical bistability requires the presence in the medium of a mode with a large amplitude (the resonant mode, which arises from the incident field). Via mode-mode interaction, the resonant mode induces gain for the side-modes. Hence, with respect to the unstable modes the system works as a novel type of laser without population inversion (GRONCHI, BENZA, LUGIATO, MEYSTRE and SARGENT [1981]). It is important to observe that \mathcal{G}_n coincides with the gain one finds in saturation spectroscopy (see SARGENT [1978]), that is with the gain experienced by a weak probe field traveling through an atomic passive medium, saturated by a strong field detuned from the probe field. \mathcal{G}_n also coincides with the differential gain of McCall [1974].

We also note that, as one sees from eq. (91), in order to allow the unstable modes to build up it is necessary that at least one of these modes has a nonvanishing initial amplitude. Hence, at least a small initial inhomogeneity of the field is necessary to trigger the instability. Fluctuations can easily achieve this goal.

Let us now consider, still for $\Delta = \theta = 0$, the case that only the two frequencies immediately and symmetrically adjacent to the resonant frequency are unstable. In the steady self-pulsing regime, the field inside the cavity is described to excellent approximation by an expression of the type

$$F(z, t') = x + A \cos \left[\alpha_1 \left(t' - \frac{z\mathcal{L}}{cL} \right) + \psi_0 \right], \quad (93)$$

where the phase ψ_0 depends on the initial conditions. Hence, using the relation of the electric field \mathcal{E} with its envelope E ,

$$\mathcal{E}(z, t) = E(z, t) \exp \left[-i\omega_0 \left(t - \frac{z}{c} \right) \right] + \text{c.c.}$$

and taking into account eqs. (9) and (47), and the relation $\Delta t = (\mathcal{L} - L)/c$, we obtain

$$\mathcal{E}(z, t) = \bar{E} \cos \left[\omega_0 \left(t - \frac{z}{c} \right) \right]$$

$$\begin{aligned}
 & + \mathcal{A} \left\{ \cos \left[(\omega_0 + \alpha_1) \left(t - \frac{z}{c} \right) + \psi_0 \right] \right. \\
 & \left. + \cos \left[(\omega_0 - \alpha_1) \left(t - \frac{z}{c} \right) - \psi_0 \right] \right\}, \tag{94}
 \end{aligned}$$

where we have introduced the symbols \bar{E} , \mathcal{A} with obvious meaning. Hence, part of the incident light is transferred from the resonant mode, of frequency ω_0 , to the adjacent modes, of frequencies $\omega_0 \pm \alpha_1$, which experience gain and build up. This gives rise to the undamped spiking behavior.

When the system is in the instability region, the dynamics involve a competition between the resonant mode and the unstable modes: when the unstable modes prevail the system approaches the self-pulsing regime; when the resonant mode dominates the dynamics, the system precipitates to the low transmission branch.

2.4.4. Case of αL large. Chaotic self-pulsing

Up to now, in studying the stability of the steady states, we have always assumed that αL is small. In this subsection, we shall drop assumption (44). Actually, the first paper which predicted a positive slope instability (BONIFACIO and LUGIATO [1978b]) treated the case of absorptive optical bistability for general values of αL and T . GRONCHI, BENZA, LUGIATO, MEYSTRE and SARGENT [1981] analyze the effects of increasing αL and T on the self-pulsing behavior in absorptive optical bistability.

In this subsection, we shall treat the absorptive + dispersive case. We start from the general Maxwell–Bloch equations (1), linearized around steady state. From eq. (3b), and taking into account the fact that the steady state field $E_{st}(z)$ obeys the boundary condition (3b) itself, we have that the boundary condition for the deviation $\delta E(z, t)$ from steady state is

$$\delta E(0, t) = R \exp(-i\delta_0) \delta E(L, t - \Delta t). \tag{95}$$

The linearized Maxwell–Bloch equations admit solutions of exponential type, namely $\delta E(z, t)$, $\delta P(z, t)$, $\delta D(z, t) \propto \exp(\lambda t)$. By inserting this ansatz into the linearized Maxwell–Bloch equations and using the boundary condition (95), one obtains an equation that determines the eigenvalues. In the limits (44), and $k \ll \gamma_\perp, \gamma_\parallel$ this equation reduces to the one discussed in § 2.4.1.

For the sake of simplicity, let us now assume that the cavity transit time \mathcal{L}/c

is much longer than all atomic relaxation times, i.e.

$$\gamma_{\perp} \mathcal{L}/c \gg 1, \quad \gamma_{\parallel} \mathcal{L}/c \gg 1. \quad (96)$$

In this situation γ_{\perp} and γ_{\parallel} are much larger than both the real and the imaginary part of many of the relevant eigenvalues λ_{n1} and λ_{n4} . In fact, $\operatorname{Re} \lambda_{n4}$ is proportional to the cavity linewidth $k = cT/\mathcal{L}$, while $\operatorname{Im} \lambda_{n4}$ is on the order of $\alpha_n = 2\pi nc/\mathcal{L}$, $n = 0, \pm 1, \dots$. In the limit

$$\gamma_{\perp} \mathcal{L}/c \rightarrow \infty, \quad \gamma_{\parallel} \mathcal{L}/c \rightarrow \infty, \quad (96')$$

γ_{\perp} and γ_{\parallel} are much larger than both the real and the imaginary parts of *all* the eigenvalues λ_{n1} and λ_{n4} . Hence, in the linearized equations for $\delta P(z, t)$ and $\delta D(z, t)$ one can neglect λ with respect to γ_{\perp} and γ_{\parallel} , which leads to a simplified eigenvalue equation. A more straightforward procedure to derive the same equation is the following: on the basis of assumption (96') we can adiabatically eliminate the atomic variables in the Maxwell–Bloch equations, that is we can set $\partial P/\partial t = \partial D/\partial t = 0$ in eqs. (1b) and (1c). Thus, using the variables ρ_F and φ defined by eq. (14) and by $\rho_F = \mu\rho/\hbar(\gamma_{\perp} \gamma_{\parallel})^{1/2}$, we obtain the equations

$$\frac{\partial \rho_F}{\partial z} + \frac{1}{c} \frac{\partial \rho_F}{\partial t} = -\alpha \frac{\rho_F}{1 + \Delta^2 + \rho_F^2}, \quad (97a)$$

$$\frac{\partial \varphi}{\partial z} + \frac{1}{c} \frac{\partial \varphi}{\partial t} = \frac{\alpha \Delta}{1 + \Delta^2 + \rho_F^2}. \quad (97b)$$

Next, we linearize these equations around the steady state. By setting

$$\delta\rho_F(z, t) = \rho_F(z, t) - \rho_{F, \text{st}}(z), \quad \delta\varphi(z, t) = \varphi(z, t) - \varphi_{\text{st}}(z)$$

we have

$$\frac{\partial \delta\rho_F}{\partial z} + \frac{1}{c} \frac{\partial \delta\rho_F}{\partial t} = -\alpha \frac{1 + \Delta^2 - \rho_{F, \text{st}}^2(z)}{[1 + \Delta^2 + \rho_{F, \text{st}}^2(z)]^2} \delta\rho_F, \quad (98a)$$

$$\frac{\partial \delta\varphi}{\partial z} + \frac{1}{c} \frac{\partial \delta\varphi}{\partial t} = -\alpha \Delta \frac{2\rho_{F, \text{st}}(z)}{[1 + \Delta^2 + \rho_{F, \text{st}}^2(z)]^2} \delta\varphi. \quad (98b)$$

By combining eq. (98b) with the stationary equation

$$\partial \rho_{F, \text{st}} / \partial z = -\alpha \rho_{F, \text{st}}(z) / [1 + \Delta^2 + \rho_{F, \text{st}}^2(z)]$$

(see eqs. (15a), (5), and (6)) and defining $\delta\bar{\varphi}(z, t) = \rho_{F, st}(z) \delta\varphi(z, t)$, we obtain

$$\frac{\partial \delta\bar{\varphi}}{\partial z} + \frac{1}{c} \frac{\partial \delta\bar{\varphi}}{\partial t} = -\frac{\alpha}{1 + \Delta^2 + \rho_{F, st}^2(z)} \delta\bar{\varphi} - \frac{2\alpha\Delta\rho_{st}^2(z)}{[1 + \Delta^2 + \rho_{F, st}^2(z)]^2} \delta\rho_F. \quad (98c)$$

The boundary condition (95) can be rephrased as

$$\delta\rho_F(0, t) = R \left[(\cos \Phi) \delta\rho_F \left(L, t - \frac{\mathcal{L} - L}{c} \right) - (\sin \Phi) \delta\bar{\varphi} \left(L, t - \frac{\mathcal{L} - L}{c} \right) \right], \quad (99a)$$

$$\delta\bar{\varphi}(0, t) = R \left[(\sin \Phi) \delta\rho_F \left(L, t - \frac{\mathcal{L} - L}{c} \right) + (\cos \Phi) \delta\bar{\varphi} \left(L, t - \frac{\mathcal{L} - L}{c} \right) \right], \quad (99b)$$

where

$$\Phi = \varphi_{st}(L) - \varphi_{st}(0) - \delta_0. \quad (100)$$

Two relations which will be useful in the sequel and which follow from eqs. (15), (5), and (6) are

$$\rho_{F, st}(z) = \rho_{F, st}(0) \exp \{ -\bar{\alpha}z\bar{D}_{st}(z) \}, \quad (101a)$$

$$\varphi_{st}(z) - \varphi_{st}(0) = \bar{\alpha}z\Delta\bar{D}_{st}(z), \quad (101b)$$

where $\bar{D}_{st}(z)$ is the space average of the population difference at steady state from 0 to z :

$$\bar{D}_{st}(z) = \frac{1}{z} \int_0^z dz' D_{st}(z') = \frac{1}{z} \int_0^z dz' \frac{1 + \Delta^2}{1 + \Delta^2 + \rho_{F, st}^2(z')}, \quad (102)$$

and $\bar{\alpha} = \alpha/(1 + \Delta^2)$ is the absorption coefficient off resonance. Equation (101a) generalizes the well known Beer absorption law to the case of a nonlinear medium. Note that $\exp[\bar{\alpha}L\bar{D}(L)]$ coincides with the quantity η defined by eq. (17).

From now on, we follow the treatment of BONIFACIO and LUGIATO [1978b]. First, we introduce the ansatz

$$\begin{Bmatrix} \delta\rho_F(z, t) \\ \delta\bar{\varphi}(z, t) \end{Bmatrix} = e^{\lambda t} \begin{Bmatrix} \delta\rho_F(z) \\ \delta\bar{\varphi}(z) \end{Bmatrix} + \text{c.c.} \quad (103)$$

and integrate eqs. (98a) and (98c), obtaining

$$\delta\rho_F(z) = C_1 \exp \left[-\frac{\lambda}{c} z - \bar{\alpha}z \bar{D}_{st}(z) \right] \frac{1 + \Delta^2 + \rho_{F,st}^2(0)}{1 + \Delta^2 + \rho_{F,st}^2(z)}, \quad (104a)$$

$$\delta\bar{\varphi}(z) = \exp \left[-\frac{\lambda}{c} z - \bar{\alpha}z \bar{D}_{st}(z) \right] \left[C_2 + C_1 \Delta \frac{\rho_{F,st}^2(z) - \rho_{F,st}^2(0)}{1 + \Delta^2 + \rho_{F,st}^2(z)} \right], \quad (104b)$$

where C_1 and C_2 are arbitrary constants. Next, we insert eqs. (103) and (104) into eqs. (99a) and (99b), thus obtaining a homogeneous system of two equations for C_1 and C_2 . The condition that this system admits nontrivial solutions gives the simplified eigenvalue equation. By setting

$$v = R \exp \left\{ -\frac{\lambda \mathcal{L}}{c} - \bar{\alpha} L \bar{D}_{st}(L) \right\}, \quad (105a)$$

$$B = \left(\frac{1 + \Delta^2 + \rho_{F,st}^2(0)}{1 + \Delta^2 + \rho_{F,st}^2(L)} \right)^{1/2}, \quad (105b)$$

$$\begin{aligned} \mathcal{S} &= [(1 + \Delta^2 + \rho_{F,st}^2(0))(1 + \Delta^2 + \rho_{F,st}^2(L))]^{-1/2} \\ &\times \left[\frac{\Delta}{2} (\rho_{F,st}^2(0) - \rho_{F,st}^2(L)) \sin \Phi \right. \\ &\left. + \left(1 + \Delta^2 + \frac{\rho_{F,st}^2(0) + \rho_{F,st}^2(L)}{2} \right) \cos \Phi \right], \end{aligned} \quad (105c)$$

the equation reads

$$B v^2 - 2 \mathcal{S} v + B^{-1} = 0. \quad (106)$$

Hence, the eigenvalues are given by

$$\lambda_{n,\pm} = -\frac{c}{\mathcal{L}} \ln \frac{\mathcal{S} \pm (\mathcal{S}^2 - 1)^{1/2}}{BR \exp(-\bar{\alpha} L \bar{D}(L))} + i\alpha_n, \quad n = 0, \pm 1, \dots \quad (107)$$

Using eqs. (100) and (101), the eigenvalues are expressed as functions of $\bar{\alpha}$, Δ , δ_0 , $\rho_{st}^2(0)$ and $\bar{D}_{st}(L)$. From these expressions, one sees (LUGIATO, ASQUINI and NARDUCCI [1982]) that eq. (107) coincides with the expression of the eigenvalues given in SNAPP, CARMICHAEL and SCHIEVE [1981] and CARMICHAEL, SNAPP and SCHIEVE [1982] obtained from the treatment of optical bistability in a ring cavity given by IKEDA [1979]. In fact, roughly one

year after the work of BONIFACIO and LUGIATO [1978a,b] on the absorptive case, Ikeda reconsidered the same model but in the general absorptive and dispersive case. By adiabatically eliminating the atomic polarization and population difference under conditions (96'), he transformed the Maxwell–Bloch equations with boundary conditions into a system of finite difference equations, with a time step equal to the cavity transit time. By linearization of the system, we obtain the eigenvalues (107). Note that all the eigenvalues λ_{n+} have the same real part and the same holds for the eigenvalues λ_{n-} . Hence, all the frequencies become simultaneously unstable when $\operatorname{Re} \lambda_{n\pm} > 0$. This is a consequence of the limit (96'). On the other hand, if one does not perform the limit (96'), only a finite set of frequencies become unstable as we have seen in § 2.4.1.

From eq. (107), one has that the steady state is unstable when

$$2\bar{B}|\mathcal{S}| > 1 + \bar{B}^2, \quad \bar{B} = BR \exp[-\bar{\alpha}L\bar{D}(L)] \quad (108)$$

For $\mathcal{S} > 0$ the condition $2\bar{B}\mathcal{S} > 1 + \bar{B}^2$ is equivalent to the condition $dY/dX < 0$, as one easily verifies using eqs. (22), (25) and (17). On the other hand, for $\mathcal{S} < 0$ the condition $2\bar{B}\mathcal{S} < -(1 + \bar{B}^2)$, which can be satisfied only for Δ and θ different from zero, leads to instabilities in the parts of the curve $X(Y)$ with positive slope. Under suitable conditions (IKEDA [1979]) several segments of the curve $X(Y)$ are unstable, and one can find ranges of values of the incident intensity in correspondence to which no stable steady state exists. In this situation the system shows a self-pulsing behavior, which can be either a regular self-pulsing with a period roughly equal to an even multiple of the cavity transit time and square-wave type pulses (Fig. 18b), or a *chaotic self-pulsing* (Fig. 18c). As it has been shown in SNAPP, CARMICHAEL and SCHIEVE [1981], this period doubling bifurcation behavior, which finally leads to chaos, is in agreement with the general theory of nonlinear maps developed by FEIGENBAUM [1978, 1979]. Following the suggestions of IKEDA, DAIDO and AKIMOTO [1980], GIBBS, HOPF, KAPLAN and SHOEMAKER [1981] built a hybrid electro-optical device which reproduced this type of behavior (Fig. 18, see also OKADA and TAKIZAWA [1981]). The problem of the possibility of instabilities of this type has been studied in FIRTH [1981] and ABRAHAM, FIRTH and WRIGHT [1982] for Fabry–Perot cavities and by WINFUL and COOPERMAN [1982] for distributed feedback bistable optical devices. KITANO, YABUZAKI and OGAWA [1981b] predicted a magnetically induced self-pulsing in optical tristability.

Since the instability predicted in BONIFACIO and LUGIATO [1978b] was derived in a context of differential equations, whereas the instability found in

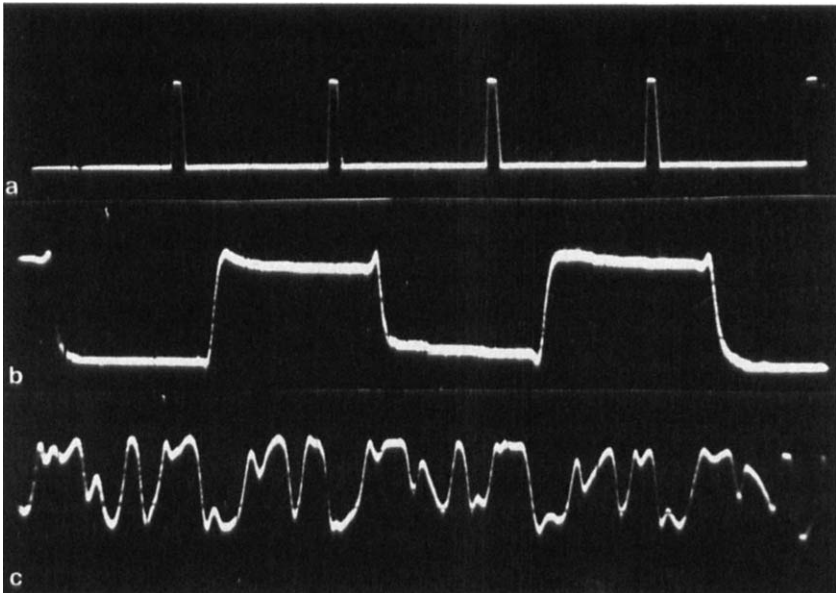


Fig. 18. Observation of chaotic behavior in a hybrid device (from GIBBS, HOPF, KAPLAN and SHOEMAKER [1981]). (a) Time calibration; one pulse every cavity transit time, equal to 40 ms. (b) Output intensity versus time in the periodic domain. (c) Intensity versus time in the chaotic regime.

IKEDA [1979] arises in a context of difference equations (nonlinear maps), for a long time the two instabilities have been considered as substantially different matters. The Bonifacio–Lugiato instability was usually considered as associated with absorptive optical bistability, and the Ikeda instability with dispersive optical bistability. However, this is wrong because, as we have shown in § 2.4.1, the Bonifacio–Lugiato instability also arises in the dispersive case. As was first proven in LUGIATO, ASQUINI and NARDUCCI [1982] and we have explicitly reported here, the Ikeda instability is a special case of the Bonifacio–Lugiato instability and it arises precisely in the limit (96'). The fundamental contribution of IKEDA [1979] was the prediction of chaos in optical bistability.

As we have seen in § 2.4.3, in the case when $\alpha L \ll 1$, $T \ll 1$, the fundamental pulsation frequency is α_1 , which corresponds to a period equal to the cavity transit time \mathcal{L}/c . On the other hand, in the Ikeda instability the period is twice the cavity transit time. This feature can be easily understood from eq. (107). In fact, the instability occurs for $\mathcal{S} < -1$ and concerns the eigenvalues λ_{n+} .

Hence, we have

$$\operatorname{Im} \lambda_{n+} = \frac{c}{\mathcal{L}} \pi + \alpha_n = 2\pi \left(2 \frac{\mathcal{L}}{c} \right)^{-1} (1 + 2n),$$

which gives a period $2\mathcal{L}/c$.

The expression (107) of the eigenvalues holds for general values of αL , T and δ_0 , in the limit (96'). Now, let us consider the case (44) which is perfectly compatible with (96'). In this situation the eigenvalues reduce to

$$\lambda_{n,\pm} = -i\alpha_n - k \left\{ 1 + \frac{2C(1 + \Delta^2)}{(1 + \Delta^2 + X)^2} \pm \mathcal{H}^{1/2} \right\}, \quad (109)$$

with

$$\mathcal{H} = \frac{4C(1 + \Delta^2)}{(1 + \Delta^2 + X)^2} \left\{ \frac{X^2 - \Delta^2(1 + \Delta^2)}{(1 + \Delta^2 + X)^2} + C\Delta\theta \right\} - \theta^2. \quad (110)$$

The expressions (109) coincide with those of λ_{n1} , λ_{n4} given by eqs. (78–81) if one introduces the limit (96'), that is if one sets $\tilde{\alpha}_n = \alpha_n/\gamma_\perp = 0$. Hence, the real part of λ_{n+} , λ_{n-} , as given by (109) coincides with $\operatorname{Re} \lambda_{04}$ and $\operatorname{Re} \lambda_{01}$ and therefore, as demonstrated in § 2.4.2, is never positive in the positive slope parts of the graph $X = X(Y)$. This means that the Ikeda instability disappears in the mean field limit (27) and requires αL and T to be large enough. However, as we have shown in § 2.4.1, one can still have a self-pulsing instability if one drops the condition (96).

On the other hand, $\operatorname{Re} \lambda_{n,\pm}$, as given by eq. (109), can be positive when $C < 0$, as in the case of the laser with injected signal (see § 2.1.7). Hence, in this case the Ikeda instability can arise even in the mean field limit (27).

Recently, it has been shown that *chaotic behavior* in dispersive optical bistability can also arise *in the mean field limit* (27) with *single-mode operation*, both for Kerr medium (IKEDA and AKIMOTO [1982]) and in the mean field model (55) when $\gamma_\perp \gg \gamma_\parallel, k$, while k and γ_\parallel have the same order of magnitude (LUGIATO, NARDUCCI, BANDY and PENNISE [1982]). Decreasing the incident field along the high transmission branch, one finds the appearance of regular pulsations that undergo a sequence of period doubling bifurcations, which finally terminates into chaos.

2.4.5. Observability of self-pulsing in all-optical systems

Let us now briefly describe the ideal conditions in which to observe self-pulsing in all-optical systems. First, one must use a ring cavity, because the instability region is strongly reduced in the case of a Fabry–Perot (CASAGRANDE, LUGIATO and ASQUINI [1980]). Second, one should fulfil as closely as possible the plane wave condition, since one cannot exclude the fact that the radial shape of the electric field decreases or destroys the self-pulsing instability region. Third, one must use a homogeneously broadened system, because inhomogeneous broadening drastically reduces the gain \mathcal{G}_n (see eq. (92)) (MC CALL [1974]). Furthermore, the elastic collision broadening should not be large, because otherwise no positive slope instability arises.

The dispersive situation $A, \theta \neq 0$ is preferable because, by playing with parameters, one can obtain the self-pulsing instability without bistability, and therefore one can exclude a priori the possibility of precipitation to the lower branch, which is a competitive process with respect to self-pulsing.

In order to ensure that at least one off-resonance cavity frequency lies in the instability range $\alpha_{\min} < \alpha_n < \alpha_{\max}$, it is necessary that the frequency spacing $2\pi c/\mathcal{L}$ is not larger than the power broadened linewidth $\gamma_{\perp}(1+X)^{1/2}$, because $\alpha_{\max} < \gamma_{\perp}(1+X)^{1/2}$. For $\gamma_{\perp} = \gamma_{\parallel}, X \gg 1$, we have $\gamma_{\perp}(1+X)^{1/2} \approx \gamma_{\perp}x = \Omega_r$, where Ω_r is the Rabi frequency of the internal field $\mu E_r/\hbar\sqrt{T}$ (compare eq. (61)). Hence, long cavities, and large power are necessary. We stress that the Ikeda instability discussed in the previous section requires the much more stringent condition $c/\mathcal{L} \ll \gamma_{\perp}$ (see eq. (96)).

Another disadvantage of the Ikeda instability is that it requires very large values of αL , on the order of 100. From all these considerations, it appears that the observation of self-pulsing is not easy, but not impossible. It remains an exciting challenge for the experimentalists.

2.5. DRESSED MODE THEORY OF OPTICAL BISTABILITY. ANALYTICAL TREATMENT OF SELF-PULSING

It is hardly reasonable to expect that a complete understanding of the self-pulsing behavior can emerge from the direct numerical solutions of the Maxwell–Bloch equations, which most often amount to a crude registration of data, without any predictive power. Furthermore, one meets with the following difficulty. In order to render the situation more transparent it is useful to consider the case (44). In this limit, however, one can identify two widely

separated time scales: the characteristic duration time of each pulse, which is on the order of the cavity transit time \mathcal{L}/c , and the characteristic variation time of the envelope of the pulses, which is longer by at least a factor T^{-1} . Thus, the problem becomes numerically complicated. These considerations point to the need for a formulation of the problem that is analytical or quasi-analytical so as to reduce the amount of numerical work. This goal can be achieved by the so-called *dressed mode theory of optical bistability* (BENZA and LUGIATO [1979b]), which is a development of Haken's theory of generalized Ginzburg–Landau equations for phase transition-like phenomena in systems far from thermal equilibrium (HAKEN [1975a,b], HAKEN and OHNO [1976a,b]). This formalism allows one to select the few dominant variables out of the infinite number of degrees of freedom of the system, thereby reducing the problem from the level of Maxwell–Bloch equations to a set of equations *in time only* for these “order parameters”. This selection of variables is obtained using *Haken's adiabatic elimination principle*. In this crucial point our procedure deviates substantially from that of HAKEN [1975b]. In fact, Haken's method is iterative and therefore it is strictly limited to a neighborhood of the critical point, where the steady state becomes unstable. This limitation is common to all the standard bifurcation theory techniques (NICOLIS and PRIGOGINE [1977]). On the contrary, our adiabatic elimination is exact in the limit (27). Hence, it allows us to consider arbitrary deviations from the critical point.

We devote our attention mainly to the simplest situation in which only the two modes that are symmetrically adjacent to the resonant one are unstable. In this case, we can reduce the problem to a set of only two differential equations, that nonetheless fully includes both nonlinearity and propagation. Thus, we obtain a simple description in terms of a two-dimensional phase space, that allows us to explore the full domain of existence of the self-pulsing solution, until it becomes itself unstable, thereby giving rise to a higher order bifurcation.

In this section, we shall consider only the resonant case $\Delta = \theta = 0$. In such a situation, we can safely consider F and \tilde{P} in eqs. (49) as real quantities. In fact, for $\Delta = \theta = 0$, the instabilities arise only from the real part of the variables, which produce the eigenvalues λ_{n1} , λ_{n2} , and λ_{n3} . Consideration of the imaginary parts does not add any interesting new feature, because the eigenvalues λ_{n4} and λ_{n5} do not attain a positive real part.

2.5.1. The dressed mode formalism

Let us start from eqs. (49) with $F^* = F$, $\tilde{P}^* = P$. Similarly to eq. (74), let us introduce the three-component vector

$$\mathbf{q}(z, t') = \begin{pmatrix} \delta F(z, t') \\ \delta P(z, t') \\ \delta D(z, t') \end{pmatrix}, \quad (111)$$

where δF , δP and δD are defined in eq. (72). Equations (49) can be reformulated in terms of the deviations (compare eqs. (73) with $A = \theta = 0$)

$$\frac{\partial \mathbf{q}}{\partial t'} = \hat{\mathcal{L}} \mathbf{q} + \psi_{\text{NL}}, \quad (112)$$

where $\hat{\mathcal{L}}$ is the operator that includes all the linear terms of the equations:

$$\hat{\mathcal{L}} = \begin{pmatrix} -c \frac{L}{\mathcal{L}} \frac{\partial}{\partial z} - k & -2Ck & 0 \\ \gamma_{\perp} \tilde{D}_{\text{st}} & -\gamma_{\perp} & \gamma_{\perp} x \\ -\gamma_{\parallel} \tilde{P}_{\text{st}} & -\gamma_{\parallel} x & -\gamma_{\parallel} \end{pmatrix}, \quad (113)$$

while ψ_{NL} is a vector which contains all the nonlinear terms

$$\psi_{\text{NL}} = \begin{pmatrix} 0 \\ \gamma_{\perp} \delta F \delta D \\ -\gamma_{\parallel} \delta F \delta P \end{pmatrix}. \quad (114)$$

Note that \mathcal{L} is not only a matrix, but also an operator on the variable z , because it contains $\partial/\partial z$.

Now, let us consider the Hilbert space, defined as follows: the generic element ψ of the space has the structure

$$\psi = \begin{pmatrix} \psi_1(z) \\ \psi_2(z) \\ \psi_3(z) \end{pmatrix}, \quad (115)$$

where $\psi_i(z)$ ($i = 1, 2, 3$) are square integrable functions in the interval $0 < z < L$. The scalar product of two elements φ, ψ is

$$(\varphi, \psi) = \sum_{i=1}^3 \int_0^L dz \varphi_i^*(z) \psi_i(z). \quad (116)$$

The vectors φ and ψ_{NL} are elements of the Hilbert space. The eigenvalue equation for the linear operator $\hat{\mathcal{L}}$ is

$$\hat{\mathcal{L}} \mathbf{O}_{nj} = \lambda_{nj} \mathbf{O}_{nj}, \quad j = 1, 2, 3, \quad (117)$$

where the eigenvalues λ_{n1} are given by eqs. (78) and (84.1), and the eigenvalues λ_{n2} and λ_{n3} are given by eqs. (78') and (83). The eigenstates \mathbf{O}_{nj} have the expression

$$\mathbf{O}_{nj} = \exp(i k_n z) \begin{pmatrix} G(\lambda_{nj}, x) \\ \frac{(\lambda_{nj}/\gamma_{||}) + 1 - x^2}{1 + x^2} \\ -\frac{x}{1 + x^2} \left(\frac{\lambda_{nj}}{\gamma_{\perp}} + 2 \right) \end{pmatrix}, \quad (118)$$

where

$$G(\lambda, x) = \left(\frac{\lambda}{\gamma_{\perp}} + 1 \right) \left(\frac{\lambda}{\gamma_{||}} + 1 \right) + x^2. \quad (119)$$

Of course, the eigenstates are defined up to a constant factor. This has been chosen in such a way that the three elements of \mathbf{O}_{nj} remain finite in the limit (27). In fact, as one easily verifies, $G(\lambda_{n3}^{(0)}, x) = 0$.

At this point, we say that the indices n and j label the *modes* of our system. We call them *dressed* because they incorporate an exact part of the atom-field interaction, namely the part that is contained in the linear operator $\hat{\mathcal{L}}$. With respect to the modes introduced in § 2.2.2, the dressed modes also include the index j , which diagonalizes the linearized part of the atom-field interaction.

We note that $\operatorname{Re} \lambda_{n1}$ is proportional to the field relaxation rate k , whereas $\operatorname{Re} \lambda_{n2}$ and $\operatorname{Re} \lambda_{n3}$ are proportional to the atomic relaxation rates γ_{\perp} and $\gamma_{||}$. Hence, the dressed modes with $j = 1$ have a dominant field character, and accordingly we shall call them *field modes*. Similarly, we shall call the dressed modes with $j = 2, 3$ *atomic modes*.

In order to introduce suitable dressed mode amplitudes, it is necessary to consider the adjoint operator $\hat{\mathcal{L}}^\dagger$. The spectrum of $\hat{\mathcal{L}}^\dagger$ is obtained from the spectrum of $\hat{\mathcal{L}}$ by the complex conjugation

$$\hat{\mathcal{L}}^\dagger \bar{O}_{nj} = \lambda_{nj}^* \bar{O}_{nj}. \quad (120)$$

Note the relations

$$\lambda_{n1}^* = \lambda_{-n1}, \quad \lambda_{n2}^* = \lambda_{-n3}. \quad (121)$$

The second equation in (121) holds provided that γ_{\parallel} has the same order of magnitude as γ_{\perp} and x is not too small. In the following, we shall always assume that these conditions are satisfied.

The eigenstates \bar{O}_{nj} have the form

$$\bar{O}_{nj} = \frac{\exp(ik_n z)}{L \mathcal{N}_{nj}^*} \begin{pmatrix} 1 \\ -2C \frac{k}{\gamma_{\perp}} \frac{(\lambda_{nj}^*/\gamma_{\parallel}) + 1}{G(\lambda_{nj}^*, x)} \\ -2C \frac{k}{\gamma_{\parallel}} \frac{x}{G(\lambda_{nj}^*, x)} \end{pmatrix}, \quad (122)$$

where the normalization constant \mathcal{N}_{nj} , whose explicit expression is given in Appendix 2, is chosen in such a way that

$$(\bar{O}_{nj}, \bar{O}_{n'j'}) = \delta_{nn'} \delta_{jj'}. \quad (123)$$

Hence, the vectors $\{\bar{O}_{nj}\}$, $\{\bar{O}_{nj}\}$ constitute a complete bi-orthonormal set of vectors in the Hilbert state. We can expand the vector q on the basis $\{\bar{O}_{nj}\}$:

$$q(t') = \sum_{nj} \xi_{nj}(t') \bar{O}_{nj}, \quad \xi_{nj}(t') = (\bar{O}_{nj}, q(t')). \quad (124)$$

The dimensionless variables ξ_{nj} , which depend on time only, are the dressed mode amplitudes. In particular, using eqs. (72), (111) and (118) we have the following expression of the normalized electric field

$$F(z, t') = x + \sum_{nj} \xi_{nj}(t') G(\lambda_{nj}, x) \exp(ik_n z). \quad (125)$$

The expression of the amplitude f_n , defined in eq. (52), is therefore

$$f_n(t') = x \delta_{n0} + \sum_j \xi_{nj}(t') G(\lambda_{nj}, x). \quad (126)$$

Next, we substitute the expansion (124) into (112) and multiply scalarly eq. (112) times \bar{O}_{nj} on the left. Using eqs. (123), (117), (116) and (114) we obtain the time evolution equations for the amplitudes ξ_{nj} :

$$\xi_{nj} = \lambda_{nj} \xi_{nj} + \sum_{n'j'} \sum_{n''j''} \Gamma(nj, n'j', n''j'') \xi_{n'j'} \xi_{n''j''}, \quad (127)$$

where the coefficients Γ are given by

$$\Gamma(nj, n'j', n''j'') = \delta_{n,n'+n''} O_{n''j'',1} \{ \gamma_{\perp} O_{nj,2}^* O_{n'j',3} - \gamma_{\parallel} O_{nj,3}^* O_{n'j',2} \}. \quad (128)$$

In eq. (128) we have called $O_{nj,i}$ ($i = 1, 2, 3$) the three components of the vector O_{nj} , without the exponential factor (see eq. (118)), and correspondingly we have called $\bar{O}_{nj,i}$ ($i = 1, 2, 3$) the three components of the vector \bar{O}_{nj} , without the factor $L^{-1} \exp(i k_n z)$.

Equation (127) governs the dressed mode dynamics. It has a linear term which arises from the part $\hat{\mathcal{L}}q$ of eq. (112) and several nonlinear terms, which arise from ψ_{NL} , and rule the mode-mode coupling. The time evolution, starting from a situation in which the system is slightly displaced from an unstable stationary state, can be described as follows. In the initial stage, due to the smallness of the deviation q and hence, of ξ_{nj} , the linear part of eq. (127) is dominant. Therefore the unstable modes ($\operatorname{Re} \lambda_{nj} > 0$) grow exponentially while the stable modes are exponentially damped. In due time, the nonlinear terms become important and eventually lead the system to a periodic self-pulsing regime. The expressions for the relevant coefficients Γ are given in Appendix B. The only important feature, in view of the following treatment, is the order of magnitude of these coefficients with respect to T . One has for any j'

$$\begin{aligned} \Gamma(n1, n'j', n''1) &= O(T), \\ \Gamma(n1, n'j', n''_3^2) &= O(T^2), \end{aligned} \quad (129)$$

$$\begin{aligned} \Gamma(n_3^2, n'j', n''1) &= O(1), \\ \Gamma(n_3^2, n'j', n''2) &= O(T), \\ \Gamma(n_3^2, n'j', n''3) &= O(T). \end{aligned} \quad (130)$$

In the following we shall restrict ourselves to the case $\gamma_{\perp} = \gamma_{\parallel} = \gamma$ in which all the expressions attain a maximum of simplicity. In this case, one finds that the coefficients $\Gamma(nj, n'j', n''j'')$ get a further factor of T with respect to that indicated in eqs. (130) when $j = 2$ and $j' = 3$ or $j = 3$ and $j' = 2$. Hence, eq.

(130) must be corrected as follows

$$\begin{aligned}\Gamma(n2, n'1, n''1), \Gamma(n2, n'2, n''1) &= O(1), \\ \Gamma(n2, n'3, n''1) &= O(T), \\ \Gamma(n2, n'1, n''2), \Gamma(n2, n'2, n''2), \\ \Gamma(n2, n'1, n''3), \Gamma(n2, n'2, n''3) &= O(T), \\ \Gamma(n2, n'3, n''2), \Gamma(n2, n'3, n''3) &= O(T^2),\end{aligned}\quad (131)$$

The order of magnitude of the coefficients $\Gamma(n3, n'j', n''j'')$ is immediately obtained by taking into account the relation

$$\Gamma^*(nj, n'j', n''j'') = \Gamma(-n\bar{j}, -n'\bar{j}', -n''\bar{j}''), \quad (132)$$

where $\bar{j} = 1$ for $j = 1$, $\bar{j} = 3$ for $j = 2$, $\bar{j} = 2$ for $j = 3$.

The dressed mode formalism outlined in this subsection is essentially a simplification of the procedure of HAKEN [1975a,b]. The distinction between field and atomic modes was introduced in BENZA and LUGIATO [1979b]. As we shall see in the next subsection, this distinction is important for the following developments.

2.5.2 Adiabatic elimination of the atomic modes (BENZA and LUGIATO [1982])

For the following steps, it is suitable to reformulate eq. (127) in terms of the variables S_{nj} , defined by

$$\xi_{nj}(t') = S_{nj}(t') \exp(-i\alpha_n t'). \quad (133)$$

Using eq. (128), we obtain

$$\dot{S}_{nj} = (\lambda_{nj} + i\alpha_n)S_{nj} + \sum_{n'j'} \sum_{n''j''} \Gamma(nj, n'j', n''j'') S_{n'j'} S_{n''j''}. \quad (134)$$

Accordingly, eq. (125) becomes

$$F(z, t') = x + \sum_{nj} S_{nj}(t') G(\lambda_{nj}, x) \exp\left[-i\alpha_n\left(t' - \frac{z\mathcal{L}}{cL}\right)\right]. \quad (135)$$

Equation (134) gives us an infinite system of equations that is fully equivalent to the original Maxwell–Bloch equations. In order to reduce the problem to a tractable dimension, the first step is to select the frequencies to be considered. Of course this selection is guided by physical intuition, on the basis of the

frequencies that are unstable. Essentially, one must guess which frequencies n have non-negligible dressed mode amplitudes S_{nj} . Of course, for each selected frequency n , one must also consider the corresponding frequency $-n$, because $S_{-n1} = S_{n1}^*$, $S_{-n2} = S_{n2}^*$.

After this selection the number of equations (134) for the amplitudes S_{nj} becomes finite, but the system is still too complicated even in the simplest setting of two unstable frequencies that we shall consider in the next section. The second crucial step to simplify the problem is the systematic use of the limit (27). More precisely, we shall perform the limit (27) simultaneously with the limit

$$t' \rightarrow \infty, \quad \tau = kt' = \text{const.} \quad (136)$$

In fact, if one performs only the limit (27), one trivializes the time evolution of the field variables, because one eliminates the interaction of the field with the atoms ($\alpha L \rightarrow 0$). This is no longer the case if we also let $t' \rightarrow \infty$, with $\tau = cTt'/\mathcal{L}$ kept constant.

Let us now analyze in detail the consequences that the use of the limits (27) and (136) imposes on eqs. (134). The first consequence is that the atomic modes, which vary at a rate γ , in this limit attain a stationary situation (i.e. $dS_{n2}/dt' = dS_{n3}/dt' = 0$). On the contrary, the field modes, which vary at a rate k , still possess a time evolution as function of τ . Hence, in the limits (27) and (136) the atomic modes are *adiabatically eliminated in an exact way*. After setting $dS_{n2}/dt' = dS_{n3}/dt' = 0$ one obtains an algebraic system of equations for the atomic mode amplitudes

$$0 = (\lambda_{n_3^2} + i\alpha_n)S_{n_3^2} + \sum_{n'j'} \sum_{n''j''} \Gamma(n_3^2, n'j', n''j'') S_{n'j'} S_{n''j''}. \quad (137)$$

By solving this system one finds the expressions of the atomic amplitudes S_{n2} , S_{n3} as functions of the field amplitudes S_{n1} . In general, the nonlinearity of the algebraic equations renders it impossible to solve these equations analytically, and therefore one must use approximate methods, such as the iterative procedure of HAKEN [1975a,b]. However, in our case the limits (27) and (136) again introduce a decisive simplification. In fact, let us consider the terms in eq. (137) such that both factors $S_{n'j'}$ and $S_{n''j''}$ are of atomic type, that is both j' and j'' are equal to 2 or 3. As one sees from eqs. (131), the corresponding factor $\Gamma(n_3^2, n'j', n''j'')$ always vanishes in the limit (27). Thus, in this limit the system (137) becomes *linear* with respect to the atomic variables S_{n2} and S_{n3} , and therefore can be solved in a standard way. A further simplification is that eqs. (137) decouple into separate subsystems, one for the amplitudes S_{n2} and

one for S_{n3} . In fact, as one sees again from eqs. (131), all the terms that couple the two sets of variables contain coefficients that vanish for $T \rightarrow 0$.

Hence, if in eqs. (137) we introduce the limit (27), the adiabatic elimination is performed *exactly and analytically*. The expressions for the atomic modes S_{n2} and S_{n3} as functions of the field modes S_{n1} are given by rational functions that do not depend on αL and T . By substituting these expressions into eqs. (134) with $j = 1$, one obtains a closed system of equations for the field modes, that play the role of order parameters in our problem. In the limit $T \ll 1$, all the terms in the thus obtained equations for the variables S_{n1} are proportional to k . In fact, as one sees from eqs. (78), $\lambda_{n1} + i\alpha_n$ is proportional to k , apart from corrections of order T^2 that vanish in the limits (27) and (136). Furthermore, as one sees from eqs. (129), the coefficients $\Gamma(n1, n'j', n''j'')$, which are the only ones that survive in the limit (27), are proportional to T and hence, to k .

Therefore, using (136) the equations for the field modes have the form

$$\frac{dS_{n1}}{d\tau} = h_n(S_{01}, S_{-11}, S_{11}, \dots). \quad (138)$$

where

$$h_n = \lambda_n^{(+)} S_{n1} + k^{-1} \sum_{n'j'} \Gamma(n1, n'j', (n - n')1) S_{n'j'} S_{(n - n')1}. \quad (139)$$

For $j' = 2, 3$, $S_{n'j'}$ is the rational function of S_{n1} , previously calculated in the adiabatic elimination of the atomic variables. Hence, h_n depends on αL and T only via $C = \alpha L/2T$.

Even when the number of quantities S_{n1} in play is not small, the system (138) can be numerically handled more easily than the Maxwell–Bloch equations, because it involves only the time variable, and most important of all, it solves the problem of separating the two main time scales of our problem (see § 2.5). The first time scale, on the order of the cavity transit time \mathcal{L}/c , is that of the pulses, and appears in the factor $\exp(-i\alpha_n t')$ in eq. (135). The second time scale, on the order of k^{-1} , is that of the pulse envelope. Equations (138) govern the time evolution of the quantities S_{n1} , that evolve on the time scale k^{-1} .

We stress that the adiabatic elimination performed in this subsection is not so restrictive as that performed in § 2.4.4. Namely, it does not require that $\gamma\mathcal{L}/c \gg 1$, but only that $\gamma/k = \gamma\mathcal{L}/cT \gg 1$. In fact, thanks to the transformation (133), the variation of the field dressed mode amplitudes S_{n1} in time is ruled by $\lambda_{n1} + i\alpha_n$, which is proportional to k (see eqs. (78)).

2.5.3. The case of two unstable modes

From now on we shall consider the simplest situation, that is the case in which only the two modes immediately and symmetrically adjacent to the resonant one are unstable. In this case, it is reasonable to guess that the dressed modes that play a dominant role are the three modes corresponding to the resonant frequency $n = 0$ plus the six modes corresponding to the adjacent frequencies $n = \pm 1$. This suggestion has been supported both by comparison with the numerical solutions of the Maxwell–Bloch equations (see next subsection) and by showing that inclusion of the adjacent modes with $n = 2$ never changes the results qualitatively, and quantitatively the correction is on the order of 10% (LUGIATO, BENZA, NARDUCCI and FARINA [1983]).

Let us now consider the nine equations (134) for the amplitudes S_{nj} ($n = +1, 0, -1; j = 1, 2, 3$), taking into account only the terms that are relevant in the limits (27) and (136). As discussed in the previous section, in this limit one automatically has $\dot{S}_{n2} = \dot{S}_{n3} = 0$. Thus one obtains two independent triplets of algebraic equations that are linear with respect to the atomic amplitudes S_{n2} and S_{n3} . The solution of the first system provides the expressions of S_{n2} as functions of the field amplitudes S_{n1} , and the solution of the second system the expressions of S_{n3} . Note that $S_{n3} = S_{-n2}^*$. By substituting these expressions into the equations for the field amplitudes one obtains a closed set of three equations for S_{11} , S_{01} and S_{-11} such as (138). These equations read

$$\begin{aligned}\frac{dS_{11}}{d\tau} &= S_{11} \bar{f}\{(S_{11} \cdot S_{-11}), S_{01}\}, \\ \frac{dS_{01}}{d\tau} &= g\{(S_{11} \cdot S_{-11}), S_{01}\}, \\ \frac{dS_{-11}}{d\tau} &= S_{-11} \bar{f}^*\{(S_{11} \cdot S_{-11}), S_{01}\},\end{aligned}\quad (140)$$

where the functions \bar{f} and g depend on S_{11} and S_{-11} only via the product $S_{11} \cdot S_{-11}$, and g is real. Furthermore, the only parameters that appear in \bar{f} and g are C , x and $\tilde{\alpha}_1 = 2\pi c/\mathcal{L}\gamma$. By setting

$$S_{11} \equiv \rho_1 e^{i\varphi}, \quad S_{01} \equiv \sigma \text{ real}, \quad (141)$$

we obtain from eqs. (140) (BENZA and LUGIATO [1982])

$$\frac{d\rho_1}{d\tau} = f(\rho_1, \sigma), \quad (142a)$$

$$\frac{d\sigma}{d\tau} = g(\rho_1, \sigma), \quad (142b)$$

$$\frac{d\varphi}{d\tau} = l(\rho_1, \sigma), \quad (143)$$

where

$$\begin{aligned} f(\rho_1, \sigma) &= \rho_1 \operatorname{Re} \bar{f}(\rho_1^2, \sigma), \\ l(\rho_1, \sigma) &= \operatorname{Im} \bar{f}(\rho_1^2, \sigma). \end{aligned} \quad (144)$$

The explicit expressions for the functions f and g are given in Appendix C. Clearly, eqs. (142a) and (142b) form a closed system of equations for ρ_1 and σ . On the other hand, eq. (143) has the solution

$$\varphi(\tau) = \varphi(\tau = 0) + \int_0^\tau d\tau' l(\rho_1(\tau'), \sigma(\tau')), \quad (145)$$

so that the expression of $\varphi(\tau)$ is obtained once the system (142) has been solved.

Let us now come back to eq. (135). Since $G(\lambda_{n3}^{(0)}, x) = 0$ (because $\lambda_{n2}^{(0)}$ and $\lambda_{n3}^{(0)}$ are the roots of the equation $G(\lambda, x) = 0$) in the limit (27) only the terms with $j = 1$ contribute. Using (141) and setting

$$\begin{aligned} p(\tau) &= 2\rho_1(\tau)|G(-i\alpha_1, x)|, \\ \delta(\tau) &= \sigma(\tau) G(0, x), \end{aligned} \quad (146)$$

eq. (135) reads

$$\begin{aligned} F(z, t') &= x + \delta(\tau) \\ &+ p(\tau) \cos \left\{ -\frac{2\pi c}{\mathcal{L}} \left(t' - \frac{z\mathcal{L}}{cL} \right) + \varphi(\tau) + \theta \right\}, \\ \tau &= kt', \quad \theta = \arg G(-i\alpha_1, x). \end{aligned} \quad (147)$$

Hence, the upper and lower envelopes of the time evolution are given by

$$F_{\substack{\text{upper} \\ \text{lower}}}(\tau) = x + \delta(\tau) \pm p(\tau). \quad (148)$$

Equation (148) shows that $\delta(\tau)$ is the half-amplitude of the oscillations, while $\tilde{\sigma}(\tau)$ is the difference between the mean value of the oscillations and the stationary value x . For $\tau \rightarrow \infty$, when the system precipitates to the low transmission state, $\tilde{p}(\infty) = 0$ and $x + \delta(\infty)$ is the value of the normalized transmitted light in the low transmission branch. When the system approaches a steady self-pulsing behavior $\tilde{p}(\infty) \neq 0$, and as one sees from eq. (145) $\varphi(\tau)$ has the form

$$\tau \rightarrow \infty, \quad \varphi(\tau) = c_1 + c_2 \tau, \quad (149)$$

where c_1 and c_2 are constant. Now

$$-\frac{2\pi c}{\mathcal{L}} t' + c_2 \tau = \left(-\frac{2\pi c}{\mathcal{L}} + c_2 k \right) t'.$$

In the limit (27), $c_2 k$ gives a vanishing correction to the frequency $2\pi c/\mathcal{L}$ and hence, we can drop it. Furthermore, we can safely assume that $\varphi(\tau = 0)$ is such that $c_1 = 0$. Therefore for $\tau \rightarrow \infty$ (147) gives

$$F(z, t') = x + \delta(\infty) + \tilde{p}(\infty) \cos \left\{ -\frac{2\pi c}{\mathcal{L}} \left(t' - \frac{z}{c'} \right) + \tilde{\sigma} \right\}. \quad (150)$$

Note that $t' - (z/c') = t - (z/c)$ (see eq. (47)). Equation (150) describes the asymptotic pulses which have a period equal to the cavity transit time \mathcal{L}/c . The envelope for $\tau \rightarrow \infty$ becomes perfectly flat and is given by $x + \delta(\infty) \pm \tilde{p}(\infty)$.

Thus, we can reason in terms of the two-dimensional phase space of the variables ρ_1 and σ . In particular, the stationary solutions ρ_{1st} and σ_{st} of eqs. (142) (i.e. the solutions of the equations $f(\rho_{1st}, \sigma_{st}) = g(\rho_{1st}, \sigma_{st}) = 0$) correspond to asymptotic (i.e. $\rho_{1st} = \rho_1(\infty)$, $\sigma_{st} = \sigma(\infty)$) self-pulsing solutions if they lie out of the σ -axis ($\rho_{1st} > 0$), and correspond to cw solutions if $\rho_{1st} = 0$, because in the latter case the amplitude \tilde{p} of the oscillations vanishes (see eqs. (146) and (150) with $\rho_1(\infty) = \rho_{st}$). The stability of a steady self-pulsing solution is checked by linearizing eqs. (142) around such a solution. At this point, we can appreciate what degree of simplification we have achieved by the dressed mode theory. In fact, we have reduced the problem from the level of Maxwell–Bloch equations to the following one: to draw the two lines $f(\rho_1, \sigma) = 0$ and $g(\rho_1, \sigma) = 0$ in order to find their intersections, that give the stationary solutions ρ_{1st} , σ_{st} . The position of these solutions depends on the values of the externally controllable parameters x and $\tilde{\alpha}_1$. Hence, the behavior of the system when we vary the external parameters is understood by simply

looking at the displacements of the stationary solutions in the phase plane. This will be illustrated in the following section.

2.5.4. Periodic self-pulsing behavior in the long time limit $\tau \rightarrow \infty$ (BENZA and LUGIATO [1981, 1982])

Figure 14 (above) shows the S-shaped curve of transmitted versus incident field for $C = 20$, and indicates the points that are unstable when condition (88) is satisfied. In the following, we shall consider only the case in which at most the two modes $n = \pm 1$ adjacent to the resonant one are unstable, and we shall analyze the behavior of the system when we vary the two externally controllable parameters x and $\tilde{\alpha}_1$. We note that x is controlled by varying the incident field y ; $\tilde{\alpha}_1 = 2\pi c/\mathcal{L}\gamma$ is controlled by varying the total length \mathcal{L} of the ring cavity, while keeping constant the length L of the atomic sample (see Fig. 1). Hence, we shall explore the plane of the variables x and $\tilde{\alpha}_1$ shown in Fig. 15 for $C = 20$. The stationary state in the high transmission branch is unstable when the point $x, \tilde{\alpha}_1$ lies in the region bounded by the lines $\alpha_{\max}(x)/\gamma, \alpha_{\min}(x)/\gamma$, and $x = x_m$, where α_{\max} and α_{\min} are defined by eq. (88), and x_m corresponds to the lower bistability threshold (compare Fig. 8). We stress that we must not explore the whole plane $x, \tilde{\alpha}_1$, because in correspondence to a part of this plane other modes, different from the adjacent modes $n = \pm 1$, are unstable. For instance, in correspondence to the shaded region in Fig. 15, the modes $n = \pm 2$ are unstable. Hence, we must leave this region out of consideration. Similarly there is a region of the plane, not indicated in Fig. 15, in correspondence to which the modes $n = \pm 3$ are unstable, and so on. All these regions must be excluded from our analysis, because we use the equations of § 2.5.3 which consider only the modes with $n = 0, \pm 1$.

In the following, we shall show the phase plane of the variables ρ_1, σ in correspondence to several values of the variables $x, \tilde{\alpha}_1$. In the phase plane, we shall draw the two lines $f(\rho_1, \sigma) = 0$ and $g(\rho_1, \sigma) = 0$. Note from eqs. (144) that the line $f(\rho_1, \sigma) = 0$ is composed by the line $\rho_1 = 0$, and the line $\text{Re } \bar{f}(\rho_1^2, \sigma) = 0$. Hence, the points $\{\rho_1 = 0, \sigma = \bar{\sigma}\}$, where $\bar{\sigma}$ are the solutions of the equation $g(0, \sigma) = 0$, are stationary solutions of the system (142) which correspond to the cw states of the system. Namely, for any given value of y we have three such solutions, which correspond to the three points A, B and C in Fig. 14. In particular, the point A in the high transmission branch corresponds to the origin of the phase plane $\rho_1 = \sigma = 0$. In all the graphs of the plane $\{\rho_1, \sigma\}$ which will follow, these three solutions will be always indicated by the same letters A, B and C.

First, let us analyze the behavior of the system when we move along the horizontal line (a) in Fig. 15. This corresponds to varying continuously the incident field along the high transmission branch, while the total length \mathcal{L} of the cavity is kept fixed, so that $\tilde{\alpha}_1 = 8$. Figure 19 shows the lines $\text{Re } \bar{f}(\rho_1^2, \sigma) = 0$ (solid line) and $g(\rho_1, \sigma) = 0$ (dashed line) for four different values of y in increasing order (see Fig. 15). Each intersection of the two lines corresponds to a self-pulsing state provided that it is stable. We see that, as soon as we enter into the instability region from the left along the line (a) in Fig. 15, a stable self-pulsing state S bifurcates from the cw state A , which has become unstable (Fig. 19a). By increasing the incident field, the amplitude of the oscillations for the solution S increases. When we go out of the instability region a second solution U bifurcates from the cw state A which is now again stable (Fig. 19b). On the contrary, the solution U is unstable. By further increasing y the two

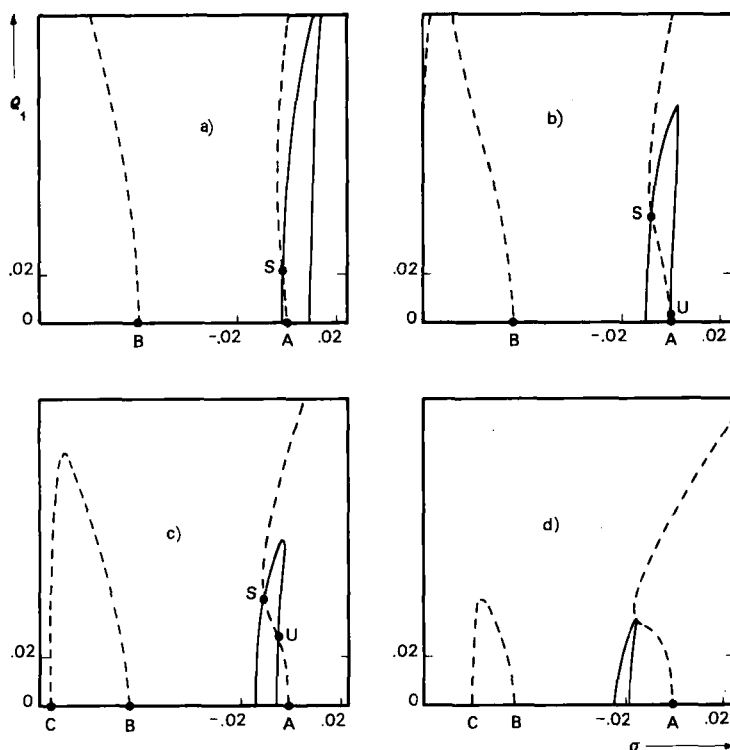


Fig. 19. Lines $\text{Re } \bar{f}(\rho_1^2, \sigma) = 0$ (solid line) and $g(\rho_1, \sigma) = 0$ (dashed line) in the phase plane $\{\rho_1, \sigma\}$ for $C = 20$, $\tilde{\alpha}_1 = 8$ and: (a) $y = 13.262$ ($x = 8.75$); (b) $y = 13.664$ ($x = 9.75$); (c) $y = 13.96$ ($x = 10$); (d) $y = 15.31$ ($x = 12$).

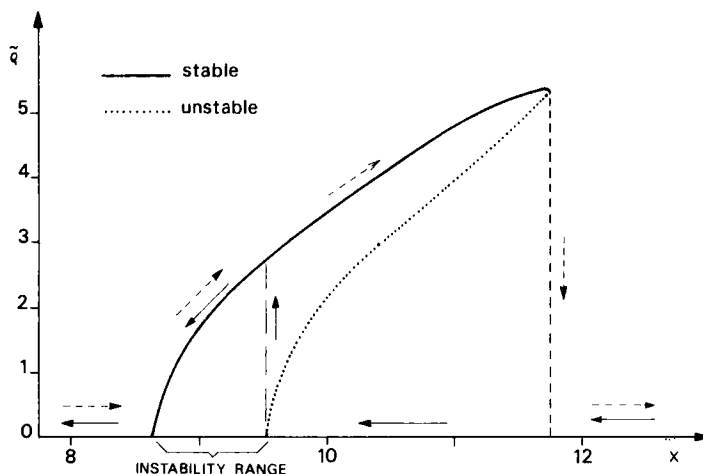


Fig. 20. Hysteresis cycle of the half-amplitude of the oscillations \tilde{p} (in the long-time limit $\tau \rightarrow \infty$) as a function of the stationary transmitted field x in the high transmission branch for $C = 20$, $\tilde{\alpha}_1 = 8$. Solid (dashed) arrows indicate the behavior of the system for decreasing (increasing) incident field.

solutions S and U become nearer and nearer (Fig. 19c) until they coalesce and disappear together (Fig. 19d) so that the system can no longer show self-pulsing. The behavior of the system when we move along the line (a) in Fig. 15 is summarized in Fig. 20, where the half-amplitude of the oscillations \tilde{p} , for solution S (full line), is graphed versus the steady state value x of the transmitted light in the high transmission branch. As shown by the arrows, one finds hysteresis when one increases and decreases the incident field. Thus, we find a *hysteresis cycle of novel type* which involves both cw and pulsing states. Precisely, Fig. 20 exhibits a second-order and a first-order phase transition. The second-order one occurs at the left boundary of the instability range. The first-order transition is manifested by the hysteresis cycle that begins on the right boundary of the instability range, where the unstable self-pulsing solution U (dotted curve in Fig. (20)) bifurcates.

Let us now consider the behavior of the system when we move along the line (b) in Fig. 15, which corresponds to $\tilde{\alpha}_1 = 5$. Figure 21 shows the phase plane for the three values of y (that is x) shown in Fig. 15. We see that now, when we enter into the instability region, no self-pulsing solution is there (Fig. 21a). In this situation, the only stable solution of system (142) is the one corresponding to the low transmission cw state C, so that if the system is initially near to the unstable high transmission state A, it precipitates to the low transmission

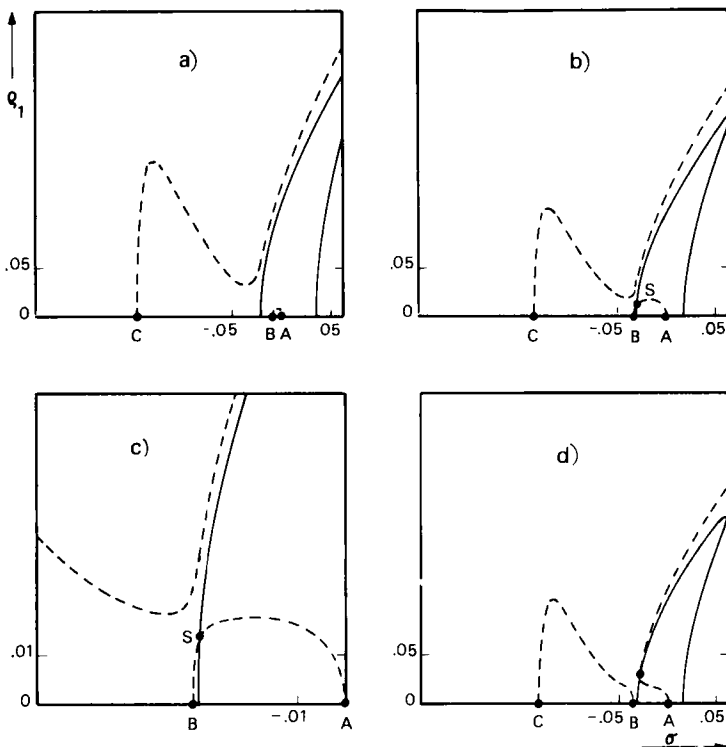


Fig. 21. Same as Fig. 19 but for $\tilde{\alpha}_1 = 5$. (a) $y = 12.49$ ($x = 6.25$); (b, c) $y = 12.573$ ($x = 6.875$); (d) $y = 12.6$ ($x = 7$). Figure 21c is an enlarged view of a part of Fig. 21b.

branch. For a suitable value of the incident field, a self-pulsing solution S appears (Figs. 21b,c). In this case, S bifurcates from the unstable cw state B , and also S is *unstable*. Increasing y slightly, the state S *becomes stable*. Note also that the shape of the curve $g(\rho_1, \sigma) = 0$ undergoes a qualitative change in the connection of its two parts (compare Figs. 21b,c,d). For larger values of y , the behavior is quite similar to that found in the case of line (a) in Fig. 15. Namely, when we go out of the instability region an unstable state U bifurcates from the cw state A . The solutions S and U become nearer and nearer until they coalesce. Figure 22 shows the behavior of the half-amplitude of the oscillations when the steady state value x , of the transmitted light in the high transmission state, is varied along the line (b) in Fig. 15. Note that in this case there is no second-order phase transition at the left boundary of the instability range, because the self-pulsing solution S is unstable. When we increase the incident

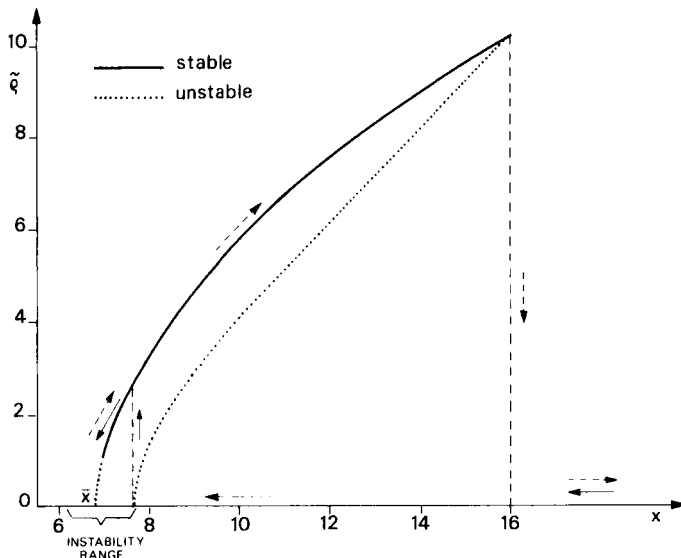


Fig. 22. Same as Fig. 20, but for $\tilde{\alpha}_1 = 5$.

field, the self-pulsing behavior appears discontinuously as soon as the solution S becomes stable.

The most striking feature that emerges from Figs. 20 and 22 is that the self-pulsing state can also exist outside the instability region. The full domain of existence of the stable self-pulsing state S is in fact the region bounded by the lines DEF and DGH in Fig. 23. We have already seen what happens when we cross the line DE from left to right (or from up to down): the self-pulsing state S bifurcates from the cw solution A in the high transmission branch. Thus, DE is a line of second-order phase transitions from cw to pulsed. On the other hand, GE is a line of first-order phase transitions, because when the system is in the cw state A and we cross it from right to left (or from down to up), we find a *discontinuous* transition from cw to pulsed. Note that line GE belongs to the boundary of the instability region but *does not belong* to the boundary of the domain of existence of the self-pulsing state.

When we cross the lines EF and GH from the inside to the outside of the domain of existence, the stable self-pulsing state coalesces with an unstable self-pulsing solution, and the two solutions disappear together while the system discontinuously jumps from the self-pulsing state to the cw regime. When we cross the line DG from right to left (or from up to down) the self-pulsing state becomes unstable. The stability analysis of eqs. (142), linearized around the

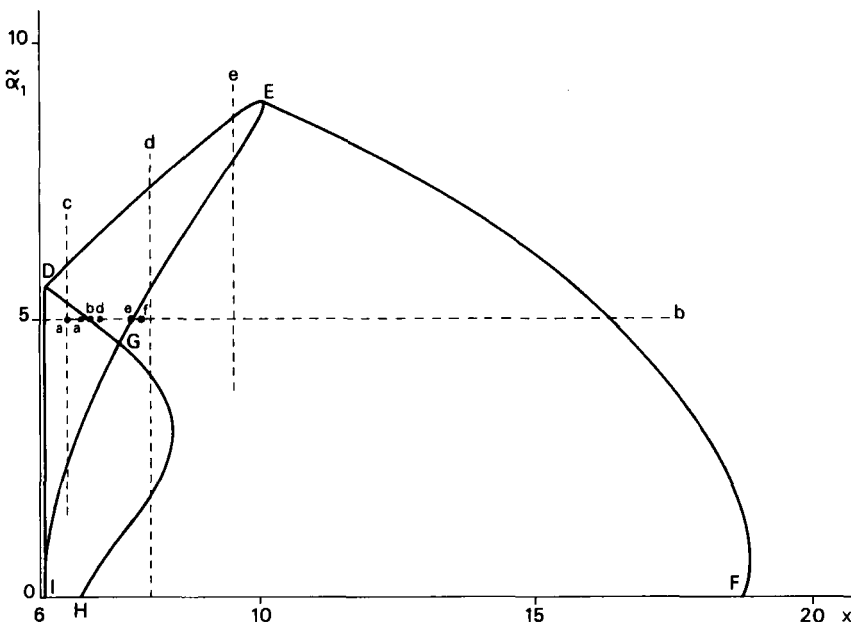


Fig. 23. The domain of existence of the stable self-pulsing state is the region DEFHGD. The lines **c**, **d**, and **e** refer to Figs. 24, 25, and 26 respectively. The points on line **b** (which coincides with line **b** in Fig. 15) correspond to Figs. 27a-f, respectively.

self-pulsing solution S , reveals that the two eigenvalues of the linearized equations are complex conjugate in correspondence to line DG. Hence, when crossing DG, we have a *Hopf bifurcation*. This will be discussed in detail in § 2.5.6.

In correspondence to the part DGI of the instability region there is always precipitation to the low transmission branch. Note that the domain of existence DEFHGD partially overlaps with the shaded region of Fig. 15, in correspondence to which the modes $n = \pm 2$ are unstable. As discussed before, this common part must be left out of consideration. The same must be done for the regions of the plane $(x, \tilde{\alpha}_1)$ in correspondence to which the modes $n = \pm 3, n = \pm 4$, etc. are unstable.

Figures 24 and 25 show the variation of the half-amplitude of the oscillations $\tilde{\beta}$ as a function of $\tilde{\alpha}_1$, when we move along the vertical lines (c) and (d) in Fig. 23, which correspond to $x = 6.5$ and $x = 8$ respectively. In order to move along these lines, one must keep the incident field fixed and vary the total length of the cavity. Note that the left-hand part of the graph in Fig. 25 cannot be reached by moving along the vertical line (d) because it is disconnected from the

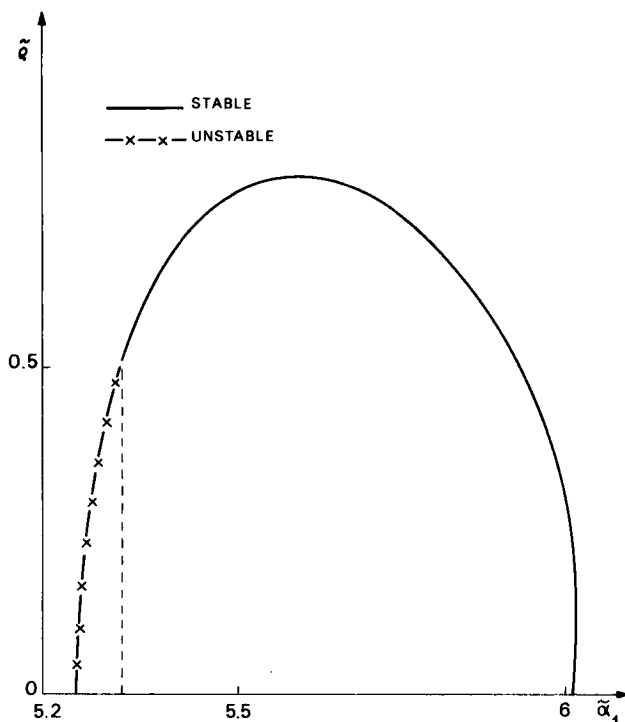


Fig. 24. The half-amplitude of the oscillations $\tilde{\rho}$ is graphed as a function of $\tilde{\alpha}_1$ for $C = 20$, $x = 6.5$.

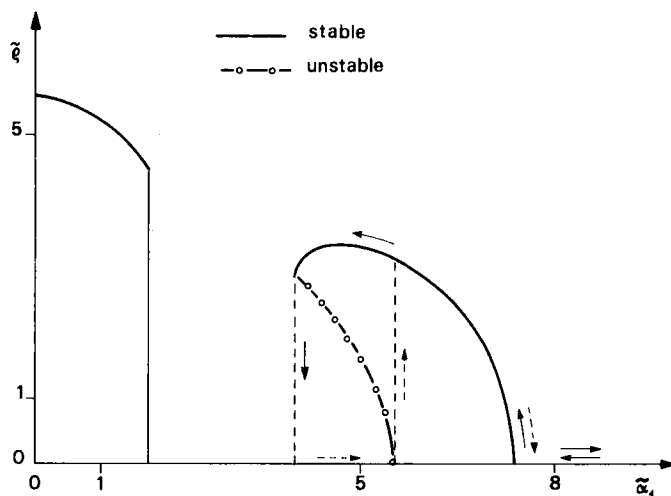


Fig. 25. Same as Fig. 24, but for $x = 8$. Solid (dashed) arrows indicate the behavior of the system when we decrease (increase) the incident field.

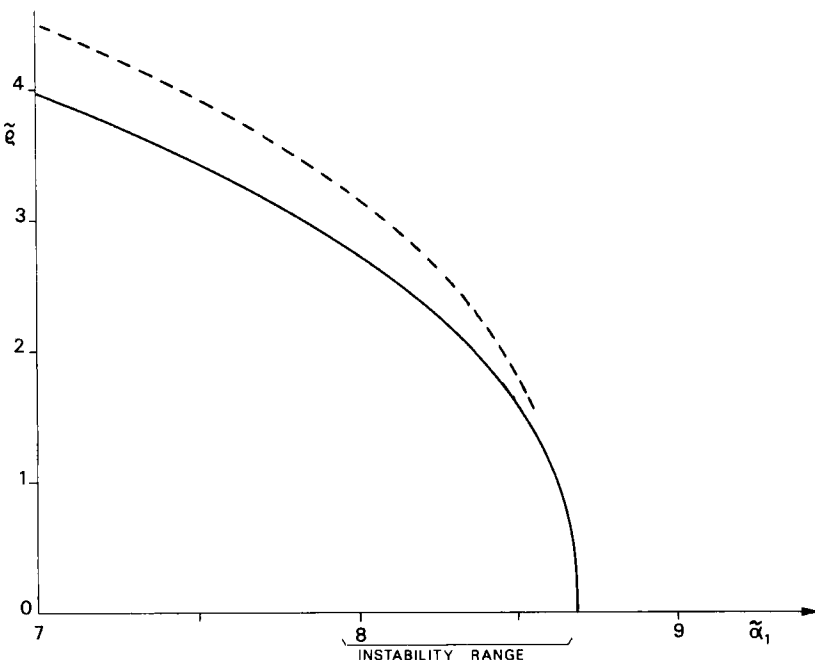


Fig. 26. Same as Fig. 24, but for $x = 9.5$. The solid line is obtained using eqs. (142), the dashed line by numerically solving the Maxwell-Bloch equations.

remaining part of the curve. The self-pulsing state corresponding to the left-hand branch in Fig. 25 can be reached only by changing the parameters x and α_1 simultaneously, in such a way that the point $(x, \tilde{\alpha}_1)$ always remains inside the domain of existence of the self-pulsing state.

Figure 26 shows the half-amplitude of the oscillations $\tilde{\beta}$ as a function of α_1 , along the line (e) in Fig. 23, which corresponds to $x = 9.5$. The broken line is obtained by numerically solving the Maxwell-Bloch equations and the full line by using eqs. (142). The agreement between the two curves is satisfactory; the 10% discrepancy is due in part to numerical errors in the solution of the Maxwell-Bloch equations, and in part to the neglect of higher order frequencies in the derivation of eqs. (142). Note that the dressed mode theory also predicts the correct behavior when the amplitude of the oscillations is comparable with the stationary field.

The results of this subsection lead us to look at optical bistability with new eyes. Now our bistable system no longer appears simply as a device with two different stationary states, but rather as a *multistable* system, in which some of

the stable steady states are cw, and some are pulsing. One can reach all the (cw and pulsing) branches of the system by suitably controlling the external parameters. In fact, in correspondence to each point in the region GEFH of the plane of the control parameters (see Fig. 23), we have three possible steady states, of which one is pulsing and two are cw (both the low and the high transmission steady states are stable in this situation).

Thus the phenomenology of optical bistability is deeply enriched. From a formal viewpoint, this is already evident from eqs. (142) that treat cw and pulsing solutions on the same footing.

2.5.5. *Transient approach to self-pulsing and precipitation* (LUGIATO, BENZA, NARDUCCI and FARINA [1981, 1983])

Up to this point, we have considered the self-pulsing behavior only in the long time limit $\tau \rightarrow \infty$. In this subsection we describe the main features of the time evolution of the envelope (148), obtained by numerically solving eqs. (142). Specifically, let us analyze how the transient changes when we move along the line (b) in Figs. 15 and 23, which corresponds to $\tilde{\alpha}_1 = 5$.

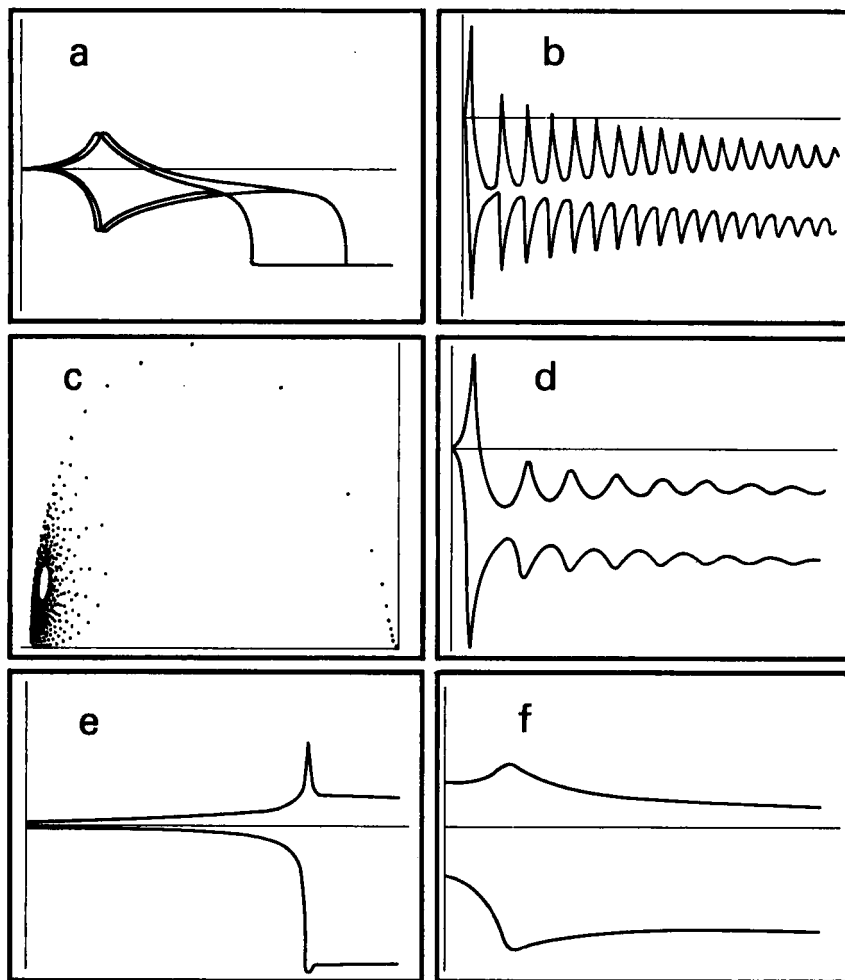
With reference to the numbered dots in Fig. 23, consider the sequence of figures 27a–f. The upper and lower solid lines in each computer solution represent the envelope of self-pulsing, while the horizontal axis is placed in correspondence with the unstable steady state amplitude x of the transmitted field. Figure 27a corresponds to operating conditions to the left of the threshold line DG in Fig. 23. The system undergoes a transient oscillation, but eventually it terminates to the stable low transmission branch. As we change the value of x in such a way that we approach the line DG from the left, the time that the system takes to precipitate becomes longer and longer, showing a pronounced critical slowing down effect. As one moves the operating point to the right of the threshold line DG, the character of the transmitted field changes drastically. Figure 27b shows the evolution of the self-pulsing envelope just to the right of the threshold. The output field, which eventually approaches a stable oscillation, undergoes an extensive transient modulation of its envelope. Sometimes this behavior is called “breathing” (MAYR, RISKEN and VOLLMER [1981]); here the effect is only a transient one. It is especially interesting to examine the envelope breathing in the phase space of the $\{\rho_1, \sigma\}$ variables. This is done in Fig. 27c. In this way the nature of the focal attractor, which is responsible for the stable self-pulsing, is made especially evident. As the operating point is moved farther away from the threshold line, the envelope modulation gradually

disappears (Fig. 27d), while the overall time scale of the approach to steady pulsing state shortens considerably. The focus changes into a node. On the other hand, when we bring the system close to the right boundary of the instability region (line EG in Fig. 23), the time scale begins to grow again (Fig. 27e), and diverges. This new critical slowing down effect arises as usual from a stability changeover. In fact, on the boundary of the instability region the real part of the eigenvalue λ_{11} vanishes.

Next, let us move to the right of the instability region, but still inside the domain of existence of the stable self-pulsing solution (point f in Fig. 23). In this case, if the system is initially only slightly displaced from the steady state in the high transmission branch (*soft excitation*), it simply returns to it, because it is now stable. On the other hand, if the initial displacement is large enough (*hard excitation*), the system approaches the stable self-pulsing state (Fig. 27f). Hence, the region DEG in Fig. 23 is the soft excitation domain, and the region EFHG the hard excitation domain. When we sweep the incident field adiabatically back and forth, as indicated in Figs. 20 and 22, we are automatically in hard excitation conditions.

Finally, if we move to the right of the line EF, no self-pulsing state exists any longer, and hence, the system returns to the steady state in the high transmission state.

Fig. 27. (facing page). (a) Transient evolution of the self-pulsing envelope, followed by precipitation to the low transmission branch. The total run time is 50 units of τ . The picture shows two runs, one for $\tilde{\alpha}_1 = 5$ and $x = 6.5$, the other for $\tilde{\alpha}_1 = 5$ and $x = 6.86$. Both correspond to operating points to the left of the threshold line DG in Fig. 23. Note the critical slowing down exhibited by the solution with $x = 6.86$, whose operating parameters are very close to the line DG. (b) Self-pulsing envelope corresponding to operating values of the parameters which are slightly to the right of the line DG ($\tilde{\alpha}_1 = 5$, $x = 6.867$). The total run time is 600 units of τ , more than ten times the length of the characteristic time scale of Fig. 27a. (c) Phase-space portrait of the solution shown in Fig. 27b. The trajectory lies in the second quadrant of the $\{\rho_1, \sigma\}$ plane. Here we are actually plotting $\tilde{\rho}$ versus $\tilde{\sigma}$ in order to allow an easy comparison of the different numerical features. (d) Same as Fig. 27b, with $\tilde{\alpha}_1 = 5$ and $x = 6.87$. The total run time is 300 units of τ . Note the rapid decrease of both the breathing effect and the overall time scale. (e) Same as Fig. 27b, with $\tilde{\alpha}_1 = 5$ and $x = 7.65$. Here the operating point is slightly on the left of the line EG in Fig. 23. The total run time is 300 units of τ . Note the marked critical slowing down. (f) Same as Fig. 27b, with $\tilde{\alpha}_1 = 5$, $x = 7.68$. Here the operating point lies in the hard excitation domain. The total run time is 15 units of τ .



2.5.6. Hopf bifurcations and unstable limit cycles

As we said in § 2.5.4, the real part of the complex conjugate eigenvalues of the linearized counterparts of eqs. (142) undergoes a sign change as the scan line crosses the threshold line DG. Because the imaginary part remains finite, the conditions for the existence of a Hopf bifurcation are met all along the line DG. Upon close inspection of the region immediately above the line DG one finds that precipitation persisted even under conditions that insured the existence of a focal attractor. This effect is consistent with the existence of an *unstable limit cycle* that erects a barrier around the attractor and makes it invisible to all trajectories, except to those that originate in the immediate neighborhood of the focus itself. This unstable limit cycle exists in a narrow layer in the plane of Fig. 23 above the line DG.

In order to confirm the presence of the unstable limit cycle in a convincing way, one can produce (LUGIATO, BENZA, NARDUCCI and FARINA [1981, 1983]) time-reversed solutions of the differential equations (142). By moving again along the line (b) of Fig. 23, we find the following features:

- i) The size of the limit cycle increases very rapidly over a very small interval above the value x_{thr} where the line (b) crosses the line DG (Figs. 28b,c).
- ii) The limit cycle is identical in shape and size when approached in a time-reversed fashion, both from its interior and from the outside.
- iii) At a sharply defined value slightly above x_{thr} , the limit cycle disappears abruptly, leaving behind a naked stable focus.

In Fig. 28d we show the time-reversed evolution of the envelope of the transmitted field for the same values of the parameters of Fig. 28c. In this case, the breathing behavior has an infinite duration in time. However, this does not correspond to a physically realizable behavior of the system because the limit cycle is unstable.

We stress that the Hopf bifurcation that we described in this subsection corresponds to the *third instability* that we found in the framework of absorptive optical bistability. The first instability is responsible for the switching between low and high transmission branches, and hence, for the emergence of the hysteresis loop for the transmitted field. The second instability is responsible for the self-pulsing, and can be induced by forcing the control parameters to fall within a well-defined domain of instability. As we have seen, stable self-pulsing can also be induced over a wider domain in the space of control parameters, provided that the system is initially perturbed by a sufficiently large excitation. The third instability occurs at the boundary between the stable self-pulsing and precipitation domains. This is connected with the bifurcation

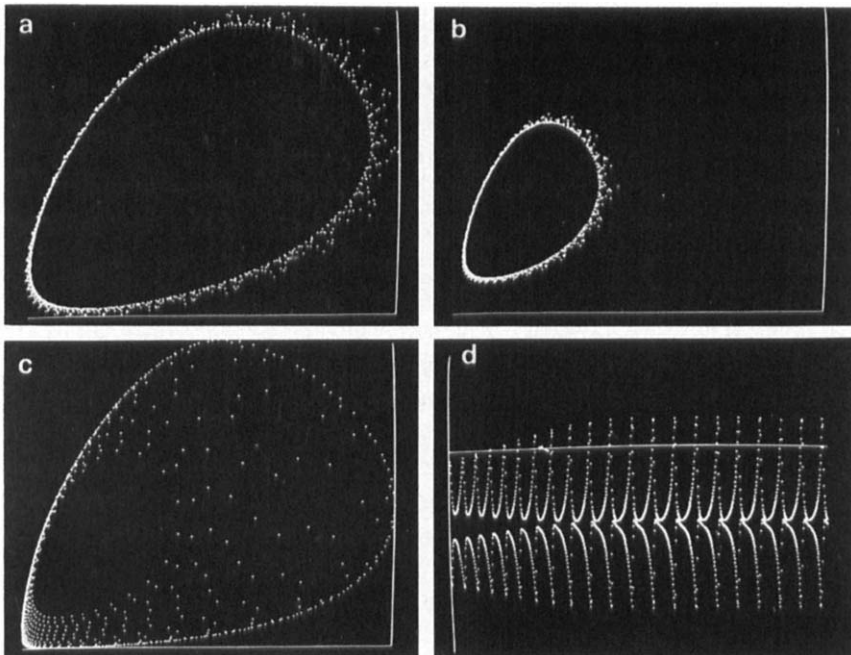


Fig. 28. (a, b) Time reversed phase space trajectory in the $\{\rho_1, \sigma\}$ phase plane reveals the presence of a limit cycle. The operating parameters are $\tilde{\alpha}_1 = 5$, $x = 6.8663$. The total run time is 1000 units of τ . Fig. 28a is an enlarged view of a part of Fig. 28b. Fig. 28b shows the window $0.0044326 \leq \rho_1 \leq 1.81622$, $-1.5024 \leq \sigma \leq -1.1139$. (c) Same as Fig. 28b, but with $x = 6.8669$. The window is the same as in Fig. 28b. Note the size increase of the limit cycle as one moves very slightly away from line DG in Fig. 23. (d) Time-reversed evolution of the envelope of the transmitted field for the same values of the parameters as in Fig. 28c. Here the envelope behaves as a perfect clock that ticks backwards in time.

of a line of stable foci and a manifold of unstable limit cycles. The stability changeover is characterized by pronounced critical slowing down and by strong self-pulsing envelope modulation.

It is reasonable to expect that, by allowing a larger number of unstable modes, one finds a richer bifurcation pattern in absorptive optical bistability. On the other hand, in the case of dispersive optical bistability for proper choices of the parameters (see for instance (96)) one has a sequence of period doubling bifurcations which eventually leads to chaotic behavior, as we discussed in § 2.4.4.

§ 3. Quantum Statistical Treatment

So far, we have systematically neglected any fluctuations, treating the time evolution of the system as completely deterministic. In this section we drop this limitation. This is necessary in order to describe the spectra of transmitted light and of fluorescent light, and the photon statistics of the transmitted light. In particular, under suitable conditions the quantum mechanical fluctuations give rise to nonclassical effects, as for instance photon antibunching or the so-called "squeezing". Furthermore, the discussion of the stability properties of the stationary states of the system is necessarily incomplete when fluctuations are not included. Finally, fluctuations become particularly important in small systems, like the miniaturized bistable devices which are presently the object of very active research in the trend toward practical optical logic devices (GIBBS, McCALL and VENKATESAN [1980], ABRAHAM and SMITH [1982b]).

There are three main sources of fluctuations in our system: (a) quantum mechanical noise, (b) thermal noise and (c) external noise, that is the fluctuations in the incident field.

3.1. THE MANY-MODE AND THE ONE-MODE MASTER EQUATIONS

The starting point of our quantum statistical theory of optical bistability is a suitable master equation that governs the time evolution of the statistical operator $W(t)$ of the system composed by the electric field and the atoms (LUGIATO [1981]). This equation, which includes all the longitudinal modes of the cavity, generalizes the well known one-mode model for the laser (WEIDLICH and HAAKE [1965a,b], HAKEN [1970]) and for optical bistability (BONIFACIO and LUGIATO [1978d]). It holds in the limit (44) and, as we shall show, in the semiclassical approximation it reproduces the Maxwell–Bloch equations (45) and (1b,c).

3.1.1. *The many-mode master equation*

We call A_n, A_n^\dagger the annihilation and creation operators of photons of the longitudinal cavity mode with frequency $\omega_c + \alpha_n$ (see (51)). We have obviously

$$[A_n, A_{n'}^\dagger] = \delta_{nn'} \quad (151)$$

On the other hand, let us consider the atoms. The i th two-level atom ($i = 1 \dots N$) is associated to the raising and lowering operators r_i^+, r_i^- and to

the inversion operator

$$r_{3i} = \frac{1}{2}(r_i^+ r_i^- - r_i^- r_i^+).$$

One has the commutation rules

$$[r_{3i}, r_j^\pm] = \pm r_i^\pm \delta_{ij}, \quad [r_i^+, r_j^-] = 2r_{3i}\delta_{ij}. \quad (152)$$

The atoms are placed inside a sample of length L (Fig. 1). Let z_i be the position of the i th atom. Following BONIFACIO and LUGIATO [1975] we introduce the collective dipole operators

$$R_n^\pm = \sum_{j=1}^N r_j^\pm \exp \left\{ \pm i \left(\frac{\omega_c}{c'} + k_n \right) z_j \right\}, \quad (153)$$

where k_n is defined by eq. (53) and $c' = cL/\mathcal{L}$. Simultaneously we consider the collective inversion operators

$$R_{3,n} = \sum_{j=1}^N r_{3j} \exp \{ -ik_n z_j \}. \quad (154)$$

In particular, $R_{3,0}$ is the one (one half) total inversion operator. The operators (153) and (154) obey the following commutation relations

$$[R_n^+, R_{n'}^-] = 2R_{3,n'-n}, \quad [R_{3,n}, R_{n'}^\pm] = \pm R_{n'\mp n}^\pm. \quad (155)$$

In particular, for each n the triple $R_n^\pm, R_{3,0}$ obeys angular momentum commutation relations

$$(R_n^+, R_n^-) = 2R_{3,0}, \quad [R_{3,0}, R_n^\pm] = \pm R_n^\pm. \quad (156)$$

Now let W_s be the statistical operator of the coupled system atom + radiation field inside the cavity (or equivalently atoms + cavity modes) in the Schrödinger picture. We use a picture in which the frequency of the incident field is eliminated. To this aim we define

$$W(t) = \exp \left[\frac{i}{\hbar} H_0 t \right] W_s(t) \exp \left[-\frac{i}{\hbar} H_0 t \right],$$

$$H_0 = \hbar\omega_0 \left(\sum_n A_n^\dagger A_n + R_{3,0} \right). \quad (157)$$

We formulate the following master equation for $W(t)$

$$\begin{aligned} \frac{dW}{dt'} = & -i\mathcal{L}_F W + \Lambda_F W - i\mathcal{L}_A W \\ & + \Lambda_A W - i\mathcal{L}_{AF} W - i\mathcal{L}_{ext} W + \Lambda_{th,ext} W, \end{aligned} \quad (158)$$

where t' is the time defined by eq. (47) and:

a) \mathcal{L}_F describes the free time evolution of the modes of the cavity

$$\begin{aligned}\mathcal{L}_F W &= \hbar^{-1} [H_F, W], \\ H_F &= \sum_n \hbar((\omega_c - \omega_0) + \alpha_n) A_n^\dagger A_n,\end{aligned}\quad (159)$$

where α_n is defined in eq. (51), and ω_0 is the frequency of the incident field.

b) Λ_F describes the damping of the modes due to the photon escape from the cavity

$$\Lambda_F W = k \sum_n \{ [A_n W, A_n^\dagger] + [A_n, W A_n^\dagger] \}, \quad (160)$$

where the cavity damping constant k is defined by eq. (33).

c) \mathcal{L}_A describes the free time evolution of the atoms:

$$\mathcal{L}_A W = \hbar^{-1} [H_A, W], \quad H_A = \hbar(\omega_a - \omega_0) R_{3,0}, \quad (161)$$

where as usual ω_a is the atomic transition frequency.

d) Λ_A describes the radiative and collisional decay of the atoms:

$$\begin{aligned}\Lambda_A W &= \sum_{i=1}^N \left\{ \frac{\gamma_{\parallel}}{2} ([r_i^-, W r_i^+] + [r_i^- W, r_i^+]) \right. \\ &\quad \left. + \left(\gamma_{\perp} - \frac{\gamma_{\parallel}}{2} \right) ([r_{3i}, W r_{3i}] + [r_{3i} W, r_{3i}]) \right\}\end{aligned}\quad (162)$$

where the part proportional to $\gamma_{\perp} - \gamma_{\parallel}/2$ is a dephasing term.*

e) \mathcal{L}_{AF} describes the interaction between the atomic system and the cavity modes in the dipole and rotating wave approximations

$$\begin{aligned}\mathcal{L}_{AF} &= \hbar^{-1} [H_{AF}, W], \\ H_{AF} &= i\hbar\bar{g} \sum_n (A_n^\dagger R_n^- - A_n R_n^+),\end{aligned}\quad (163)$$

where the coupling constant \bar{g} is given by

$$\bar{g} = \left(\frac{2\pi\omega_0 L}{\hbar V \mathcal{L}} \right)^{1/2} \mu. \quad (164)$$

* Strictly speaking, when the temperature is greater than zero there is also an upward transition term, which has the same form as the first term in eq. (162), with r_i^+ and r_i^- exchanged. We neglect this term, which produces only a negligible correction to the quantum fluctuation term in eq. (177), below.

f) \mathcal{L}_{ext} takes into account the presence of the external field

$$\mathcal{L}_{\text{ext}} = \hbar^{-1} [H_{\text{ext}}, W], \quad H_{\text{ext}} = i\hbar k \alpha_0 (A_0^+ - A_0), \quad (165)$$

where α_0 is given by

$$\alpha_0 = \left(\frac{V\mathcal{L}}{8\pi\hbar\omega_0 L} \right)^{1/2} \frac{E_1}{\sqrt{T}}. \quad (166)$$

This term injects a coherent field inside the cavity. In fact, if one neglects \mathcal{L}_{AF} and $A_{\text{th,ext}}$ one easily verifies that in the long time limit all the modes approach the vacuum state, except the resonant mode $n = 0$ which approaches the coherent state $|\alpha_0\rangle$.

g) $A_{\text{th,ext}}$ takes into account thermal fluctuations and simulates the fluctuations of the incident field (SCHENZLE and BRAND [1978], DRUMMOND, MCNEIL and WALLS [1980b]) in the limit in which they can be described as a white noise:

$$A_{\text{th,ext}} W = 2k \sum_n \bar{n}_n [A_n, [W, A_n^\dagger]]. \quad (167)$$

In the case of thermal fluctuations, \bar{n} is given by

$$\bar{n}_n = \frac{1}{\exp[\beta\hbar(\omega_c + \alpha_n)] - 1}, \quad \beta = \frac{1}{k_B T}, \quad (168)$$

where k_B is Boltzmann's constant and T is the temperature (not to be confused with the transmissivity coefficient of the mirrors, which is indicated by the same symbol in this chapter). In the case of fluctuations of the incident field $\bar{n}_n = 0$ for $n \neq 0$, while \bar{n}_0 measures the strength of these fluctuations. In the general case, \bar{n}_n is the sum of the contributions from thermal and external fluctuations.

3.1.2. Connection with the semiclassical theory

Let us now derive from the master equation (158) the time evolution equations for the mean values $\langle A_n \rangle(t') = \text{Tr}(A_n W(t'))$, $\langle R_n^- \rangle(t')$, and $\langle R_{3n} \rangle(t')$. This is easily done using the commutation rules (151), (152), (155) and the definitions (153), (154). We obtain

$$\langle \dot{A}_n \rangle = -i((\omega_c - \omega_0) + \alpha_n) \langle A_n \rangle - k[\langle A_n \rangle - \alpha_0 \delta_{n0}] + \bar{g} \langle R_n^- \rangle, \quad (169a)$$

$$\langle \dot{R}_n^- \rangle = 2\bar{g} \sum_{n'} \langle A_{n'} R_{3,n-n'} \rangle - \gamma_\perp (1 + i\Delta) \langle R_n^- \rangle, \quad (169b)$$

$$\begin{aligned} \langle \dot{R}_{3,n} \rangle &= -\bar{g} \sum_{n'} [\langle A_{n'}^\dagger R_{n'+n}^- \rangle + \langle A_{n'} R_{n'-n}^+ \rangle] \\ &\quad - \gamma_\parallel [\langle R_{3,n} \rangle + \frac{1}{2}N\delta_{n0}], \end{aligned} \quad (169c)$$

where we have assumed that $\sum_{i=1}^N \exp(ik_n z_i) = N\delta_{n0}$, as one has for a lattice structure of the atomic system (BONIFACIO and LUGIATO [1975]). The equation for $\langle R_n^+ \rangle$ is immediately obtained from eq. (169b), by taking into account that

$$\langle R_n^- \rangle = \langle R_n^+ \rangle^*, \quad \langle A_n \rangle = \langle A_n^\dagger \rangle^*, \quad \langle R_{3,n} \rangle = \langle R_{3,-n} \rangle^*.$$

Next, we introduce the *semiclassical approximation*, that is, we factorize the mean values of the products of a field and an atomic operator into the corresponding products of mean values (for instance $\langle A_{n'} R_{3,n''} \rangle \rightarrow \langle A_{n'} \rangle \langle R_{3,n''} \rangle$). This approximation becomes exact in the thermodynamic limit $N \rightarrow \infty$, $V \rightarrow \infty$ with $N/V = \text{constant}$. Thus, equations (169) become identical to eq. (54), provided one makes the following correspondences

$$\begin{aligned} f_n &= \mu \left(\frac{8\pi\omega_0 L}{\hbar\gamma_\perp\gamma_\parallel V\mathcal{L}} \right)^{1/2} \langle A_n \rangle, \\ p_n &= - \left(\frac{N}{2} \sqrt{\frac{\gamma_\parallel}{\gamma_\perp}} \right)^{-1} \langle R_n^- \rangle, \\ d_n &= - \left(\frac{N}{2} \right)^{-1} \langle R_{3,n} \rangle. \end{aligned} \quad (170)$$

This is easily verified using eqs. (53), (166), (2), (164), (7a), and (33), and the definitions $k\theta = \omega_n - \omega_0$, and $C = \alpha L/2T$. This result proves that, in the semiclassical approximation, the master equation reproduces eqs. (54) and hence, the Maxwell–Bloch equations (45) and (1b,c) which are equivalent to eq. (54).

3.1.3. The one-mode master equation

With only one exception (BENZA and LUGIATO [1981]), all the papers that deal with the quantum statistical treatment of optical bistability use the *one-mode approximation*. Accordingly, in the following we shall use the master

equation (158), but neglecting all the off-resonance modes $n \neq 0$. Furthermore, we shall use the notations A , R^\pm , R_3 and \bar{n} instead of A_0 , R_0^\pm , $R_{3,0}$ and \bar{n}_0 . The model that we obtain in such a way is the quantum statistical analogue of the semiclassical mean field model (55) (BONIFACIO and LUGIATO [1978d]).

In introducing the one-mode approximation, we assume that the values of the parameters are such that no self-pulsing instability can arise (see § 2.4). Furthermore, since the phenomena that we are going to describe occur on a time scale much longer than the cavity transit time, we can replace the time t' , defined by eq. (47), by the real time t .

For the following treatment it is useful to introduce an alternative expression of the interaction Hamiltonian H_{AF} restricted to the resonant mode $n = 0$:

$$H_{\text{AF}} = i\hbar\bar{g} \sum_{i=1}^N (A^\dagger \tilde{r}_i^- - A \tilde{r}_i^+), \quad (163')$$

where

$$\tilde{r}_i^\pm = r_i^\pm \exp\left(\pm i \frac{\omega_c}{c'} z_i\right). \quad (171)$$

The three operators \tilde{r}_i^\pm , r_{3i} obey the same commutation rules (152). In the following, we shall always use \tilde{r}_i^\pm , but we shall systematically drop the superscript \sim .

Finally, in the following sections, we shall always *restrict ourselves to the resonant situation* $\Delta = \theta = 0$, because no particularly interesting novelty arises in the general case $\Delta, \theta \neq 0$.

3.2. THE FOKKER-PLANCK EQUATION FOR THE GENERALIZED WIGNER FUNCTION

The master equation (158) is too complicated to be solved exactly, even in the one-mode approximation. Further approximations must be introduced. The first one exploits the presence of a smallness parameter in our system. This parameter is the inverse of the saturation photon number (which corresponds to the saturation intensity I_s defined in eq. (7.3)), given by

$$N_s = \frac{\gamma_\perp \gamma_\parallel}{4\bar{g}^2}. \quad (172)$$

In order to introduce this approximation, we begin translating eq. (158), restricted to $n = 0$, into a c-number partial differential equation. This can be

performed via the characteristic function technique devised by Haken and coworkers (HAKEN [1970]). Precisely, one introduces a characteristic function by which five c-number quantities are associated with the operators R^\pm , R_3 , A and A^\dagger . The Fourier transform of this function is a quasi-probability distribution in five variables. Its time evolution is governed by a classical looking partial differential equation, which is derived from the master equation by suitable techniques. By means of this distribution, one can calculate the expectation values of products of operators in suitable order as classical mean values of the corresponding c-number variables. This procedure, which creates a bridge between the quantum mechanical density operator and the classical density function, generalizes the notions of the Wigner function (WIGNER [1932]), and of the Glauber P -function (GLAUBER [1963a,b]). The time evolution equation for the distribution function contains derivatives of all orders. The condition $N_s \gg 1$ allows us to introduce the *Fokker–Planck approximation*, which consists of neglecting the terms with derivatives of order higher than second.

A crucial point concerns the ordering prescription for the operators in the characteristic function. Actually, different choices such as normal, antinormal, or symmetrical ordering, lead to different quasiprobability distributions, which in turn give normal, antinormal or symmetrical-ordered expectation values, respectively. The distributions themselves obey different equations according to the chosen ordering prescription.

In order to treat laser fluctuations, Haken and coworkers (HAKEN [1970]) adopted the normal ordering prescription, which is the most natural one in quantum optics, and therefore used a generalized Glauber distribution. However, as was first shown in GRONCHI and LUGIATO [1978], this procedure is not suitable in the case of optical bistability, because it leads to a Fokker–Planck equation whose diffusion matrix is not in general positive definite. In order to avoid this difficulty, the proper choice is that of symmetrical ordering. Hence, the characteristic function is

$$C(\xi, \xi^*, \eta, \zeta, \zeta^*, t) = \\ = \text{Tr}[\exp(i\xi R^- + i\xi^* R^+ + i\eta R_3 + i\zeta A + i\zeta^* A^\dagger) W(t)], \quad (173)$$

whose Fourier transform $P_w(\bar{v}, \bar{v}^*, \bar{m}, \beta, \beta^*, t)$ is a generalization of the Wigner function to include the atomic variables. P_w is normalized to unity and is always real but not necessarily positive, hence, it is a quasiprobability distribution. The moments of P_w give symmetrized expectation values, for instance

$$\int d_2 \bar{v} d\bar{m} d_2 \beta P_w(\bar{v}, \bar{v}^*, \bar{m}, \beta, \beta^*, t) \cdot \beta^* \beta = \frac{1}{2} [\langle A^\dagger A \rangle(t) + \langle A A^\dagger \rangle(t)], \quad (174)$$

where $d_2\bar{v} = d(\operatorname{Re} \bar{v}) d(\operatorname{Im} \bar{v})$, etc. The partial differential equation which rules the evolution of P_w can be derived either via the simple constructive procedure of GRONCHI and LUGIATO [1978], which is summarized in Appendix D, or via suitable techniques (GILMORE [1974]) which allow us to disentangle the exponential in eq. (173) into a product of exponentials, and hence, allow the operator approach of HAKEN [1970]. For $\Delta = \theta = 0$, and in terms of the normalized variables, corresponding to eqs. (10) and (48),

$$\begin{aligned} x &= \frac{\beta}{\sqrt{N_s}}, \quad y = \frac{\alpha_0}{\sqrt{N_s}}, \\ v &= -\left(\frac{N}{2}\sqrt{\frac{\gamma_{\parallel}}{\gamma_{\perp}}}\right)^{-1}\bar{v}, \quad m = -\left(\frac{N}{2}\right)^{-1}\bar{m}, \end{aligned} \quad (175)$$

this equation reads (GRONCHI and LUGIATO [1978])

$$\begin{aligned} \frac{\partial}{\partial t} P_w(v, v^*, m, x, x^*, t) &= \\ \left\{ -\frac{\partial}{\partial v} [-\gamma_{\perp}(v - mx)] - \frac{\partial}{\partial v^*} [-\gamma_{\perp}(v^* - mx^*)] \right. \\ &\quad \left. - \frac{\partial}{\partial m} \{-\gamma_{\parallel}[m - 1 + \frac{1}{2}(v^*x + vx^*)]\} \right\} \\ &\quad - \frac{\partial}{\partial x} [-k(x - y + 2Cv)] - \frac{\partial}{\partial x^*} [-k(x^* - y + 2Cv^*)] \\ &\quad + \frac{\gamma_{\perp}^2}{k} \frac{1}{2CN_s} \left[\frac{\partial^2}{\partial v^* \partial v} - \frac{\bar{d}^2}{4} \frac{\partial}{\partial m} \left(\frac{\partial}{\partial v} v + \frac{\partial}{\partial v^*} v^* \right) + \frac{\bar{d}^2}{4} \frac{\partial^2}{\partial m^2} (1 - m) \right] \\ &\quad + \frac{k}{N_s} (1 + 2\bar{n}) \frac{\partial^2}{\partial x^* \partial x} \left\} P_w(v, v^*, m, x, x^*, t) + O\left(\frac{1}{N_s^{3/2}}\right), \end{aligned} \quad (176)$$

where $\bar{d} = \gamma_{\parallel}/\gamma_{\perp}$ and we have taken into account the relation

$$C = \frac{\bar{g}^2 N}{2k\gamma_{\perp}} \quad (176')$$

which follows immediately from the definition $C = \alpha L/2T$ and eqs. (7a), (2), (33) and (164). Since $N_s \gg 1$, we can introduce the Fokker–Planck approxi-

mation, neglecting the terms which are not explicitly written in eq. (176). Thus eq. (176) becomes a Fokker–Planck equation. Furthermore, the drift (i.e. first-order derivative) terms are larger than the diffusion (i.e. second-order derivative) terms by a factor of N_s . This fact ensures the smallness of fluctuations. If we also drop the diffusion terms, we recover the deterministic semi-classical description (55).

While the drift coefficients do not depend on the ordering prescription, the diffusion coefficients do. The matrix of the diffusion coefficients in eq. (176) is positive definite for all values of the parameters, at least in the physically relevant domain $|m| \leq 1$.

3.2.1. Good cavity case: adiabatic elimination of the atomic variables

The Fokker–Planck equation (176) is still too complicated to be solved, even at steady state. This situation is greatly simplified in the two limit situations, that in § 2.3.1 were called “good cavity case” and “bad cavity case”. In fact, in the first case we can *adiabatically eliminate* the atomic variables from the Fokker–Planck equation, in the second the field variables. The adiabatic elimination can be performed following the procedure of GORDON [1967] and HAKEN [1977].

In the good cavity case $k \ll \gamma_{\perp}, \gamma_{\parallel}$ we obtain the following closed Fokker–Planck equation for the field variables (LUGIATO [1979], LUGIATO, CASAGRANDE and PIZZUTO [1982]):

$$\begin{aligned} k^{-1} \frac{\partial}{\partial t} P_w(x, x^*, t) = & \left\{ -\frac{\partial}{\partial x} \left[y - x - \frac{2Cx}{1 + |x|^2} \right] + \text{c.c.} \right. \\ & - \frac{C}{2N_s} \frac{\partial^2}{\partial x^2} x^2 \frac{(1 + |x|^2)^2 + 1 + \bar{d}}{(1 + |x|^2)^3} + \text{c.c.} \\ & \left. + \frac{1}{N_s} \frac{\partial^2}{\partial x^* \partial x} \left[1 + 2\bar{n} + C \frac{(1 + |x|^2)^2(2 + |x|^2) - (1 + \bar{d})|x|^2}{(1 + |x|^2)^3} \right] \right\} P_w(x, x^*, t), \end{aligned} \quad (177)$$

where $P_w(x, x^*, t)$ is obtained from the full distribution by integration over $\text{Re } v$, $\text{Im } v$ and m . It will be useful to rephrase eq. (177) in polar coordinates

$$x = r \exp(i\varphi). \quad (178)$$

We obtain

$$\begin{aligned}
 k^{-1} \frac{\partial}{\partial t} P_w(r, \varphi, t) = & \frac{1}{r} \left\{ \frac{\partial}{\partial r} r \left[r + \frac{2Cr}{1+r^2} - y \cos \varphi \right] + \frac{\partial}{\partial \varphi} y \sin \varphi \right. \\
 & + \frac{1}{4N_s} \left[\frac{\partial}{\partial r} r \frac{\partial}{\partial r} \left(1 + 2\bar{n} + 2C \frac{r^4 + (1-\bar{d})r^2 + 1}{(1+r^2)^3} \right) \right. \\
 & \left. \left. + (1 + 2\bar{n} + 2C) \frac{1}{r} \frac{\partial^2}{\partial \varphi^2} \right] \right\} P_w(r, \varphi, t), \quad (177')
 \end{aligned}$$

from which one sees by simple inspection that the diffusion matrix is positive definite, since $\bar{d} \leq 2$. In eq. (177') we have neglected a contribution proportional to $N_s^{-1} \ll 1$ in the drift term. The same approximation is used in eq. (237), below.

3.2.2. Bad cavity case: adiabatic elimination of the field variables

In the bad cavity case $k \gg \gamma_{\perp}, \gamma_{\parallel}$, we can adiabatically eliminate the field variables from eq. (176). Thus, we obtain the following Fokker–Planck equation for the atomic variables (LUGIATO [1979])

$$\begin{aligned}
 \frac{\partial}{\partial t} P_w(v, v^*, m, t) = & \left\{ -\gamma_{\perp} \left[\frac{\partial}{\partial v} (-v + ym - 2Cmv) + \text{c.c.} \right] \right. \\
 & - \gamma_{\parallel} \frac{\partial}{\partial m} [1 - m - \frac{1}{2}y(v + v^*) + 2Cv^*v] \\
 & + \frac{\gamma_{\perp}^2}{k} \frac{1}{2CN_s} \left[\frac{\partial^2}{\partial v^* \partial v} (1 + 2Cm^2) - \left(\frac{\partial^2}{\partial v^* \partial m} \bar{d} (\frac{1}{4}\bar{d}v + Cmv) + \text{c.c.} \right) \right. \\
 & \left. \left. + \frac{\partial^2}{\partial m^2} \frac{\bar{d}^2}{2} \left(\frac{1-m}{2} + Cv^*v \right) \right] \right\} P_w(v, v^*, m, t), \quad (179)
 \end{aligned}$$

where $P_w(v, v^*, m, t)$ is obtained from the full distribution by integration over $\text{Re } x$ and $\text{Im } x$.

Furthermore, we obtain the following “adiabatic formula”

$$\hat{x} = y - 2Cr^-, \quad (180)$$

where the operator \hat{x} corresponds to the c-number variable x , while \hat{r} corresponds to v :

$$\hat{x} = \frac{A}{\sqrt{N_s}}, \quad \hat{r} = - \left(\frac{N}{2} \sqrt{\frac{\gamma_{||}}{\gamma_{\perp}}} \right)^{-1} R^{-}. \quad (181)$$

Equation (180) reduces the calculation of expectation values and time correlation functions of field quantities to expectation values and correlation functions of atomic quantities. For instance, $\langle x \rangle(t) = y - 2C\langle \hat{r}^- \rangle$, etc. Of course eq. (180) holds only for $k \gg \gamma_{\perp}, \gamma_{||}$.

3.3. SPECTRUM OF TRANSMITTED LIGHT

The spectrum $S(\omega)$ of the transmitted light is given by the Fourier transform of the time correlation function at steady state $\langle A^\dagger(t) A(0) \rangle_{st}$:

$$S(\omega) = \frac{1}{\pi} \operatorname{Re} \int_0^\infty dt \exp[-i(\omega - \omega_0)t] \langle A^\dagger(t) A(0) \rangle_{st}. \quad (182)$$

Hence, to obtain the spectrum one must calculate the fluctuations of the system around the steady state. More specifically, for any given incident field y let us choose one of the two stable steady states, and let us call x_{st} the normalized transmitted field in the chosen state. Subdividing $A(t)$ into the stationary mean value $\langle A \rangle_{st} = x_{st} \sqrt{N_s}$ (see eq. (181)), and the fluctuation $\delta A(t) = A(t) - \langle A \rangle_{st}$, we have that $S(\omega)$ is composed of a coherent and an incoherent part

$$S(\omega) = S_{coh}(\omega) + S_{inc}(\omega), \quad (183)$$

$$S_{coh}(\omega) = N_s x_{st}^2 \delta(\omega - \omega_0), \quad (184)$$

$$S_{inc}(\omega) = \frac{1}{\pi} \operatorname{Re} \int_0^\infty dt \exp[-i(\omega - \omega_0)t] \langle \delta A^\dagger(t) \delta A(0) \rangle_{st}. \quad (185)$$

The coherent or classical part has the same frequency as the injected field and is proportional to the intensity x_{st}^2 of the transmitted field. The incoherent part is the quantum mechanical contribution and arises from the fluctuations around the steady state.

It is useful to also introduce the hermitian and antihermitian parts of the

operator \hat{x} defined by eq. (181):

$$\hat{x}_1 = \frac{\hat{x} + \hat{x}^\dagger}{2}, \quad \hat{x}_2 = \frac{\hat{x} - \hat{x}^\dagger}{2i}. \quad (186)$$

In terms of these operators, the incoherent part of the spectrum has the expression

$$\begin{aligned} S_{\text{inc}}(\omega) = & \frac{N_s}{\pi} \operatorname{Re} \int_0^\infty dt \exp[-i(\omega - \omega_0)t] \\ & \times [\langle \delta\hat{x}_1(t) \delta\hat{x}_1(0) \rangle_{\text{st}} + \langle \delta\hat{x}_2(t) \delta\hat{x}_2(0) \rangle_{\text{st}} \\ & + i\langle \delta\hat{x}_1(t) \delta\hat{x}_2(0) \rangle_{\text{st}} - i\langle \delta\hat{x}_2(t) \delta\hat{x}_1(0) \rangle_{\text{st}}]. \end{aligned} \quad (185')$$

In the bad cavity case, taking into account that from eq. (180) we have $\delta\hat{x} = -2C\delta\hat{r}^-$, the expression of $S_{\text{inc}}(\omega)$ to be used is

$$S_{\text{inc}}(\omega) = \frac{4C^2 N_s}{\pi} \operatorname{Re} \int_0^\infty dt \exp[-i(\omega - \omega_0)t] \langle \delta\hat{r}^+(t) \delta\hat{r}^-(0) \rangle_{\text{st}}. \quad (187)$$

The integrated incoherent spectrum is given by

$$S_{\text{inc}}^{(\text{int})} = \int_0^\infty d\omega S_{\text{inc}}(\omega) = \langle \delta\hat{A}^\dagger \delta\hat{A} \rangle_{\text{st}}; \quad (188)$$

in the bad cavity case it becomes

$$S_{\text{inc}}^{(\text{int})} = 4C^2 N_s \langle \delta\hat{r}^+ \delta\hat{r}^- \rangle_{\text{st}}. \quad (188')$$

The reflected field (Fig. 1) is given by (compare eqs. (3a,b))

$$\begin{aligned} E_R(t) = & -\sqrt{R} E_I + \sqrt{RT} E(L, t - \Delta t) \\ = & \sqrt{R} [E_T(t - \Delta t) - E_I]. \end{aligned} \quad (189)$$

Hence, the coherent part of the spectrum of reflected light is given by $RN_s(y - x_{\text{st}})^2 \delta(\omega - \omega_0)$, and is in a sense complementary to the coherent part of the transmitted light. On the other hand, the incoherent part of the spectrum of reflected light is identical to that of transmitted light, apart from a factor of $R \approx 1$.

In this section we assume that thermal fluctuations and external field fluctuations are negligible, hence, we set $\bar{n} = 0$ in eqs. (176) and (177).

3.3.1. Good cavity case

In the case $k \ll \gamma_{\perp}, \gamma_{\parallel}$ we start from eq. (177). As for $N_s \gg 1$ the fluctuations are small, we can linearize the Fokker–Planck equation (177) around steady state. Hence, we introduce the deviations from steady state

$$x' = x - x_{st}, \quad (x^*)' = x^* - x_{st}. \quad (190)$$

The linearized Fokker–Planck equation takes a particularly simple form in terms of the variables (compare eq. (186))

$$x'_1 = \frac{x' + (x^*)'}{2}, \quad x'_2 = \frac{x'_1 - (x^*)'}{2i} \quad (191)$$

It reads (LUGIATO [1979], CASAGRANDE and LUGIATO [1980])

$$\begin{aligned} k^{-1} \frac{\partial}{\partial t} P_w(x'_1, x'_2, t) = & \left\{ \frac{\partial}{\partial x'_1} \lambda x'_1 + \frac{\partial}{\partial x'_2} \lambda_{\varphi} x'_2 \right. \\ & + \frac{1}{4N_s} \left[1 + 2C \frac{x_{st}^4 + (1 - \bar{d})x_{st}^2 + 1}{(1 + x_{st}^2)^3} \right] \frac{\partial^2}{\partial x'^2_1} \\ & \left. + \frac{1 + 2C}{4N_s} \frac{\partial^2}{\partial x'^2_2} \right\} P_w(x'_1, x'_2, t), \end{aligned} \quad (192)$$

where

$$\lambda = \left. \frac{dy}{dx} \right|_{x_{st}} = 1 + 2C \frac{1 - x_{st}^2}{(1 + x_{st}^2)^2}, \quad \lambda_{\varphi} = \frac{y}{x_{st}} = 1 + \frac{2C}{1 + x_{st}^2} \quad (193)$$

and the function $y(x)$ is defined by eq. (32). Note that $\tilde{\lambda}$ and λ_{φ} coincide with $-\lambda_n^{(+)}$ and $-\lambda_n^{(-)}$ respectively, if one puts $n = 0$ (resonant mode) in eqs. (84). They also coincide with $-k^{-1}\lambda_1$ and $-k^{-1}\lambda_2$ given by eq. (58).

To obtain the incoherent part of the spectrum, according to eq. (185') we must calculate the time correlation functions $\langle \delta\dot{x}_1(t) \delta\dot{x}_1(0) \rangle_{st}$, etc. To do that we use the regression theorem (LAX [1967]) which ensures that the time correlation functions $\langle \delta\dot{x}_1(t) \delta\dot{x}_1(0) \rangle_{st}$, and $\langle \delta\dot{x}_1(t) \delta\dot{x}_2(0) \rangle_{st}$, obey the same time evolution equation as $\langle \delta\dot{x}_1 \rangle(t)$, and similarly, the time correlation functions $\langle \delta\dot{x}_2(t) \delta\dot{x}_2(0) \rangle_{st}$, and $\langle \delta\dot{x}_2(t) \delta\dot{x}_1(0) \rangle_{st}$, obey the same time evolution equation as $\langle \delta\dot{x}_2 \rangle(t)$. Since $\langle \delta\dot{x}_i \rangle(t) = \langle x'_i \rangle(t)$ ($i = 1, 2$), the equations for $\langle \delta\dot{x}_i \rangle(t)$ are immediately obtained from eq. (192), and read

$$\langle \delta\dot{x}_1 \rangle(t) = -k\tilde{\lambda}\langle \delta\dot{x}_1 \rangle(t), \quad \langle \delta\dot{x}_2 \rangle(t) = -k\lambda_{\varphi}\langle \delta\dot{x}_2 \rangle(t). \quad (194)$$

Hence, from eq. (185') we have

$$S_{\text{inc}}(\omega) = \frac{N_s}{\pi} \operatorname{Re} \int_0^\infty dt \exp[-i(\omega - \omega_0)t] \\ \times [e^{-k\lambda t} (\langle \delta\hat{x}_1^2 \rangle_{\text{st}} + i\langle \delta\hat{x}_1 \delta\hat{x}_2 \rangle_{\text{st}}) \\ + e^{-k\lambda_\varphi t} (\langle \delta\hat{x}_2^2 \rangle_{\text{st}} - i\langle \delta\hat{x}_2 \delta\hat{x}_1 \rangle_{\text{st}})]. \quad (195)$$

The variances $\langle \delta\hat{x}_1^2 \rangle_{\text{st}}$, etc. are also easily obtained from eq. (192). In fact, taking into account that $\langle (x'_i)^2 \rangle(t) = \langle (\delta\hat{x}_i)^2 \rangle(t)$ ($i = 1, 2$) and $\langle x'_1 x'_2 \rangle(t) = (1/2)\langle \delta\hat{x}_1 \delta\hat{x}_2 + \delta\hat{x}_2 \delta\hat{x}_1 \rangle(t)$ (compare eq. (174)) we have

$$\langle \delta\hat{x}_1^2 \rangle_{\text{st}} = \frac{1}{4N_s \tilde{\lambda}} \left(1 + 2C \frac{x_{\text{st}}^4 + (1 - \bar{d})x_{\text{st}}^2 + 1}{(1 + x_{\text{st}}^2)^3} \right), \quad (196a)$$

$$\langle \delta\hat{x}_2^2 \rangle_{\text{st}} = \frac{1}{4N_s \lambda_\varphi} (1 + 2C), \quad (196b)$$

$$\frac{1}{2}(\langle \delta\hat{x}_1 \delta\hat{x}_2 \rangle_{\text{st}} + \langle \delta\hat{x}_2 \delta\hat{x}_1 \rangle_{\text{st}}) = 0. \quad (196c)$$

By combining eq. (196c) with the commutation rule $[\delta\hat{x}_1, \delta\hat{x}_2] = i/2N_s$, we have

$$\langle \delta\hat{x}_1 \delta\hat{x}_2 \rangle_{\text{st}} = -\langle \delta\hat{x}_2 \delta\hat{x}_1 \rangle_{\text{st}} = \frac{i}{4N_s} \quad (196c')$$

Finally, by inserting eq. (196a,b) and (196c') into eq. (195) we obtain (LUGIATO [1979])

$$S_{\text{mc}}(\omega) = \frac{Ck}{2\pi} \frac{x_{\text{st}}^2}{1 + x_{\text{st}}^2} \left\{ \frac{2x_{\text{st}}^2 + 1 - \bar{d}}{(1 + x_{\text{st}}^2)^2} \frac{1}{(\omega - \omega_0)^2 + k^2 \tilde{\lambda}^2} \right. \\ \left. + \frac{1}{(\omega - \omega_0)^2 + k^2 \lambda_\varphi^2} \right\}. \quad (197)$$

Hence, $S_{\text{inc}}(\omega)$ is given by the superposition of two Lorentzians, whose weights are inversely proportional to $\tilde{\lambda}$ and λ_φ , respectively. Note, however, that the weight of the first Lorentzian is not always positive.

According to eq. (188), the integrated incoherent spectrum is given by

$$S_{\text{inc}}^{(\text{int})} = \frac{C}{2} \frac{x_{\text{st}}^2}{1 + x_{\text{st}}^2} \left\{ \frac{2x_{\text{st}}^2 + 1 - \bar{d}}{(1 + x_{\text{st}}^2)^2} \frac{1}{\lambda} + \frac{1}{\lambda_\varphi} \right\}. \quad (198)$$

Let us now analyze the spectrum for $C \gg 1$, first in the purely radiative case $\gamma_{\parallel} = 2\gamma_{\perp} \equiv \gamma$ (i.e. $\bar{d} = 2$), then for $\gamma_{\parallel} \ll \gamma_{\perp}$ (i.e. $\bar{d} \ll 1$):

a) $\bar{d} = 2$ ($\gamma_{\parallel} = 2\gamma_{\perp}$). For $y \ll C$ (so that $x_{st} \ll 1$, $y \approx 2Cx_{st}$) it follows from eqs. (198) and (193) that $S_{inc}^{(int)}$ is proportional to x_{st}^4 , and hence, to y^4 . On the other hand, for $y \gg C$ (i.e. $x_{st} \approx y$), $S_{inc}^{(int)}$ saturates to the value $C/2$. Furthermore $S_{inc}^{(int)}$ diverges when the bistability thresholds y_M and y_m (see Fig. 8) are approached, because $\tilde{\lambda} \rightarrow 0$. (compare § 2.3.1). In the neighborhood of y_M and y_m the linearization of the Fokker-Planck equation fails.

Let us now consider the lineshape $S_{inc}(\omega)$. As shown by eq. (197), for $k \ll \gamma_{\perp}$, γ_{\parallel} the linewidth is scaled by the empty cavity halfwidth k . The relevant eigenvalues $\tilde{\lambda}$ and λ_{φ} are always real. For $y \ll C$ it follows from eq. (193) that $\lambda_{\varphi} \approx \tilde{\lambda} \approx 2C$. Hence, the width of the spectrum is $4Ck$, much larger than the empty-cavity width $2k$. Since $C \propto N$, in this situation the linewidth is proportional to the number of atoms (*cooperative line broadening*). As one sees from eq. (197), in this situation the weight of the first Lorentzian is negative. Consequently the line gets a hole in the middle, so that it takes the shape of a doublet (Fig. 29a,b). This is a purely quantum mechanical effect, as we shall show in § 3.3.3.

Increasing y the doublet character disappears (Fig. 29c). Approaching the upper bistability threshold y_M the spectrum becomes a narrow line (Fig. 29d). In fact $\tilde{\lambda} \rightarrow 0$ so that the soft-mode contribution from the first term in eq. (197) dominates the cooperative background from the second term. This *line narrowing* is clearly a manifestation of the critical slowing down illustrated in § 2.3.1.

When we cross the threshold $y = y_M$, jumping to the one-atom branch, the spectrum changes discontinuously from a narrow line to a line whose width coincides with the empty cavity width $2k$ (Fig. 29e). In fact, for $y \gtrsim y_M$ one has $x \approx y$, and from eq. (193) we have $\lambda_{\varphi} \approx \tilde{\lambda} \approx 1$. For $y \gg y_M$, the incoherent part of the spectrum does not change increasing y (Fig. 29f). In fact, one finds

$$S_{inc}(\omega) \approx \frac{C}{2\pi} \frac{k}{(\omega - \omega_0)^2 + k^2}. \quad (197')$$

Let us now decrease y along the one-atom branch. Approaching the lower bistability threshold $y = y_m$ the line becomes narrower and narrower, because again $\tilde{\lambda} \rightarrow 0$ (see Fig. 22g,h). Finally, crossing the lower threshold, the spectrum suddenly broadens because the system jumps to the cooperative branch.

b) $\bar{d} \ll 1$ ($\gamma_{\parallel} \ll \gamma_{\perp}$). In this case, the behavior of $S_{inc}(\omega)$ is qualitatively similar to that of the case $\bar{d} = 2$, except for $y \ll C$. In fact, for $\bar{d} \ll 1$, both weights

in eq. (197) are always positive, so that for $y \ll C$ the spectrum is not a doublet but a single line of width $4Ck$.

These results have been generalized to the case $\Delta, \theta \neq 0$ in DRUMMOND and WALLS [1981].

The spectrum of transmitted light in the good cavity case, including all the longitudinal modes of the cavity, is given in BENZA and LUGIATO [1981], on the basis of the many-mode master equation (158). Their paper also describes the behavior of this spectrum when we approach the self-pulsing instability domain.

3.3.2. Bad cavity case

The details of the calculation of $S_{\text{inc}}(\omega)$ for $k \gg \gamma_{\perp}, \gamma_{\parallel}$ starting from the Fokker–Planck equation (179) are given in LUGIATO [1979]. Again, one finds that $S_{\text{inc}}(\omega)$ is given by the superposition of few Lorentzians which are peaked at $\omega = \omega_0 + \text{Im } \lambda_i$, and have width $-\text{Re } \lambda_i$, where λ_i are the eigenvalues of the linearized semiclassical mean field equations (see § 2.3.1). Namely, the relevant eigenvalues $-\lambda_i$ are

$$\lambda_{\frac{\alpha}{\beta}} = \frac{\gamma_{\perp}}{2} \left\{ \bar{d} + \frac{y}{x_{\text{st}}} \pm \left[\left(\bar{d} - \frac{y}{x_{\text{st}}} \right)^2 - 4\bar{d}x_{\text{st}}(2x_{\text{st}} - y) \right]^{1/2} \right\}, \quad (199)$$

$$\lambda_{\gamma} = \gamma_{\perp} \frac{y}{x_{\text{st}}} = \gamma_{\perp} \lambda_{\phi}. \quad (200)$$

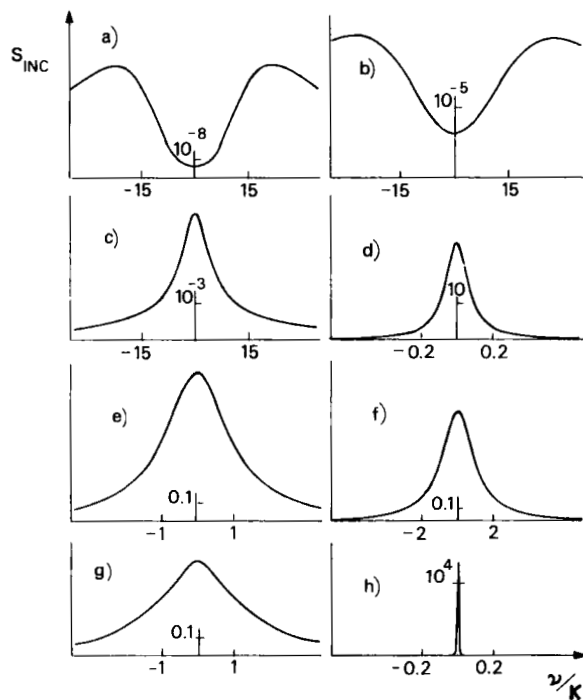
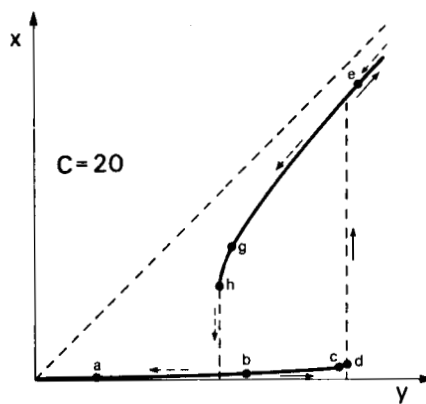
The real part of the root λ_{β} coincides with the damping constant $\bar{\lambda}$ discussed in § 2.3.1; when (x, y) lies on the cooperative branch λ_{β} is well approximated by expression (59). When $\lambda_{\frac{\alpha}{\beta}}$ are real $S_{\text{inc}}(\omega)$ is given by the superposition of three Lorentzians:

$$S_{\text{inc}}(\omega) = \frac{C\gamma_{\perp}^2}{\pi k} \sum_{i=\alpha, \beta, \gamma} w_i \frac{\lambda_i}{(\omega - \omega_0)^2 + \lambda_i^2}, \quad (201)$$

where

$$w_{\gamma} = \frac{1}{2\lambda_{\gamma}} \frac{x_{\text{st}}^2}{1 + x_{\text{st}}^2},$$

$$w_{\frac{\alpha}{\beta}} = \mp \frac{1}{2\lambda_{\frac{\alpha}{\beta}}} \frac{x_{\text{st}}^2}{1 + x_{\text{st}}^2} \frac{1}{\lambda_{\alpha}^2 - \lambda_{\beta}^2} [(\bar{d} - 1)\lambda_{\alpha}^2 - \gamma_{\parallel}(\bar{d} - 1 - 2x_{\text{st}}^2)]. \quad (202)$$



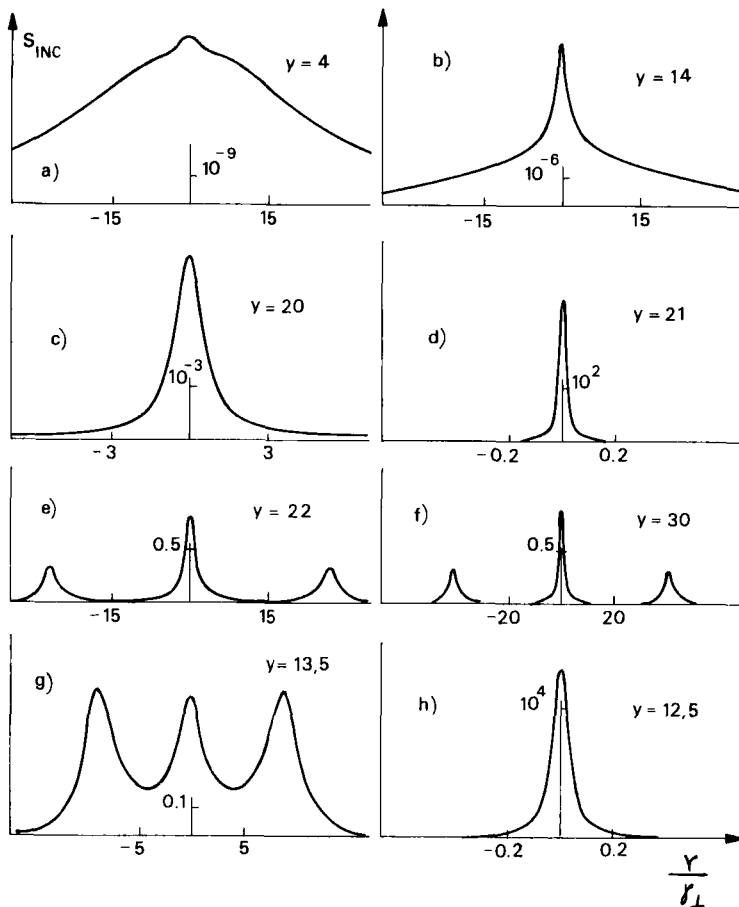


Fig. 30. Hysteresis cycle of the incoherent part of the spectrum $S_{\text{inc}}(\omega)$ of the transmitted light in the *bad cavity case* $k \gg \gamma_{\perp}, \gamma_{\parallel}$ for $\gamma_{\parallel} = 2\gamma_{\perp}$, $C = 20$. The points of the (x, y) plane corresponding to (a)–(h) are indicated in Fig. 29. See also caption of Fig. 29.

Fig. 29. (facing page). Hysteresis cycle of the incoherent part of the spectrum $S_{\text{inc}}(\omega)$ of the transmitted light in the *good cavity case* $k \ll \gamma_{\perp}, \gamma_{\parallel}$ for $\gamma_{\parallel} = 2\gamma_{\perp}$, $C = 20$. The point of the (x, y) plane corresponding to (f) does not appear because y is too large. Here and in figure 30 we have (i) $v = \omega - \omega_0$, where ω_0 is the frequency of the incident field, (ii) S_{inc} is given in units $C/2\pi k$, (iii) the scale varies from diagram to diagram as indicated, (iv) y has the values (a) $y = 4.06$, (b) $y = 14.193$, (c) $y = 20.589$, (d) $y = 21.026$, (e) $y = 21.995$, (f) $y = 31.33$, (g) $y = 13.39$, (h) $y = 12.48$.

When $\lambda_\alpha, \lambda_\beta$ are complex conjugate one puts

$$\frac{\lambda_\alpha}{\lambda_\beta} = \lambda_R \pm i\lambda_I \quad (203)$$

and obtains

$$S_{inc}(\omega) = \frac{C\gamma_\perp^2}{\pi k} \left\{ w_\gamma \frac{\lambda_\gamma}{(\omega - \omega_0)^2 + \lambda_\gamma^2} + g(\omega - \omega_0) + g(\omega_0 - \omega) \right\}, \quad (204)$$

where

$$g(v) = \frac{1}{8} \frac{1}{\lambda_R^2 - \lambda_I^2} \frac{\gamma_\perp^3}{(v - \lambda_I)^2 + \lambda_R^2} \left\{ 2\bar{d}^2(2x_{st}^2 + 1 - \bar{d}) - \frac{v}{\gamma_\perp \lambda_R} [(\bar{d} - 1)(\lambda_R^2 + \lambda_I^2) - \gamma_\parallel^2(\bar{d} - 1 - 2x_{st}^2)] \right\} \frac{x_{st}^2}{1 + x_{st}^2}. \quad (205)$$

For $\gamma_\parallel = 2\gamma_\perp$ eqs. (201) and (204) coincide with the formulas independently derived in AGARWAL, NARDUCCI, GILMORE and FENG [1978a,b] via quantum mechanical Langevin equations.

According to eq. (188'), the integrated spectrum is given by

$$S_{inc}^{(int)} = C \frac{\gamma_\perp}{k} \frac{x_{st}^4}{(1 + x_{st}^2)y(y/x_{st} + \bar{d})[y/x_{st} + x_{st}(2x_{st} - y)]} \times \left\{ \frac{\bar{d}}{2}(2x_{st} + y) + \left(1 - \frac{\bar{d}}{2}\right) \frac{y}{x_{st}^2} \left[x_{st}(2x_{st} - y) + \frac{y}{x_{st}} + \bar{d} \right] \right\}. \quad (206)$$

For $y \ll C$ we have $S_{inc}^{(int)} \propto x_{st}^4$ as in the good cavity case. For $y \gg C$ $S_{inc}^{(int)}$ saturates to the value $\gamma_\perp C/k$. Furthermore $S_{inc}^{(int)}$ diverges as usual when we approach the bistability thresholds y_M and y_m .

As we see from eqs. (199) and (200), in the bad cavity case the linewidth of the transmitted field is scaled by the atomic linewidth γ_\perp . The hysteresis cycle of the spectrum for $\gamma_\parallel = 2\gamma_\perp \equiv \gamma$ is shown in Fig. 30 for $C \gg 1$. When the system is on the cooperative branch, $\lambda_\alpha, \lambda_\beta$ are real, so that the spectrum $S_{inc}(\omega)$ is a single line. For $y \ll C$ one has $\lambda_\alpha \approx \lambda_\gamma \approx C\gamma, \lambda_\beta \approx \gamma$. In these conditions the contribution of the term proportional to w_β in eq. (201) is negligible, so that the spectrum is a broad line (Fig. 30a) whose halfwidth is γC , which coincides with the cooperative linewidth γ_R of pure superfluorescence (BONIFACIO and LUGIATO [1975]). Since $C \propto N$, in this situation the linewidth

is proportional to the number of atoms (cooperative line broadening) exactly as in the good cavity case. Increasing y along the cooperative branch, the peak corresponding to the soft mode λ_β emerges from the cooperative background (Fig. 30b). Approaching the upper bistability threshold we have the usual line narrowing, in which the soft mode dominates and the cooperative background is completely negligible (Fig. 30c,d). This line narrowing is accompanied by strong atom-atom correlations (LUGIATO [1979]).

Let us now cross the threshold $y = y_M$, so that the system jumps to the one-atom branch. The roots $\lambda_\alpha, \lambda_\beta$ are complex conjugate, so that the spectrum suddenly becomes a triplet (Fig. 30e). This means a *discontinuous* appearance of a *Dynamical Stark Effect*. For $y \gg y_M$ one has $x_{st} \approx y$ and $\lambda_\gamma \approx \frac{1}{2}\gamma, \lambda_R \approx \frac{3}{4}\gamma, \lambda_I \approx \frac{1}{2}\gamma\sqrt{2}$ (compare eqs. (60) and (61)). Hence, since $\lambda_I \gg \lambda_R, x_{st} \gg 1$, $S_{inc}(\omega)$ takes the simple form

$$S_{inc}(\omega) \propto \left\{ \frac{\frac{1}{2}\gamma}{((\omega - \omega_0)^2 + \frac{1}{4}\gamma^2)} + \frac{1}{2} \left[\frac{\frac{3}{4}\gamma}{((\omega - \omega_0 - \Omega_I)^2 + \frac{9}{16}\gamma^2)} + \frac{\frac{3}{4}\gamma}{((\omega - \omega_0 + \Omega_I)^2 + \frac{9}{16}\gamma^2)} \right] \right\}, \quad (207)$$

where Ω_I is the Rabi frequency of the incident field, defined in eq. (61). Equation (207) coincides with the lineshape predicted for the spectrum of fluorescent light in the high intensity situation by the one-atom theory of resonance fluorescence (MOLLOW [1969]). For $C \gg 1$ one has $\Omega_I \gg \gamma$, so that the sidebands are well separated from the central line (Fig. 30f).

Let us now decrease y along the one-atom branch. The two sidebands get nearer and nearer to the central line (Fig. 30g) until in the vicinity of the lower threshold $y = y_m$ the roots $\lambda_\alpha, \lambda_\beta$ become real and one again has a line narrowing, because the linewidth $2\lambda_\beta$ tends to zero (Fig. 30h).

3.3.3. Nonclassical effects in the transmitted field

In the previous subsection we have seen that, in the good cavity case (eq. (197)), the weight of the first Lorentzian in the expression for $S_{inc}(\omega)$ is negative in the purely radiative case $\bar{d} = 2$ for $y \ll C$. This is a consequence of the fact that, if we consider the Fokker-Planck equation for the Glauber P -function equivalent to eq. (177'), its radial diffusion coefficient is negative in these conditions. In fact, this coefficient is proportional to the weight of the first

Lorentzian in eq. (197). Moreover, in general, the lack of positive definiteness in the Fokker–Planck equation for the Glauber P -function (or generalized Glauber P -function) is an indication of the rise of nonclassical effects in the transmitted field. These effects arise specifically from the noncommutative character of the creation and annihilation operators.

The most well known effect is *photon antibunching* which is defined as follows. Let us consider the second-order correlation function

$$g^{(2)}(t) = \frac{\langle A^\dagger(0) A^\dagger(t) A(t) A(0) \rangle_{\text{st}}}{\langle A^\dagger A \rangle_{\text{st}}^2}.$$

For purely coherent light $g^{(2)}(t) = 1$; one has *bunching* when $g^{(2)}(t) > 1$ (GLAUBER [1963]) and *antibunching* for $g^{(2)}(t) < 1$. Let us now analyze this problem in the case of optical bistability (DRUMMOND and WALLS [1980], CASAGRANDE and LUGIATO [1980]). By taking into account the first of eqs. (181), and that $x_{\text{st}} = O(1)$, $\delta\hat{x} = O(N_s^{-1/2})$, we obtain, after simple calculations,

$$g^{(2)}(0) = 1 + \frac{4}{x_{\text{st}}^2} \left(\langle \delta\hat{x}_1^2 \rangle_{\text{st}} - \frac{1}{4N_s} \right) + O(N_s^{-3/2}). \quad (208)$$

Using eqs. (196a) and (193) we have

$$\langle \delta\hat{x}_1^2 \rangle_{\text{st}} - \frac{1}{4N_s} = \frac{C}{2\tilde{\lambda}N_s} \frac{x_{\text{st}}^2(2x_{\text{st}}^2 + 1 - \bar{d})}{(1 + x_{\text{st}}^2)^3}. \quad (209)$$

For $\bar{d} = 2$ (purely radiative case) and $x_{\text{st}} \ll 1$ (i.e. $y \ll C$), it follows from eq. (209) that $\langle \delta\hat{x}_1^2 \rangle - (1/4N_s)$ is negative, hence, there is antibunching. As we see from eqs. (208) and (209), this effect is small, since $N_s \gg 1$. Note that the expression (209) is proportional to the weight of the first Lorentzian in (197). As shown by CASAGRANDE and LUGIATO [1980] $g^{(2)}(t) = g^{(2)}(0) \exp(-k\tilde{\lambda}t)$. Furthermore, the antibunching effect in the cooperative branch also arises in the bad cavity case.

Another nonclassical effect that has become popular in recent years is the so-called “squeezing”. The squeezed states are characterized by the fact that the variance in one of the two quadrature components is smaller than in the coherent Glauber states. Namely, let us consider the two operators

$$A_1 = \frac{A + A^\dagger}{2}, \quad A_2 = \frac{A - A^\dagger}{2i}. \quad (210)$$

In the coherent states, which are minimum uncertainty states, one has

$$\langle \delta A_1^2 \rangle_{\text{st}} = \langle \delta A_2^2 \rangle_{\text{st}} = 1/4. \quad (211)$$

The state is squeezed when $\langle \delta A_1^2 \rangle < 1/4$ or $\langle \delta A_2^2 \rangle < 1/4$ (one cannot have both simultaneously because of Heisenberg's indetermination rule). This type of state is important in the framework of optical communication, interferometry and gravitational wave detection (YUEN [1976], MEYSTRE and SCULLY [1983]).

Now, since $\delta A_1 = \sqrt{N_s} \delta \dot{x}_1$, we see immediately from eq. (209) that, in the case of optical bistability (for $A = \theta = 0$) when there is photon antibunching there is also squeezing in the component A_1 . This effect is small because $\langle \delta A_1^2 \rangle_{\text{st}}$ always remains larger than 0.21 (LUGIATO and STRINI [1982a]). However, it increases in the case of multiphoton bistability where one finds that $\langle \delta A_1^2 \rangle_{\text{st}}$ can be as small as 1/16 (LUGIATO and STRINI [1982b,c]). In optical bistability, antibunching and squeezing are cooperative effects which arise from atom–atom correlations.

We observe that thermal and external fluctuations tend to destroy the antibunching and squeezing effects. In fact, if $\bar{n} \neq 0$ in eq. (177) we obtain, instead of eq. (209),

$$\langle \delta \dot{x}_1^2 \rangle - \frac{1}{4N_s} = \frac{1}{2\lambda N_s} \left[\frac{x_{\text{st}}^2(2x_{\text{st}}^2 + 1 - \bar{d})}{(1 + x_{\text{st}}^2)^3} + \bar{n} \right]. \quad (209')$$

Hence, if \bar{n} is large enough expression (209') is positive for all values x_{st} . Also atomic number fluctuations tend to destroy nonclassical effects (DRUMMOND and WALLS [1981]).

We stress that the nonclassical effects discussed in this section arise from atom–atom correlations. In fact, previous treatments which neglected atom–atom correlations (see for instance BONIFACIO, GRONCHI and LUGIATO [1978]) led to a Fokker–Planck equation for the Glauber P -function with a positive definite diffusion matrix, and hence, without antibunching and squeezing. In LUGIATO, CASAGRANDE and PIZZUTO [1982] it is shown that the procedure based on the generalized Wigner distribution is more complete and accurate than these previous treatments.

3.4. SPECTRUM OF FLUORESCENT LIGHT

In this section we consider the spectrum $I(\omega)$ of the fluorescent light emitted at 90° with respect to the incident light. It is proportional to the Fourier

transform of the time correlation function $\sum_{i=1}^N \langle r_i^+(t) r_i^-(0) \rangle_{\text{st}}$, where r_i^\pm are the raising and lowering operators of the i th two-level atom (see § 3.1.3)

$$I(\omega) \propto \frac{1}{\pi} \operatorname{Re} \int_0^\infty dt \exp[-i(\omega - \omega_0)t] \sum_{i=1}^N \langle r_i^+(t) r_i^-(0) \rangle_{\text{st}}. \quad (212)$$

By subdividing $r_i^\pm(t)$ into the stationary mean value $\langle r_i^\pm \rangle_{\text{st}} = \langle R^\pm \rangle_{\text{st}}/N$ and the fluctuation $\delta r_i^\pm(t) = r_i^\pm(t) - \langle r_i^\pm \rangle_{\text{st}}$, we show that $I(\omega)$ is composed of a coherent and an incoherent part:

$$I(\omega) = I_{\text{coh}}(\omega) + I_{\text{inc}}(\omega), \quad (213)$$

$$I_{\text{coh}}(\omega) \propto \sum_{i=1}^N |\langle r_i^- \rangle|^2 \delta(\omega - \omega_0) = N^{-1} |\langle R^- \rangle_{\text{st}}|^2 \delta(\omega - \omega_0), \quad (214a)$$

$$I_{\text{inc}}(\omega) \propto \frac{N}{\pi} \operatorname{Re} \int_0^\infty dt \exp[-i(\omega - \omega_0)t] \langle \delta r_1^+(t) \delta r_1^-(0) \rangle_{\text{st}}, \quad (214b)$$

where in eq. (214b) we have replaced the index i by 1 on account of the symmetry between the atoms.

Using eqs. (170) and (50) we show immediately that

$$I_{\text{coh}}(\omega) \propto \frac{N}{4} \bar{d} \frac{x_{\text{st}}^2}{(1 + x_{\text{st}}^2)} \delta(\omega - \omega_0). \quad (215)$$

The integrated spectrum $I_F = \int d\omega I(\omega)$ is given by

$$I_F \propto \sum_{i=1}^N \langle r_i^+ r_i^- \rangle_{\text{st}} = \frac{N}{2} + \langle R_3 \rangle_{\text{st}} = \frac{N}{2} \frac{x_{\text{st}}^2}{1 + x_{\text{st}}^2}, \quad (216)$$

where we have again used eqs. (170) and (50). On the other hand, from eq. (215) we obtain

$$I_{\text{coh}}^{(\text{int})} = \int d\omega I_{\text{coh}}(\omega) \propto \frac{N}{4} \bar{d} \frac{x_{\text{st}}^2}{(1 + x_{\text{st}}^2)^2}. \quad (217)$$

Hence, the integrated incoherent spectrum is given by

$$I_{\text{inc}}^{(\text{int})} = I_F - I_{\text{coh}}^{(\text{int})} \propto \frac{N}{2} \frac{x_{\text{st}}^2}{(1 + x_{\text{st}}^2)^2} \left(1 - \frac{\bar{d}}{2} + x_{\text{st}}^2 \right). \quad (218)$$

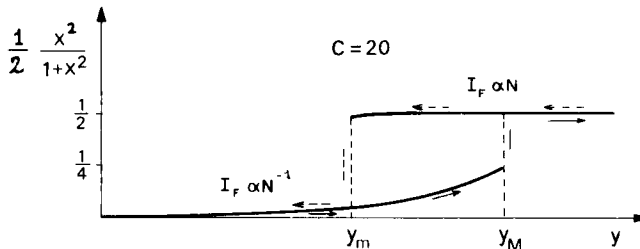


Fig. 31. Hysteresis cycle of the total fluorescent intensity I_F , which is proportional to the population of the upper level, $(N/2)(x^2/1+x^2)$.

From eqs. (217) and (218) we get

$$\frac{I_{\text{coh}}^{(\text{int})}/I_{\text{inc}}^{(\text{int})}}{1 - \frac{\bar{d}}{2} + \frac{x_{\text{st}}^2}{2}} = \frac{\bar{d}/2}{\bar{d}}. \quad (218')$$

For $\bar{d} \ll 1$ one always has $I_{\text{coh}}^{(\text{int})} \ll I_{\text{inc}}^{(\text{int})}$. For $\bar{d} = 2$ one has that $I_{\text{coh}}^{(\text{int})} \gg I_{\text{inc}}^{(\text{int})}$ in the cooperative stationary state, and the contrary in the one-atom stationary state.

Let us now focus our attention on the fluorescent intensity emitted in a unit solid angle at 90° , which is proportional to (216). Its hysteresis cycle is shown in Fig. 31. In the one-atom branch, where $x_{\text{st}} = y$, this intensity is proportional to the number of atoms as usual. On the other hand, in the cooperative branch, where $x_{\text{st}} \approx y/2C \propto N^{-1}$, the fluorescent intensity is inversely proportional to the number of atoms. This is a remarkable cooperative effect (BONIFACIO and LUGIATO [1976]). The first observations of the hysteresis cycle of the fluorescent intensity have been made recently by GRANT and KIMBLE [1982] (Fig. 32) and ARECCHI, GIUSFREDI, PETRIELLA and SALIERI [1982].

3.4.1. Calculation of the incoherent part of the spectrum

The time evolution equation for the time correlation function $\langle r_1^+(t) r_1^-(0) \rangle_{\text{st}}$ in eq. (214b) is immediately obtained from the master eq. (158), restricted to the resonant mode $n = 0$, via the regression theorem (LAX [1967]). In fact, on using the commutation rules (151), (152) and the form (163') of the interaction Hamiltonian we obtain the equation

$$\langle r_1^+ \rangle(t) = 2\bar{g} \langle A^\dagger r_{31} \rangle(t) - \gamma_\perp \langle r_1^+ \rangle(t).$$

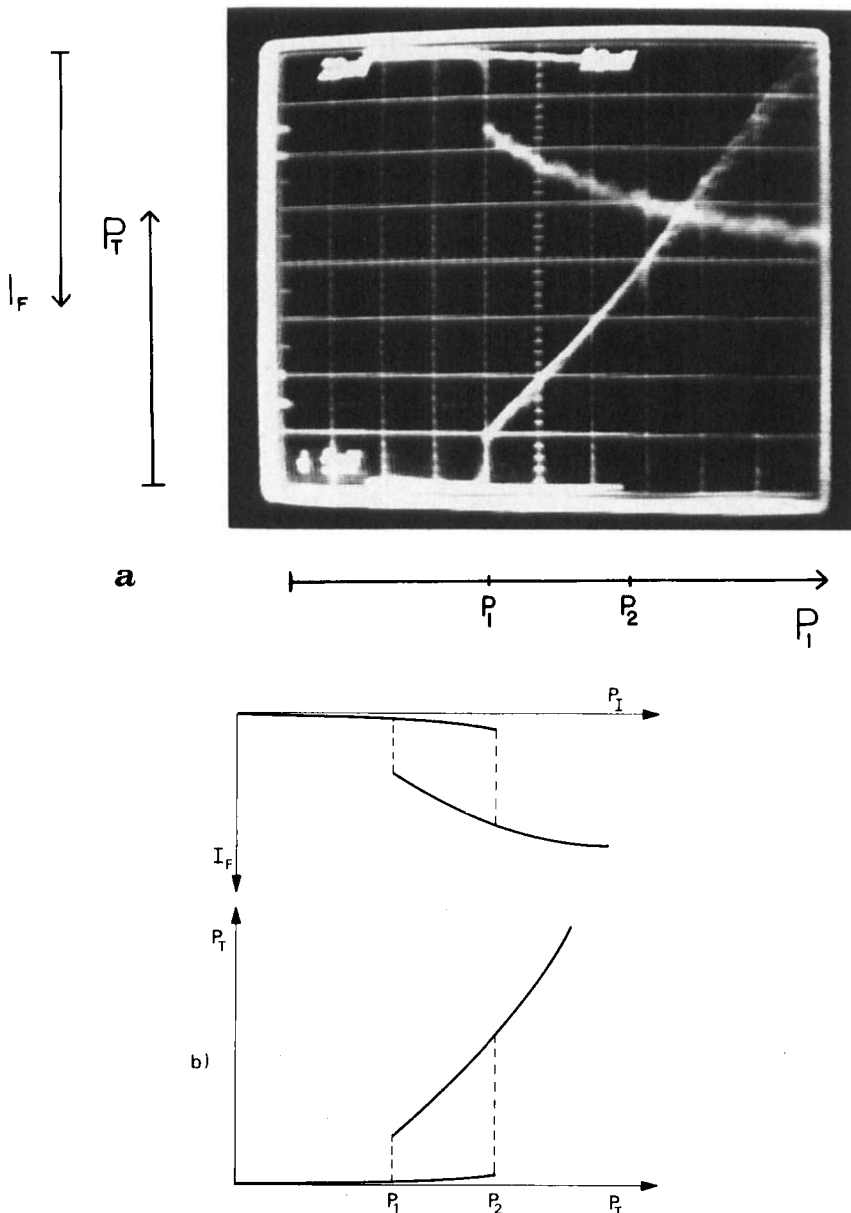


Fig. 32. Simultaneous observation of output power P_T and fluorescent intensity I_F in an atomic beam of sodium traveling through a confocal cavity (from KIMBLE [1982]). The bistability is purely absorptive. Figure 32b explains the picture in Fig. 32a. In this experiment $C = \alpha L \mathcal{F}/2\pi = 35$, where the cavity finesse \mathcal{F} is $\mathcal{F} \approx 210$. The time taken to switch the incident power up and down is 10 ms. The switching points occur at $P_1 = 0.63$ mW and $P_2 = 1$ mW.

The regression theorem states that the time evolution equation of $\langle r_1^+(t) r_1^-(0) \rangle_{st}$ has the same form as that of $\langle r_1^+ \rangle(t)$. Hence, it reads

$$\frac{d}{dt} \langle r_1^+(t) r_1^-(0) \rangle_{st} = 2\bar{g} \langle A^\dagger(t) r_{31}(t) r_1^-(0) \rangle_{st} - \gamma_\perp \langle r_1^+(t) r_1^-(0) \rangle_{st}. \quad (219a)$$

We shall consider eq. (219a) together with the time evolution equations for $\langle r_1^-(t) r_1^-(0) \rangle_{st}$ and $\langle r_{31}(t) r_1^-(0) \rangle_{st}$, which read

$$\frac{d}{dt} \langle r_1^-(t) r_1^-(0) \rangle_{st} = 2\bar{g} \langle A(t) r_{31}(t) r_1^-(0) \rangle_{st} - \gamma_\perp \langle r_1^-(t) r_1^-(0) \rangle_{st}, \quad (219b)$$

$$\begin{aligned} \frac{d}{dt} \langle r_{31}(t) r_1^-(0) \rangle_{st} &= -\bar{g} (\langle A(t) r_1^+(t) r_1^-(0) \rangle_{st}) \\ &- \langle A^\dagger(t) r_1^-(t) r_1^-(0) \rangle_{st} - \gamma_\parallel (\langle r_{31}(t) r_1^-(0) \rangle_{st} + \frac{1}{2} \langle r_1^- \rangle_{st}). \end{aligned} \quad (219c)$$

Next, we introduce the deviations of r_1^\pm , r_{31} , A and A^\dagger from their respective stationary values,

$$\begin{aligned} r_1^\pm(t) &= \langle r_1^\pm \rangle_{st} + \delta r_1^\pm(t), & r_{31}(t) &= \langle r_{31} \rangle_{st} + \delta r_{31}(t), \\ A(t) &= \langle A \rangle_{st} + \delta A(t), \end{aligned} \quad (220)$$

and insert eq. (220) into eqs. (219). By taking into account the fact that, at steady state, one has (using eq. (151), (152) and (158)) and setting $d\langle r_1^\pm \rangle/dt = d\langle r_{31} \rangle/dt = 0$

$$\begin{aligned} 0 &= 2\bar{g} \langle A^\dagger r_{31} \rangle_{st} - \gamma_\perp \langle r_1^+ \rangle_{st} \\ &= 2\bar{g} (\langle A^\dagger \rangle_{st} \langle r_{31} \rangle_{st} + \langle \delta A^\dagger \delta r_{31} \rangle_{st}) - \gamma_\perp \langle r_1^+ \rangle_{st}, \end{aligned} \quad (221a)$$

$$0 = 2\bar{g} (\langle A \rangle_{st} \langle r_{31} \rangle_{st} + \langle \delta A \delta r_{31} \rangle_{st}) - \gamma_\perp \langle r_1^- \rangle_{st}, \quad (221b)$$

$$\begin{aligned} 0 &= -\bar{g} (\langle A \rangle_{st} \langle r_1^+ \rangle_{st} + \langle \delta A \delta r_1^+ \rangle_{st} + \langle A^\dagger \rangle_{st} \langle r_1^- \rangle_{st} + \langle \delta A^\dagger \delta r_1^- \rangle_{st}) \\ &- \gamma_\parallel (\langle r_{31} \rangle_{st} + 1/2), \end{aligned} \quad (221c)$$

we obtain the equations

$$\begin{aligned} \frac{d}{dt} \langle \delta r_1^+(t) \delta r_1^-(0) \rangle_{st} &= 2\bar{g} \{ \langle A^\dagger \rangle_{st} \langle \delta r_{31}(t) \delta r_1^-(0) \rangle_{st} \\ &+ \langle r_{31} \rangle_{st} \langle \delta A^\dagger(t) \delta r_1^-(0) \rangle_{st} + \langle \delta A^\dagger(t) \delta r_{31}(t) \delta r_1^-(0) \rangle_{st} \} \\ &- \gamma_\perp \langle \delta r_1^+(t) \delta r_1^-(0) \rangle_{st}, \end{aligned} \quad (222a)$$

$$\begin{aligned} \frac{d}{dt} \langle \delta r_1^-(t) \delta r_1^-(0) \rangle_{st} &= 2\bar{g} \{ \langle A \rangle_{st} \langle \delta r_{31}(t) \delta r_1^-(0) \rangle_{st} \\ &+ \langle r_{31} \rangle_{st} \langle \delta A(t) \delta r_1^-(0) \rangle_{st} + \langle \delta A(t) \delta r_{31}(t) \delta r_1^-(0) \rangle_{st} \} \\ &- \gamma_\perp \langle \delta r_1^-(t) \delta r_1^-(0) \rangle_{st}, \end{aligned} \quad (222b)$$

$$\begin{aligned} \frac{d}{dt} \langle \delta r_{31}(t) \delta r_1^-(0) \rangle_{st} &= -\bar{g} \{ \langle A \rangle_{st} \langle \delta r_1^+(t) \delta r_1^-(0) \rangle_{st} \\ &+ \langle r_1^+ \rangle_{st} \langle \delta A(t) \delta r_1^-(0) \rangle_{st} + \langle \delta A(t) \delta r_1^+(t) \delta r_1^-(0) \rangle_{st} \\ &+ \langle A^\dagger \rangle_{st} \langle \delta r_1^-(t) \delta r_1^-(0) \rangle_{st} + \langle r_1^- \rangle_{st} \langle \delta A^\dagger(t) \delta r_1^-(0) \rangle_{st} \\ &+ \langle \delta A^\dagger(t) \delta r_1^-(t) \delta r_1^-(0) \rangle_{st} - \gamma_\parallel \langle \delta r_{31}(t) \delta r_1^-(0) \rangle_{st}. \end{aligned} \quad (222c)$$

A crucial point in the quantum statistical treatment of a system with normal fluctuations is the consideration of the scaling properties of the quantities in play, with respect to the size of the system (this is precisely what we did in § 3.2 when we took into account the smallness of the quantity N_s^{-1} , which is proportional to N^{-1}). For instance, one has $\langle A \rangle_{st} \propto N^{1/2}$, $\delta A \propto N^0$. In fact, $\langle \delta A^\dagger(t) \delta A(0) \rangle_{st} \propto N^0$ (see § 3.3.1). Similarly, if we consider the macroscopic polarization operators $R^\pm = \sum_i r_i^\pm$, one has $\langle R^\pm \rangle_{st} \propto N$, $\delta R^\pm \propto N^{1/2}$. In fact, $\langle \delta R^+(t) \delta R^-(0) \rangle_{st} \propto N$, $\langle \delta A^\dagger(t) \delta R^-(0) \rangle_{st} \propto N^{1/2}$, etc. Following this line, one would be tempted to guess that $\delta r_1^\pm \propto N^{-1/2}$. However this is not true in general. In fact, let us consider $\langle \delta r_1^+ \delta r_1^- \rangle_{st}$. We have

$$\begin{aligned} \langle \delta r_1^+ \delta r_1^- \rangle_{st} &= \langle r_1^+ r_1^- \rangle_{st} - \langle r_1^+ \rangle_{st} \langle r_1^- \rangle_{st} \\ &= \langle r_{31} \rangle_{st} + 1/2 - \langle r_1^+ \rangle_{st} \langle r_1^- \rangle_{st} \propto N^0. \end{aligned}$$

Hence, $\langle \delta r_1^+(t) \delta r_1^-(0) \rangle_{st} \propto N^0$. On the other hand,

$$\begin{aligned} \langle \delta r_i^+(t) \delta r_j^-(0) \rangle_{st} &\propto N^{-1} \quad \text{for } i \neq j, \text{ because} \\ \sum_{i \neq j} \langle \delta r_i^+(t) \delta r_j^-(0) \rangle_{st} &= \langle \delta R^+(t) \delta R^-(0) \rangle_{st} \\ &- \sum_{i=1}^N \langle \delta r_i^+(t) \delta r_i^-(0) \rangle_{st} \propto N. \end{aligned}$$

On the basis of these scaling arguments, let us consider the order of magnitude of the various terms in the right hand side of eq. (222a). Taking into account that

$$\begin{aligned} \bar{g} &\propto N^{-1/2}, \quad \langle A^\dagger \rangle_{st} \propto N^{1/2}, \quad \langle \delta r_{31}(t) \delta r_1^-(0) \rangle_{st} \propto N^0, \\ \langle r_{31} \rangle_{st} &\propto N^0, \quad \langle \delta A^\dagger(t) \delta r_1^-(0) \rangle_{st} \propto N^{-1/2}, \end{aligned}$$

$$\begin{aligned}\langle \delta A^\dagger(t) \delta r_{31}(t) \delta r_1^-(0) \rangle_{st} &\propto N^{-1/2}, \\ \langle \delta r_1^+(t) \delta r_1^-(0) \rangle_{st} &\propto N^0.\end{aligned}$$

one concludes that the first and last terms in the right-hand side of eq. (222a) are of order N^0 , whereas the others are of order N^{-1} . Quite similar considerations can be repeated for eqs. (222b) and (222c). Hence, in the limit of large N eqs. (222) reduce to

$$\begin{aligned}\frac{d}{dt} \langle \delta r_1^+(t) \delta r_1^-(0) \rangle_{st} &= 2\bar{g} \langle A^\dagger \rangle_{st} \langle \delta r_{31}(t) \delta r_1^-(0) \rangle_{st} \\ &- \gamma_\perp \langle \delta r_1^+(t) \delta r_1^-(0) \rangle_{st},\end{aligned}\tag{223a}$$

$$\begin{aligned}\frac{d}{dt} \langle \delta r_1^-(t) \delta r_1^-(0) \rangle_{st} &= 2\bar{g} \langle A \rangle_{st} \langle \delta r_{31}(t) \delta r_1^-(0) \rangle_{st} \\ &- \gamma_\perp \langle \delta r_1^-(t) \delta r_1^-(0) \rangle_{st},\end{aligned}\tag{223b}$$

$$\begin{aligned}\frac{d}{dt} \langle \delta r_{31}(t) \delta r_1^-(0) \rangle_{st} &= \\ &= -\bar{g} \{ \langle A \rangle_{st} \langle \delta r_1^+(t) \delta r_1^-(0) \rangle_{st} + \langle A^\dagger \rangle_{st} \langle \delta r_1^-(t) \delta r_1^-(0) \rangle_{st} \} \\ &- \gamma_\parallel \langle \delta r_{31}(t) \delta r_1^-(0) \rangle_{st}.\end{aligned}\tag{223c}$$

Equations (223) give a closed system of equations which has the same form as the corresponding set of equations for the fluorescence of the single atom (MOLLOW [1969]) apart from the replacement of the incident field α_0 with the selfconsistent internal field $\langle A \rangle_{st}$ (LUGIATO [1980b], CARMICHAEL [1981]). The initial conditions for eqs. (223) are

$$\begin{aligned}\langle \delta r_1^+(0) \delta r_1^-(0) \rangle_{st} &= \langle r_1^+ r_1^- \rangle_{st} - \langle r_1^+ \rangle_{st} \langle r_1^- \rangle_{st} \\ &= \frac{1}{2} \frac{x_{st}^2}{(1 + x_{st}^2)^2} (1 - \frac{1}{2}\bar{d} + x_{st}^2),\end{aligned}\tag{224a}$$

$$\langle \delta r_1^-(0) \delta r_1^-(0) \rangle_{st} = -\frac{\bar{d}}{4} \frac{x_{st}^2}{(1 + x_{st}^2)^2},\tag{224b}$$

$$\langle \delta r_{31}(0) \delta r_1^-(0) \rangle_{st} = \frac{1}{4} \bar{d}^{1/2} \frac{x_{st}^3}{(1 + x_{st}^2)^2}.\tag{224c}$$

Since the initial conditions also coincide with those of the one-atom resonance fluorescence after replacement of α_0 by $\langle A \rangle_{\text{st}}$, the expression of the incoherent part of the spectrum is immediately obtained from that given in MOLLOW [1969].

These results are valid for general values of the parameters k , γ_{\perp} , γ_{\parallel} and hence, hold both for a bad and for a good quality cavity. Usually, the regression theorem transfers to the steady state spectrum the behavior (relaxation times, etc.) of the transient approach to steady state. This occurs, for instance, for the one-atom resonance fluorescence and for the spectrum of *transmitted* light in optical bistability. However, as shown by the previous results, this is not the case for the spectrum of *fluorescent* light in optical bistability. This fact is due to the anomalous scaling of the one-atom deviations δr_i^{\pm} , δr_{3i} when they enter into a correlation function for a single atom only. This implies that atom–atom correlations do not play any role in determining the spectrum of fluorescent light, contrary to what occurs for the spectrum of transmitted light.

3.4.2. Comparison of the spectra of fluorescent and transmitted light

In the good cavity case $k \ll \gamma_{\perp}, \gamma_{\parallel}$, the spectrum of fluorescent light is quite different from that of transmitted light. For instance, in the high transmission branch, the spectrum of fluorescent light has a three-peaked structure. On the contrary, the incoherent part of the spectrum of transmitted light is one-peaked and for sufficiently large values of the incident field the linewidth is the empty cavity width (see eq. (197')).

However, in the bad cavity case $k \ll \gamma_{\perp}, \gamma_{\parallel}$, the hysteresis cycle of the incoherent part of the spectrum of fluorescent light shows some similarities with that of the transmitted light, especially in the high transmission branch. In particular, one finds in both cases the discontinuous appearance of the resolved triplet when we increase the incident field, starting from zero (Discontinuous Dynamical Stark Effect). However, the spectrum of fluorescent light does not show line narrowing at the boundaries of the hysteresis cycle, contrary to what we found for the spectrum of the transmitted light. Furthermore, there is no cooperative broadening in the low transmission branch for $y \ll C$. In fact, in the case of fluorescent light, the cooperative behavior only arises via the internal field $\langle A \rangle_{\text{st}}$, which is in general quite different from the incident field. Additional cooperative effects such as line narrowing or broadening are absent, since, as we have seen, atom–atom correlations do not enter into play in the calculation of the spectrum of fluorescent light.

We end this subsection with a comparison between the energy emitted by the system as incoherent transmitted light and the energy emitted as incoherent fluorescent light. This comparison comes naturally because, while in the case of the fluorescent light the incoherent part has, roughly speaking, the same order of magnitude as the coherent one, in the case of the transmitted light the coherent part, which is proportional to the transmitted number of photons $N_s x_{st}^2$, always dominates the incoherent one.

From the master equation (158), as well as from the Fokker–Planck equation (176), one easily obtains the energy balance equation

$$\begin{aligned} \frac{d}{dt} (\langle A^\dagger A \rangle + \langle R_3 \rangle) &= \\ &= k\alpha_0^2 - k\langle A^\dagger A \rangle - k\langle (A^\dagger - \alpha_0)(A - \alpha_0) \rangle - \gamma_{||}(\frac{1}{2}N + \langle R_3 \rangle). \end{aligned} \quad (225)$$

The meaning of the various terms on the right-hand side of eq. (225) is:

$$\begin{aligned} k\alpha_0^2 &\propto \text{incident energy per unit time}, \\ k\langle A^\dagger A \rangle &\propto \text{transmitted energy per unit time}, \\ k\langle (A^\dagger - \alpha_0)(A - \alpha_0) \rangle &\propto \text{reflected energy per unit time}, \\ \gamma(\frac{1}{2}N + \langle R_3 \rangle) &\propto \text{fluorescent light emitted per unit time in all directions}, \\ (\gamma_{||} - \gamma)(\frac{1}{2}N + \langle R_3 \rangle) &\propto \text{energy dissipated in the atomic sample per unit time}; \end{aligned} \quad (226)$$

γ is the natural lifetime, $(\gamma_{||} - \gamma)$ is the inelastic collision rate.

In turn, the transmitted energy is subdivided into a coherent part $k|\langle A \rangle|^2$ and an incoherent part $k|\langle \delta A^\dagger \rangle|^2$, and the total fluorescent energy is composed of a coherent part $\gamma N \langle r_1^+ \rangle \langle r_1^- \rangle$ and an incoherent part $\gamma N \langle \delta r_1^+ \delta r_1^- \rangle$. Let us now compare at steady state the energy emitted as incoherent fluorescent light and the energy emitted as incoherent transmitted light, both per unit time and solid angle. In doing that, we must take into account that the fluorescent light is emitted in all directions, that is in a solid angle 4π , whereas the transmitted light is emitted in a diffraction solid angle λ_0^2/S , where λ_0 is the wavelength of the incident field and $S = V/L$ is the section of the region containing the atom.

We consider the case $k \gg \gamma_{\perp}$, $\gamma_{||}$, $\gamma_{||} = 2\gamma_{\perp} = \gamma$. Furthermore, we consider for definiteness the situation $y \gg y_M$ (one-atom stationary state). In this condition, the incoherent fluorescent light practically coincides with the total fluorescent light. From eqs. (216) and (226) we show that the fluorescent energy emitted per unit time and solid angle is proportional to

$$\mathcal{P}_{\text{inc}}^{(\text{fl})} = \gamma \frac{N}{2} \frac{1}{4\pi}, \quad (227)$$

where we have taken into account that, in the present conditions, $x_{st}^2/(1 + x_{st}^2) \approx 1$. On the other hand, from eqs. (226), (188) and (206) we show that the incoherent transmitted energy per unit time and solid angle is proportional to

$$\mathcal{P}_{inc}^{(tr)} = C \gamma_{\perp} \frac{S}{\lambda_0^2}. \quad (228)$$

Since for $\gamma_{\perp} = \gamma/2$ from eq. (33), (176'), (164) and the relation $\gamma = 4\omega_0^3\mu^2/3\hbar c^3$ (ALLEN and EBERLY [1975]) we have

$$C = \frac{3}{8\pi T} \frac{N\lambda_0^2}{S}, \quad (229)$$

and the ratio between eqs. (227) and (228) is

$$\frac{\mathcal{P}_{inc}^{(fl)}}{\mathcal{P}_{inc}^{(tr)}} = \frac{2}{3} T. \quad (230)$$

Hence, the two energies have roughly the same order of magnitude.

3.5. PHOTON STATISTICS OF THE TRANSMITTED LIGHT AT STEADY STATE

As we anticipated, optical bistability is an example of a first-order-like phase transition in an open system, far from thermal equilibrium. As is well known, this behavior is shown also by other systems in quantum optics, for instance the laser with saturable absorber (KASANTSEV, RAUTIAN and SURDUTOVICH [1970], SALOMAA and STENHOLM [1973], SCOTT, SARGENT and CANTRELL [1975], LUGIATO, MANDEL, DEMBINSKI and KOSSAKOWSKI [1978]), the dye laser (BACZYNISKI, KOSSAKOWSKI and MARSZALEK [1976], SCHAEFER and WILLIS [1976]), sub/second harmonic generation (WOO and LANDAUER [1971], DRUMMOND, McNEIL and WALLS [1980a]), and the bidirectional ring laser (MANDEL, ROY and SINGH [1981]). The characteristic feature of optical bistability is that it occurs in a purely passive system and that it never exhibits a second-order transition. Hence, optical bistability plays the role of a prototype of first-order transition in optical systems, exactly as the usual laser, with active atoms only, is the prototype of second-order phase transition (DEGIORGIO and SCULLY [1970], GRAHAM and HAKEN [1970]). To work out this analogy, one must analyze in full detail the fluctuations of the system. In fact, in the bistable situation, only one of the two stationary solutions is

absolutely stable, while the other is only metastable. The semiclassical treatment is unable to tell us which one of the two is absolutely stable. Actually, the linear stability analysis checks the stability of the stationary solutions only against the “small” fluctuations around each steady state. Also, in the linearized treatment of the previous sections, we have analyzed only the small fluctuations around the stationary solutions, thereby treating stable and metastable states on the same footing. However, the system can also develop “large” fluctuations which make the system “tunnel” from the metastable to the stable solution. The probability of such large fluctuations is extremely small, as we shall show in § 3.6.1; however, to analyze the thermodynamic stability of the steady states, one must develop a treatment which works out the full spectrum of fluctuations. This treatment has been given so far only for the good quality case $k \ll \gamma_{\perp}, \gamma_{\parallel}$ (BONIFACIO, GRONCHI and LUGIATO [1978], LUGIATO, CASAGRANDE and PIZZUTO [1982]), the only exception being DRUMMOND [1982]. In the following subsections, we shall discuss the steady state solution of the Fokker–Planck equation (177).

3.5.1. The case of thermal and external fluctuations

In this subsection, we shall assume that the intrinsic quantum mechanical fluctuations are negligible with respect to the thermal and the external field fluctuations. Hence, in the diffusion coefficients of eq. (177) we keep only the terms proportional to \bar{n} . It is suitable to express this Fokker–Planck equation in terms of the real part x_1 and the imaginary part x_2 of the variable x (compare eqs. (186) and (191)). We obtain

$$k^{-1} \frac{\partial P_w(x_1, x_2, t)}{\partial t} = \left\{ \frac{\partial}{\partial x_1} \frac{\partial \tilde{V}_y}{\partial x_1} + \frac{\partial}{\partial x_2} \frac{\partial \tilde{V}_y}{\partial x_2} + \bar{q} \left(\frac{\partial^2}{\partial x_1^2} + \frac{\partial^2}{\partial x_2^2} \right) \right\} P_w(x_1, x_2, t), \quad (231)$$

where \tilde{V}_y is the mechanical potential defined in eq. (63) and

$$\bar{q} = \frac{1}{2} \frac{\bar{n}}{N_s}. \quad (232)$$

In this situation the diffusion coefficient is constant. This case is usually called “additive noise” (SCHENZLE and BRAND [1978]).

At steady state we put $\partial P_w / \partial t = 0$. Since eq. (231) obeys the detailed balance conditions (HAKEN [1977]), the steady state equation can easily be solved. The

solution is (BONIFACIO, GRONCHI and LUGIATO [1978], SCHENZLE and BRAND [1978])

$$P_w^{(st)}(x_1, x_2) = \mathcal{N} \exp \left\{ -\frac{1}{\bar{q}} \tilde{\mathcal{V}}_y(x_1, x_2) \right\}, \quad (233)$$

where \mathcal{N} is the normalization constant determined by the condition $\int dx_1 dx_2 P_w^{(st)}(x_1, x_2) = 1$. The function $P_w^{(st)}$ describes the fluctuations of the transmitted field at steady state, and in particular its photon statistics.

As we see from eq. (233), in the situation of thermal and external noise the mechanical potential $\tilde{\mathcal{V}}_y$ plays the role of a generalized free energy, which determines the stability of the steady states. In fact, the extrema of the function $\tilde{\mathcal{V}}_y$ (i.e. the points where $\partial \tilde{\mathcal{V}}_y / \partial x_1 = \partial \tilde{\mathcal{V}}_y / \partial x_2 = 0$) coincide with the semiclassical solutions. The unstable state (if any) corresponds to a saddle point of the free energy, the absolutely stable stationary state corresponds to the absolute minimum of the function $\tilde{\mathcal{V}}_y(x_1, x_2)$, while the metastable state (if any) corresponds to the relative minimum.

The number of peaks of the distribution $P_w^{(st)}$ is equal to the number of minima of the potential $\tilde{\mathcal{V}}_y$. Hence, for $0 \leq y \leq y_m$ (see Fig. 8), the probability distribution has one peak in correspondence with the cooperative stationary solution x_a . For $y_m < y < y_M$, $P_w^{(st)}$ has two peaks at $x_1 = x_a, x_2 = 0$ and $x_1 = x_c, x_2 = 0$. For $y \geq y_M$, the probability distribution again has one peak, corresponding to the one-atom stationary solution x_c . The parameter \bar{q} controls the width of the peaks; the smaller is \bar{q} , the narrower are the peaks. The smallness of \bar{q} also has another important consequence: the range of values of y in which the two peaks have comparable areas is very small. In other words, in the largest part of the bistable region $y_m < y < y_M$, one of the two peaks is absolutely dominant over the other. Only in a narrow transition region is the probability distribution really double peaked. In this region, it is more proper to speak of two metastable states instead of one stable and one metastable state. In fact, the system can jump randomly from one to the other minimum of the free energy, due to the action of fluctuations. These jumps occur with characteristic times τ_L and τ_R , discussed in § 3.6.1. The width of the transition region tends to zero in the thermodynamic limit $N \rightarrow \infty, V \rightarrow \infty$ with N/V constant. In this limit \bar{q} tends to zero. If we consider the mean value $\langle x \rangle_{st} = \langle x_1 \rangle_{st}$ of the transmitted field, calculated from eq. (233), we find the discontinuous transition (Fig. 33)

$$\langle x \rangle_{st} \xrightarrow{\bar{q} \rightarrow 0} \begin{cases} x_a & \text{for } y < \tilde{y}, \\ x_c & \text{for } y > \tilde{y}, \end{cases} \quad (234)$$

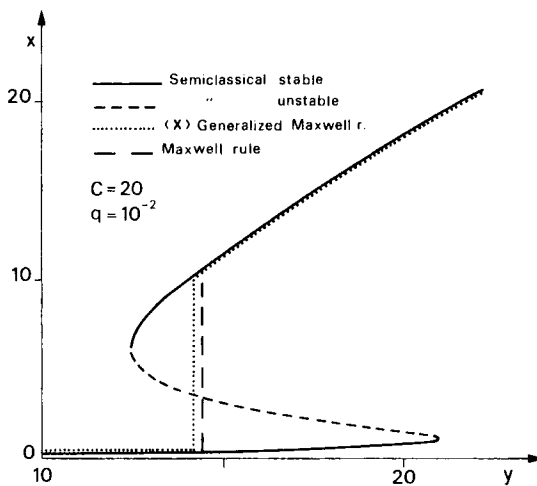


Fig. 33. Semiclassical stationary solutions, Maxwell rule and mean value of the normalized field amplitude x .

where the value \tilde{y} is specified by the condition

$$V_{\tilde{y}}(x_a) = V_{\tilde{y}}(x_c). \quad (234')$$

The definition of $V_y(x)$ is given in eq. (64), and we have taken into account that the minima of the generalized free energy \tilde{V}_y are on the real axis.

Clearly this behavior strongly resembles first-order phase transitions in equilibrium systems. Equation (234) coincides with the well known Maxwell rule, because it cuts the semiclassical curve in the (x, y) plane in such a way that one obtains two regions of equal area. In fact, the latter condition amounts to fixing the value \tilde{y} of y in such a way that

$$\begin{aligned} \int_{x_b}^{x_a} dx \left(x + \frac{2Cx}{1+x^2} - \tilde{y} \right) &= \int_{x_b}^{x_c} dx \left(\tilde{y} - x - \frac{2Cx}{1+x^2} \right) \\ \Rightarrow \int_{x_a}^{x_c} dx \left(x + \frac{2Cx}{1+x^2} - \tilde{y} \right) &= 0. \end{aligned} \quad (235)$$

From eq. (64), one sees that condition (235) coincides with (234').

3.5.2. General case. Effects of the intrinsic quantum fluctuations

Let us now also include the intrinsic quantum fluctuations, so that we consider the full eq. (177'). It is suitable to reformulate this equation in terms of the probability distribution

$$\bar{P}_w(r, \varphi) = r P_w(r, \varphi), \quad (236)$$

which obeys the normalization condition $\int_0^\infty dr \int_0^{2\pi} d\varphi \bar{P}(r, \varphi, t) = 1$. We have (see last sentence in § 3.2.1)

$$k^{-1} \frac{\partial \bar{P}_w(r, \varphi, t)}{\partial t} = \left\{ \frac{\partial}{\partial r} \left[r \left(1 + \frac{2C}{1+r^2} \right) - y \cos \varphi + q \frac{\partial}{\partial r} D(r) \right] \right. \\ \left. + \frac{\partial}{\partial \varphi} \left[\frac{y}{r} \sin \varphi + q \left(1 + \frac{1+2\bar{n}}{2C} \right) \frac{1}{r^2} \frac{\partial}{\partial \varphi} \right] \right\} \bar{P}_w(r, \varphi, t), \quad (237)$$

where

$$q = C/2N_s \quad (238a)$$

$$D(r) = \frac{1+2\bar{n}}{2C} + \frac{r^4 + (1-\bar{d})r^2 + 1}{(1+r^2)^3}. \quad (238b)$$

The parameter q rules the strength of the fluctuations. From eq. (238b) we see that now the amplitude diffusion coefficient is not constant, but is intensity dependent. This is because intrinsic fluctuations give rise to “multiplicative noise” (SCHENZLE and BRAND [1978]). In this situation saturation effects are important not only in the average motion, but also in the fluctuations.

Unfortunately, eq. (237) cannot be solved exactly at steady state because it involves two variables and does not obey the detailed balance conditions. However, a very well approximated expression for the amplitude stationary distribution can be easily obtained in the following way. At a semiclassical level, the phase has only one stationary value, $\varphi = 0$. At a quantum statistical level, the phase will fluctuate around $\varphi = 0$, but these fluctuations are small because the diffusion constant q is small. Hence, at steady state, one can linearize eq. (237) *with respect to the phase only*, so that $\cos \varphi$ is simply replaced by 1. At this point, one can integrate eq. (237) with respect to the phase, obtaining the following closed equation for the amplitude distribution $P(r, t) = \int_0^{2\pi} d\varphi \bar{P}_w(r, \varphi, t)$:

$$k^{-1} \frac{\partial P(r, t)}{\partial t} = - \frac{\partial}{\partial r} \left\{ K(r) - q \frac{\partial}{\partial r} D(r) \right\} P(r, t), \quad K(r) = y - r - \frac{2Cr}{1+r^2}. \quad (239)$$

In steady state, from eq. (239) we obtain

$$\left\{ K(r) + q \frac{\partial}{\partial r} D(r) \right\} P^{st}(r) = 0. \quad (239')$$

The solution of this equation is (BONIFACIO, GRONCHI and LUGIATO [1978], LUGIATO, CASAGRANDE and PIZZUTO [1982]):

$$P^{(st)}(r) = \mathcal{N} D^{-1}(r) \exp \left[-\frac{1}{q} U_y(r) \right], \quad (240)$$

where \mathcal{N} is the normalization constant and

$$U_y(r) = \int dr' K(r')/D(r'). \quad (241)$$

Hence, in this case, the role of generalized free energy is played by $U_y(r)$, which is different from the mechanical potential $V_y(r)$, because $D(r)$ is not constant. Clearly the equation $dU_y/dr = 0$, which determines the extrema of the potential, coincides with the semiclassical state equation (32). For $q \ll 1$, the factor $D^{-1}(r)$ in eq. (240) produces a negligible shift in the position of the extrema of distribution $P^{(st)}(r)$, which then coincide with the extrema of $U_y(r)$. Hence, the stable semiclassical solutions correspond to most probable values (i.e. peaks of the distribution function), while the unstable solutions correspond to least probable values. In particular, for $C > 4$ in the bistable situation $y_m < y < y_M$ (see Fig. 8), $P^{(st)}(r)$ has two peaks at $r = x_a$ and $r = x_c$. Exactly as described in the previous subsection, the parameter q controls the width of the peaks and of the transition region. For $q \ll 1$, distribution (240) can be very well approximated by the superposition of two Gaussians

$$P^{(st)}(r) = w_a G_a(r) + w_c G_c(r), \quad (242)$$

where ($i = a, c$)

$$G_i(r) = \frac{1}{\sigma_i \sqrt{2\pi}} \exp \left\{ -(r - x_i)^2 / 2\sigma_i^2 \right\},$$

$$\sigma_i^{-2} = \frac{1}{q} \left(\frac{d^2 U_y}{dr^2} \right)_{x_i}, \quad (243a)$$

while the weights w_i , which obey the normalization condition $w_a + w_c = 1$, are given by

$$w_i = \frac{\sigma_i D^{-1} x_i \exp\left[-\frac{1}{q} U_y(x_i)\right]}{\sum_{j=a,b} \sigma_j D^{-1}(x_j) \exp\left[-\frac{1}{q} U_y(x_j)\right]}. \quad (243b)$$

Of course, for $y < y_m$ and $y > y_M$ one of the two Gaussians in (242) is missing. When $\bar{n} = 0$, for $y \rightarrow 0$ the probability distribution approaches the Wigner function of the vacuum state, as it must be, while for $y \rightarrow \infty$ it approaches the Wigner function corresponding to the coherent state $|\alpha_0\rangle = |\sqrt{N_s} y\rangle$.

The approximation (242) fails only in the neighborhood of the two discontinuity points $y = y_m$ and $y = y_M$. From eq. (242) we obtain the following expressions for the first moments:

$$\begin{aligned} \langle r \rangle_{st} &= \langle \hat{x} \rangle_{st} = w_a x_a + w_c x_c, \\ \sigma^2 &\equiv \langle \hat{x}^\dagger \hat{x} \rangle_{st} - \langle \hat{x} \rangle_{st}^2 = \langle r \rangle_{st}^2 - \langle r^2 \rangle_{st} - \frac{1}{2N_s} \\ &= w_a \sigma_a^2 + w_c \sigma_c^2 + w_a w_c (x_a - x_c)^2 - \frac{1}{2N_s}. \end{aligned} \quad (244)$$

where we have used the first of eqs. (181), (178) and (174). Figure 34 shows the mean value $\langle x \rangle_{st}$ and the relative fluctuation $\sigma^2/\langle \hat{x} \rangle_{st}^2$ as a function of y for $C = 20$, $\bar{n} = 0$ (negligible thermal and external fluctuations), and $q = 10^{-2}$ (this value of q is chosen for pedagogical reasons, in order not to have a too narrow transition region). The mean value coincides with one of the two semiclassical solutions everywhere except in the transition region, which is centered on the value of y , such that

$$w_a = w_c \Rightarrow \langle x \rangle_{st} = \frac{1}{2}(x_a + x_c). \quad (244')$$

This condition requires that the two peaks have equal areas. Out of the transition region the absolutely stable stationary solution is the one which practically coincides with $\langle x \rangle_{st}$ while the other is metastable.

As we see from Fig. 34, the fluctuation $\sigma^2/\langle \hat{x} \rangle_{st}^2$ is always very small except in the narrow transition region, where we find a remarkable peak. This behavior is easily understood from eq. (244). In fact, out of the transition region one has

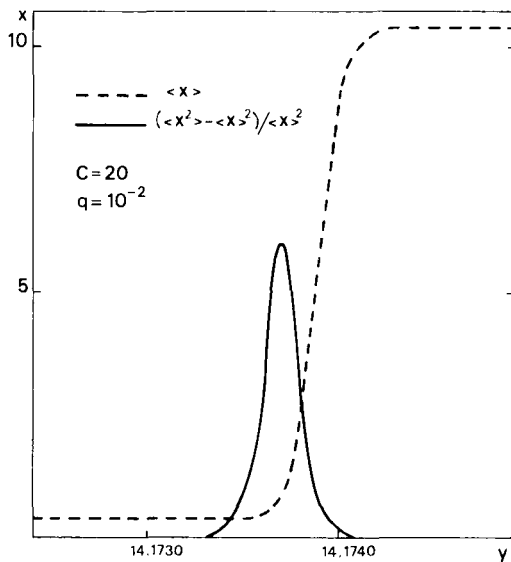


Fig. 34. Mean value and relative fluctuation of the transmitted field.

practically $w_a = 0$ or $w_c = 0$, so that $\sigma^2 = \sigma_c^2 - 1/2N_s$ or $\sigma^2 = \sigma_a^2 - 1/2N_s$, respectively. In the transition region, both w_a and w_c are of the order of unity, so that $\sigma^2 \approx w_a w_c (x_a - x_c)^2 \gg \sigma_a^2, \sigma_c^2$. In other words, the strong competition between the two peaks of the probability distribution gives the drastic increase of fluctuations in the transition region.

In the thermodynamic limit $q \rightarrow 0$, we again obtain (234), where now however, the value \bar{y} is determined by the condition

$$U_{\bar{y}}(x_a) = U_{\bar{y}}(x_b) \quad (245)$$

instead of (234'). Since $U_y \neq V_y$, condition (245) gives a *generalized Maxwell rule* different from the usual one, as is clearly indicated in Fig. 33 (BONIFACIO, GRONCHI and LUGIATO [1978]). This clearly indicates the nonthermodynamic character of the transition. A similar phenomenon arises in chemical reactions (NICOLIS and LEFEVER [1977]).

We end this subsection with a remark on the interpretation of $\langle \hat{x} \rangle_{st}$. In the usual situation (one-peaked distribution function), the mean value practically coincides with the most probable value. This is no longer the case in the transition region, in which the probability distribution has two peaks of comparable areas. In fact, in this region, there is a practically vanishing probability of finding $x = \langle \hat{x} \rangle_{st}$ as a result of a single measurement. Hence, the mean value

$\langle \hat{x} \rangle_{\text{st}}$ must be interpreted in a strictly statistical sense. That is, the results of the single experiments will be (with overwhelming probability for $q \ll 1$) very near to x_a and x_c . The statistical average of these results gives $\langle \hat{x} \rangle_{\text{st}}$.

3.6. TRANSIENT BEHAVIOR: QUANTUM STATISTICAL TREATMENT

In this subsection we illustrate the main features of the transient behavior that depend on fluctuations. In particular, the discussion of the metastable states necessarily requires the calculation of their lifetime. This general problem was first considered many years ago by KRAMERS [1940], and later in great detail by LANDAUER (see for instance LANDAUER [1962]). We shall restrict ourselves to the good cavity case, and for simplicity we shall base our discussion on the one-dimensional Fokker–Planck equation (239). For the sake of definiteness, we consider the same problem as in § 2.3.1, but in a quantum statistical context (LUGIATO, FARINA and NARDUCCI [1980]). Namely, we consider an ensemble of systems which are initially in the stationary state, corresponding to the value y_0 of the incident field, so that $P(r, 0) = P_{y_0}^{(\text{st})}(r)$. At $t = 0$, the external field is suddenly switched to a new value y_{op} , which is slightly different from y_0 . Hence, in the course of time, the distribution $P(r, t)$ will approach the new stationary solution of eq. (239), $P_{y_{\text{op}}}^{(\text{st})}(r)$ corresponding to the new value y_{op} of the incident field. We wish to illustrate the main features of the time evolution of $P(r, t)$ for $q \ll 1$.

We assume that both y_0 and y_{op} are well inside the bistability region $y_m < y < y_M$ (Fig. 8). Hence, from eq. (242), $P(r, 0)$ is well represented by the superposition of two Gaussians

$$P(r, 0) = w_a^{(0)} G_a^{(0)}(r) + w_c^{(0)} G_c^{(0)}(r), \quad (246)$$

where $w_a, w_c = 1 - w_a$, and G_a and G_c , are given by eqs. (243a) and (243b). The index (0) indicates that these quantities are calculated with x_a and x_c being the stable solutions of eq. (32), corresponding with the value y_0 of the incident field.

For $q \ll 1$, the time evolution of $P(r, t)$ occurs in two quite separate stages (LUGIATO, FARINA and NARDUCCI [1980]). In the first one, there is a *local relaxation process* in which the two peaks in eq. (246) evolve independently of each other. If the difference between y_0 and y_{op} is small enough, the evolution of each peak is described by the Fokker–Planck equation (239), linearized around the corresponding semiclassical steady state. That is, the evolution, say, of peak a is governed by eq. (239), linearized around the value $r = x_a^{(\text{op})}$, where

$x_a^{(op)}$ is the semiclassical solution corresponding with the value y_{op} of the incident field. Hence, this stage occurs on a time scale of the order of $(k\tilde{\lambda}_a)^{-1}$, $(k\tilde{\lambda}_c)^{-1}$, where $\tilde{\lambda}_a$ and $\tilde{\lambda}_c$ are given by the first of eqs. (193) with $x_{st} = x_a$, $x_{st} = x_c$.

At the end of this stage the probability distribution $P(r)$ has the form

$$P(r) = w_a^{(0)} G_a^{(op)}(r) + w_c^{(0)} G_c^{(op)}(r), \quad (247)$$

where now the two Gaussians are given by eq. (243a), with x_a and x_c corresponding to the final value y_{op} of the external field. Hence, the shape of the two peaks in eq. (247) is identical to that of the corresponding peaks in the stationary distribution $P_{y_{op}}^{(st)}(r)$, but the weights w_a and w_c are different, because they still correspond to the initial value y_0 of the incident field. This is because, up to this point, the time evolution has been only a local relaxation without any flux of probability between the two peaks.

In the second stage of the time evolution, which occurs on a much longer time scale, one has a transfer of probability from one peak to the other, which leads eventually to the final distribution, that is given by

$$P(r, \infty) = w_a^{(op)} G_a^{(op)}(r) + w_c^{(op)} G_c^{(op)}(r). \quad (248)$$

This stage is usually called “tunneling”, because it consists of a flux of probability across the “barrier” of the free energy $U_{y_{op}}(r)$ (see eq. (241)). In fact, as we know, this potential has two minima, at $r = x_a^{(op)}$ and $r = r_c^{(op)}$, separated by a barrier centered on the unstable point $r = x_b^{(op)}$. This long-time stage is discussed in the next subsection.

3.6.1. The tunneling process

The picture of the time evolution given above is consistent with the spectrum of eigenvalues of the Fokker–Planck operator. In fact, if we write eq. (239) in the form

$$\frac{\partial P(r, t)}{\partial t} = \Lambda P(r, t), \quad (249)$$

for $q \ll 1$ the linear operator Λ exhibits a nearly degenerate pair of lowest lying eigenvalues $\lambda_0 = 0$ and $\lambda_1 \neq 0$, and a large gap between λ_1 and the remaining part of the spectrum. As usual, the lowest eigenvalue $\lambda_0 = 0$ corresponds to the steady state solution, while λ_1 , in this case, is related to the eigenfunction of the Fokker–Planck operator that describes the long-time approach to steady

state. On the other hand, the remaining eigenvalues are related to the short-time, local relaxation process that we described above. In the long time limit, in which only the lowest two eigenvalues are important for the description of our bistable system, the function $P(r, t)$ is well approximated by

$$P(r, t) = P_{y_{\text{op}}}^{(\text{st})}(r) + \exp(-\lambda_1 t) u_1(r), \quad (250)$$

where u_1 is the eigenfunction of the Fokker–Planck operator A , corresponding to λ_1 . In this case, the probability of occupation of the left peak

$$w_a(t) \equiv \int_0^{x_b^{(\text{op})}} P(r, t) dr, \quad (251)$$

where $x_b^{(\text{op})}$ is the unstable point of the potential $U_{y_{\text{op}}}(r)$, obeys the very simple equation

$$\frac{dw_a(t)}{dt} = -\lambda_1(w_a(t) - w_a(\infty)), \quad (252)$$

where

$$w_a(\infty) = \int_0^{x_b^{(\text{op})}} P_{y_{\text{op}}}^{(\text{st})}(r) dr \approx w_a^{(\text{op})}. \quad (253)$$

Equation (252) can be reformulated as a rate equation of the form

$$\frac{dw_a(t)}{dt} = -\frac{1}{\tau_L} w_a + \frac{1}{\tau_R} (1 - w_a), \quad (254)$$

where τ_L and τ_R are the escape times out of the left and right wells of the potential $U_{y_{\text{op}}}(r)$, respectively. In fact, on comparing eq. (252) with eq. (254), one finds

$$\frac{1}{\tau_L} + \frac{1}{\tau_R} = \lambda_1, \quad (255a)$$

$$\frac{1}{\tau_R} = \lambda_1 w_a(\infty), \quad (255b)$$

from which follows

$$\frac{1}{\tau_L} = \lambda_1(1 - w_a(\infty)). \quad (255c)$$

In addition, it is worth observing that

$$\frac{\tau_L}{\tau_R} = \frac{w_a(\infty)}{1 - w_a(\infty)}. \quad (256)$$

We now calculate the eigenvalue λ_1 by a procedure that takes its premises from KRAMERS [1940], after allowance is made for the r -dependence of the diffusion coefficient (BONIFACIO, LUGIATO, FARINA and NARDUCCI [1981]). An alternative approach is that based on the first passage time method (STRATONOVICH [1963], FARINA, NARDUCCI, YUAN and LUGIATO [1980], ENGLUND, SCHIEVE, ZUREK and GRAGG [1981]). The probability current density $J(r, t)$ is given by (see eq. (239))

$$J(r, t) = \left\{ K(r) - q \frac{\partial}{\partial r} D(r) \right\} P(r, t). \quad (257)$$

On using eq. (251), we at once obtain

$$\frac{dw_a(t)}{dt} = -J(x_b^{(op)}, t), \quad (258)$$

where we have taken into account that $J(0, t) = 0$, because $r = 0$ is a reflecting boundary of the potential. As shown in BONIFACIO, LUGIATO, FARINA and NARDUCCI [1981], in the long-time limit $J(r, t)$ is practically independent of r in the neighborhood of $x_b^{(op)}$; this property holds, in practice, from $x_b^{(op)}$ to almost $x_a^{(op)}$ and $x_c^{(op)}$.

In order to evaluate $J(x_b^{(op)}, t)$ we now consider the following identity of KRAMERS [1940] after a suitable modification has been applied to accommodate the r -dependence of the diffusion coefficient

$$\exp\left(\frac{U_{y_{op}}(r)}{q}\right) J(r, t) = -q \frac{\partial}{\partial r} \left[D(r) P(r, t) \exp\left(\frac{U_{y_{op}}(r)}{q}\right) \right]. \quad (259)$$

If we integrate eq. (259) between the two minima $x_a^{(op)}$ and $x_c^{(op)}$ of the potential, and observe that the function $\exp[U_{y_{op}}(r)/q]$ is very sharply peaked around $x_b^{(op)}$, where $J(r, t)$ is practically constant, we obtain

$$\begin{aligned} & \int_{x_a^{(op)}}^{x_c^{(op)}} dr \exp\left[\frac{U_{y_{op}}(r)}{q}\right] J(r, t) \approx \int_{x_b^{(op)} - \varepsilon}^{x_b^{(op)} + \varepsilon} dr \exp\left[\frac{U_{y_{op}}(r)}{q}\right] J(r, t) \\ & \approx J(x_b^{(op)}, t) \int_{x_b^{(op)} - \varepsilon}^{x_b^{(op)} + \varepsilon} dr \exp\left[\frac{U_{y_{op}}(r)}{q}\right] \simeq J(x_b^{(op)}, t) \int_{x_a^{(op)}}^{x_c^{(op)}} dr \exp\left[\frac{U_{y_{op}}(r)}{q}\right]. \end{aligned} \quad (260)$$

The parameter ε , which is of the order of \sqrt{q} , is introduced only to guarantee the validity of the step by which $J(r, t)$ is factorized outside the integral sign. The last step is justified because $\exp[U_{y_{\text{op}}}(r)/q]$ is very small with respect to $\exp[U_{y_{\text{op}}}(x_b)/q]$ around both $x_a^{(\text{op})}$ and $x_c^{(\text{op})}$. Hence, after integrating both sides of eq. (259) from $x_a^{(\text{op})}$ to $x_c^{(\text{op})}$ and using eq. (260), we obtain

$$J(x_b^{(\text{op})}, t) = q \left\{ \left[DP \exp \left(\frac{U_{y_{\text{op}}}(r)}{q} \right) \right]_{r=x_a^{(\text{op})}} - \left[DP \exp \left(\frac{U_{y_{\text{op}}}(r)}{q} \right) \right]_{r=x_c^{(\text{op})}} \right\} / \int_{x_a^{(\text{op})}}^{x_c^{(\text{op})}} dr \exp \left(\frac{U_{y_{\text{op}}}(r)}{q} \right). \quad (261)$$

Finally, from eqs. (258), (261) and (251), we conclude that

$$\begin{aligned} \frac{dw_a}{dt} = & \frac{q \left[DP \exp \left(\frac{U_{y_{\text{op}}}(r)}{q} \right) \right]_{r=x_a^{(\text{op})}}}{\left[\int_{x_a^{(\text{op})}}^{x_c^{(\text{op})}} dr \exp \left(\frac{U_{y_{\text{op}}}(r)}{q} \right) \right] \left[\int_0^{x_b^{(\text{op})}} dr P(r) \right]} w_a \\ & + \frac{q \left[DP \exp \left(\frac{U_{y_{\text{op}}}(r)}{q} \right) \right]_{r=x_c^{(\text{op})}}}{\left[\int_{x_a^{(\text{op})}}^{x_c^{(\text{op})}} dr \exp \left(\frac{U_{y_{\text{op}}}(r)}{q} \right) \right] \left[\int_{x_b^{(\text{op})}}^{\infty} dr P(r) \right]} (1 - w_a). \end{aligned} \quad (262)$$

As a consequence, upon identification of eq. (254) with eq. (262) we find

$$\frac{1}{\tau_L} = \frac{q \left[DP \exp \left(\frac{U_{y_{\text{op}}}(r)}{q} \right) \right]_{r=x_a^{(\text{op})}}}{\left[\int_{x_a^{(\text{op})}}^{x_c^{(\text{op})}} dr \exp \left(\frac{U_{y_{\text{op}}}(r)}{q} \right) \right] \left[\int_0^{x_b^{(\text{op})}} dr P(r) \right]}, \quad (263a)$$

$$\frac{1}{\tau_R} = \frac{q \left[DP \exp \left(\frac{U_{y_{\text{op}}}(r)}{q} \right) \right]_{r=x_c^{(\text{op})}}}{\left[\int_{x_a^{(\text{op})}}^{x_c^{(\text{op})}} dr \exp \left(\frac{U_{y_{\text{op}}}(r)}{q} \right) \right] \left[\int_{x_b^{(\text{op})}}^{\infty} dr P(r) \right]}. \quad (263b)$$

Note that even if P is time-dependent, the right-hand sides in eqs. (263a,b) are actually independent of time. In fact, for example,

$$P(x_a^{(op)}, t) / \int_0^{x_b^{(op)}} dr P(r, t)$$

is the ratio between the height and the area of the left peak of the distribution. As the peak remains undeformed in shape during the long time evolution, this ratio remains constant in time. This fact can also be seen immediately from the long-time expression for $P(r, t)$ (compare eqs. (247) and (248))

$$P(r, t) = w_a(t) G_a^{(op)}(r) + (1 - w_a(t)) G_c^{(op)}(r). \quad (264)$$

In fact, for $q \ll 1$ we have $G_c^{(op)}(x_a^{(op)}) \approx 0$. Thus τ_L and τ_R can be evaluated by setting $P = P_{y_{op}}^{(st)}(r)$ so that, from eq. (240) we obtain

$$\begin{aligned} \tau_L &= \left[\int_{x_a^{(op)}}^{x_c^{(op)}} dr \exp\left(\frac{U_{y_{op}}(r)}{q}\right) \right] \left[\int_0^{x_b^{(op)}} dr D^{-1}(r) \exp\left(-\frac{U_{y_{op}}(r)}{q}\right) \right], \\ \tau_R &= \left[\int_{x_a^{(op)}}^{x_c^{(op)}} dr \exp\left(\frac{U_{y_{op}}(r)}{q}\right) \right] \left[\int_{x_b^{(op)}}^{\infty} dr D^{-1}(r) \exp\left(-\frac{U_{y_{op}}(r)}{q}\right) \right]. \end{aligned} \quad (265)$$

It is simple to produce an analytic approximation to eq. (265) in the limit of small fluctuations ($q \ll 1$). In the neighborhood of $x_b^{(op)}$ we can approximate $U_{y_{op}}(r)$ with

$$U_{y_{op}}(r) \simeq U_{y_{op}}(x_b^{(op)}) - \frac{1}{2} \left| \frac{d^2 U_{y_{op}}}{dr^2} \right|_{x_b^{(op)}} (r - x_b^{(op)})^2, \quad (266)$$

so that the first integral in eq. (265) becomes

$$\int_{x_a^{(op)}}^{x_c^{(op)}} dr \exp\left(\frac{U_{y_{op}}(r)}{q}\right) \simeq \frac{\sqrt{2\pi}}{\left\{ \left| \frac{d^2 U_{y_{op}}}{dr^2} \right|_{x_b^{(op)}} \right\}^{1/2}} \exp\left(\frac{U_{y_{op}}(x_b^{(op)})}{q}\right). \quad (267)$$

The second integral can be handled in a similar way after expanding the sharply peaked integral around $r = x_a^{(op)}$ or $r = x_c^{(op)}$. The final result for τ_L takes the form

$$\tau_L \simeq \frac{2\pi}{D(x_a^{(op)}) \left\{ \left(\frac{d^2 U_{y_{op}}}{dr^2} \right)_{x_a^{(op)}} \left| \frac{d^2 U_{y_{op}}}{dr^2} \right|_{x_b^{(op)}} \right\}^{1/2}} \exp\left(\frac{U_{y_{op}}(x_b^{(op)}) - U_{y_{op}}(x_a^{(op)})}{q}\right). \quad (268a)$$

In a similar way, the escape time from the right to the left well can be shown to be approximately equal to

$$\tau_R \simeq \frac{2\pi}{D(x_c^{(op)}) \left\{ \left(\frac{d^2 U_{y_{op}}}{dr^2} \right)_{x_c^{(op)}} \left| \frac{d^2 U_{y_{op}}}{dr^2} \right|_{x_b^{(op)}} \right\}^{1/2}} \exp \left(\frac{U_{y_{op}}(x_b^{(op)}) - U_{y_{op}}(x_c^{(op)})}{q} \right). \quad (268b)$$

We note the appearance of the characteristic ratio $\Delta U/q$, which plays a similar role in this problem as the activation thermal-energy ratio in chemical reactions.

As we pointed out in eq. (255a), the sum of the reciprocals of the escape times τ_L and τ_R gives the first nonzero eigenvalue λ_1 of the Fokker–Planck operator in the limit when the fluctuations are small. The eigenvalue λ_1 , in turn, governs the global evolution of the entire probability distribution for long times.

As we see from eq. (268), the escape times are not determined by the mechanical potential V_y , but by the generalized free energy U_y . The difference between the two of them lies in the fact that U_y incorporates the dependence of the diffusion coefficient on the amplitude r (eq. 241)). The importance of the variation of the noise along the path in determining the escape times has been emphasized by LANDAUER (see for instance LANDAUER [1978]).

If one plots λ_1 as a function of y in the bistable domain $y_m < y < y_M$ (see Fig. 8), one sees that it exhibits a sharp minimum in the region where $\tau_L \approx \tau_R$. In fact, as we see from eq. (268), λ_1 is mainly determined by the larger of the left and right “barriers” $U_y(x_b) - U_y(x_a)$ and $U_y(x_b) - U_y(x_c)$. When $\tau_L \approx \tau_R$, the two barriers are substantially equal and attain their minimum value. The region where $\tau_L \approx \tau_R$ coincides in turn with the transition region, because from eq. (256) it follows that $\tau_L = \tau_R$ means $w_a(\infty) = 1 - w_a(\infty) = w_c(\infty)$, which is precisely the condition that characterizes the transition region (compare eq. (244')). This can also be checked from the explicit expression (268) and (243a,b). Thus, λ_1 shows a kind of critical slowing down behavior (SCHENZLE and BRAND [1979]) of a purely statistical nature, in contrast with the semi-classical critical slowing down described in § 2.3. Furthermore, the value of y_{op} at which λ_1 is minimum is the one which insures the greatest stability of the bistable system against spontaneous switching due to noise, and appears to be optimum as a bias for logical operation. That is, it corresponds to the so-called holding intensity.

We finally note that a tunneling effect has been nicely observed and analyzed in bidirectional ring lasers (MANDEL, ROY and SINGH [1981]).

3.7. REMARKS ON THE OBSERVABILITY OF QUANTUM STATISTICAL EFFECTS

The relevance of fluctuations in our system is “measured” by the parameters \bar{q} (see eq. (232)), which governs the thermal fluctuations and the external field fluctuations, and q (see eq. (238a)), which rules intrinsic quantum fluctuations. The quantity \bar{q} is controlled by the temperature and the stability of the injected laser field. For a large system, the parameter q is ordinarily very small. On the other hand, the miniaturized optical bistable devices, presently considered as candidates for memory elements, may well present much more pronounced quantum effects. It must be said, however, that the description of fluctuations in these systems is necessarily much more complicated than the one given here, because it involves the dynamics of semiconductors instead of two-level systems (see GOLL and HAKEN [1980], and STEYN-ROSS and GARDINER [1982]).

The only quantum phenomenon which does not present basic difficulties in its observation is the spectrum of the fluorescent light. However, in order to observe the spectrum of the transmitted or reflected light one meets the difficulty that the classical coherent part is much more intense than the incoherent part, which is the interesting one and arises from fluctuations. One can conceive of depressing the coherent part by some interferometric method or by exploiting the fact that the coherent part is polarized, whereas the incoherent part is not, but an adequate elimination seems difficult. Perhaps heterodyne detection can help in this connection. In order to observe the nonclassical effects described in § 3.3.3 (i.e., photon antibunching and “squeezing”), one has the further difficulty of ensuring that the intrinsic quantum fluctuations are much larger than the thermal and external fluctuations.

The analysis in § 3.6.1 is basic to discuss the *reliability* of our system as an optical memory. In fact, τ_L and τ_R give the lifetime of the metastable states. From eq. (268) we see that, for $q \ll 1$, these lifetimes are extremely (not to say astronomically) long. Hence, the system will not switch spontaneously from one branch to the other, and this ensures the reliability of our optical bistable system. On the other hand, this very desirable feature turns out to be very bad with respect to the observation of the effects described in § 3.5 (bimodal distribution function, generalized Maxwell rule, and anomalous fluctuations in the transition region). In fact, it is necessary to wait for times that are longer than τ_L and τ_R in order to allow the system to reach steady state from a statistical viewpoint.

In conclusion, the fluctuation effects become easily accessible only when either the external fluctuations are large (but in this case the intrinsic quantum fluctuations remain hidden), or when the system is small enough.

Concluding Note

This article reflects the state of the art in the theory of optical bistability in early June 1982, when it was mailed to the editor. Therefore, with a few exceptions, the references do not cover the papers appeared after that time, in particular many contributions to the 12th International Quantum Electronics Conference in Munich, Germany, June 1982, and to the Topical Conference on optical bistability in Rochester, N.Y., June 1983. Here I can only mention the paper by GRANT and KIMBLE [1983] on the observation of critical slowing down at optical frequencies. Doctors Hyatt Gibbs and Sam McCall are preparing a book on optical bistability, which will contain an up-to-date list of references.

Acknowledgements

First of all I wish to thank Rodolfo Bonifacio, with whom I shared the satisfaction of working out many of the results described in this article, and Hermann Haken, because all these results have been directly inspired by his fundamental work in quantum optics and synergetics. I am grateful to Lorenzo Narducci for his present precious collaboration and for his help in the preparation of this manuscript. Many thanks are due also to all the other friends with whom I had the privilege of collaborating on some aspects of my research on optical bistability. At the University of Milan my thanks go to Gino Benza, Frederico Casagrande, Marziale Milani, Laura Asquini and Giuliano Strini; abroad to Stan Dembinski, Jim Farina, Andrzej Kossakowski, Paul Mandel, Pierre Meystre, Murray Sargent and Jimmy Yuan. Furthermore, I thank friends with whom I had particularly stimulating discussions on this subject: Eitan Abraham, Tito Arecchi, Ennio Arimondo, Charles Bowden, Ernst Brun, Claude Cohen-Tannoudji, Vittorio Degiorgio, Joe Eberly, Fritz Haake, John Hermann, Gerd Leuchs, Sam McCall, Ben Mollow, Marlan Scully, Dan Walls and Herbert Walther. I am grateful to Hyatt Gibbs, Adriano Gozzini, Fred Hopf, Jeff Kimble and Richard Shoemaker for giving me permission to include in this paper pictures of some of their experiments. Last but not least, I wish to thank Piero Caldirola, because his wise leadership of our theoretical group created the ideal conditions to work on Physics.

Appendix A. Derivation of eqs. (45) and (46) in the limit of small absorption, transmission and detuning

Let us consider a stationary solution $E_{\text{st}}(z)$, $P_{\text{st}}(z)$ and $D_{\text{st}}(z)$ of the Maxwell–Bloch equations (1) with the boundary condition (3.2). We introduce the deviations from the stationary values

$$\begin{aligned}\delta E(z, t) &= E(z, t) - E_{\text{st}}(z), \\ \delta P(z, t) &= P(z, t) - P_{\text{st}}(z), \\ \delta D(z, t) &= D(z, t) - D_{\text{st}}(z).\end{aligned}\quad (\text{A.1})$$

In terms of these deviations the Maxwell–Bloch equations can be rephrased as

$$\frac{\partial \delta E}{\partial t} + c \frac{\partial \delta E}{\partial z} = -g \delta P, \quad (\text{A.2a})$$

$$\frac{\partial \delta P}{\partial t} = \frac{\mu}{\hbar} [E_{\text{st}}(z) \delta D + D_{\text{st}}(z) \delta E + \delta E \delta D] - [\gamma_{\perp} + i(\omega_a - \omega_0)] \delta P, \quad (\text{A.2b})$$

$$\frac{\partial \delta D}{\partial t} = -\frac{\mu}{2\hbar} [(E_{\text{st}}(z) \delta P^* + P_{\text{st}}^*(z) \delta E + \delta E \delta P^*) + \text{c.c.}] - \gamma_{\parallel} \delta D. \quad (\text{A.2c})$$

On the other hand, from eq. (3.2) we obtain the following boundary condition for δE :

$$\delta E(0, t) = R \exp(-i\delta_0) \delta E(L, t - \Delta t), \quad (\text{A.3})$$

where we have taken into account that

$$E_{\text{st}}(0) = E_1 \sqrt{T} + R \exp(-i\delta_0) E_{\text{st}}(L).$$

Condition (A.3) differs from a pure periodicity condition in space due to the presence of the factor $R \exp(-i\delta_0)$ and of the retardation Δt . Since it is convenient to work with the periodicity condition, we introduce the following transformation of variables

$$\tilde{\delta E} = w(z, T) \delta E, \quad \tilde{\delta P} = w(z, T) \delta P, \quad \tilde{\delta D} = \delta D, \quad (\text{A.4})$$

$$w(z, T) = \exp \left[\frac{z}{L} \ln (R \exp(-i\delta_0)) \right], \quad t' = t + \Delta t \frac{z}{L} = t + \frac{\mathcal{L} - L}{c} \frac{z}{L}. \quad (\text{A.5})$$

Using (A.4) and (A.5) one verifies that (A.3) reduces to

$$\delta\tilde{E}(0, t') = \delta\tilde{E}(L, t'). \quad (\text{A.6})$$

while the time evolution equations (A.2) become

$$\frac{\partial\delta\tilde{E}}{\partial t'} + c \frac{L}{\mathcal{L}} \frac{\partial\delta\tilde{E}}{\partial z} = \frac{c}{\mathcal{L}} [\ln R - i\delta_0] \delta\tilde{E} - g \frac{L}{\mathcal{L}} \delta P, \quad (\text{A.7a})$$

$$\begin{aligned} \frac{\partial\delta\tilde{P}}{\partial t'} &= \frac{\mu}{\hbar} \{ w(z, T) E_{\text{st}}(z) \delta\tilde{D} + D_{\text{st}}(z) \delta\tilde{E} + \delta\tilde{E} \delta\tilde{D} \} \\ &\quad - [\gamma_{\perp} + i(\omega_a - \omega_0)] \delta P, \end{aligned} \quad (\text{A.7b})$$

$$\begin{aligned} \frac{\partial\delta\tilde{D}}{\partial t'} &= -\frac{\mu}{2\hbar} \{ [(w^*(z, T))^{-1} E_{\text{st}}(z) \delta P^* + (w(z, T))^{-1} P^*(z) \delta E \\ &\quad + |w(z, T)|^{-2} \delta\tilde{E} \delta\tilde{P}^*] + \text{c.c.} \} - \gamma_{\parallel} \delta\tilde{D}. \end{aligned} \quad (\text{A.7c})$$

For $T \ll 1$, $\ln R \simeq -T$, so that using eq. (33) and the relation $\delta_0 = \theta T$, eq. (A.7a) becomes

$$\frac{\partial\delta\tilde{E}}{\partial t'} + c \frac{L}{\mathcal{L}} \frac{\partial\delta\tilde{E}}{\partial z} = -k(1 + i\theta) \delta\tilde{E} - g \frac{L}{\mathcal{L}} \delta\tilde{P}. \quad (\text{A.8})$$

Furthermore, for $T \ll 1$ one has that $w(z, T)$ can be replaced by unity in eqs. (A.7b) and (A.7c).

Let us now consider the stationary fields in the limit (44), in which they are practically uniform in space. By setting the derivatives with respect to time equal to zero in the Maxwell–Bloch equations (1), and integrating eq. (1a) with respect to z to first order in αL (i.e. gL), we obtain

$$E_{\text{st}}(L) - E_{\text{st}}(0) = -g \frac{L}{c} P_{\text{st}}, \quad (\text{A.9})$$

$$0 = \frac{\mu}{\hbar} E_{\text{st}} D_{\text{st}} - [\gamma_{\perp} + i(\omega_a - \omega_0)] P_{\text{st}}, \quad (\text{A.10a})$$

$$0 = -\frac{\mu}{2\hbar} (E_{\text{st}} P_{\text{st}}^* + E_{\text{st}}^* P_{\text{st}}) - \gamma_{\parallel} (D_{\text{st}} - \frac{1}{2}N). \quad (\text{A.10b})$$

Next, we combine eq. (A.9) with the boundary condition (3b). By the relation $\delta_0 = \theta T$, neglecting the terms proportional to powers of T higher than first and

using eq. (33), we obtain the equation

$$0 = -ik\theta E_{st} - k \left(E_{st} - \frac{E_1}{\sqrt{T}} \right) - g \frac{L}{\mathcal{L}} P_{st}, \quad (\text{A.11})$$

where we have replaced $E_{st}(L)$ by E_{st} .

Finally, we take into account that, in the limit (44), $\tilde{\delta}E = \delta E$, etc. since $w(z, T) = 1$. Hence, using eq. (A.1) and summing eqs. (A.8) and (A.11), we obtain eq. (45). On the other hand, by summing eqs. (A.7.2) (with $w(z, T) = 1$) and (A.10.1), eqs. (A.7.3) and (A.10.2), we recover eqs. (1.2) and (1.3) respectively. Furthermore, since E_{st} is independent of z we obtain, from eqs. (A.6) and (A.1), the standard periodicity boundary condition (46).

Appendix B. The coefficients Γ in eq. (127)

Let us enlist the explicit expressions of the coefficients $\Gamma(nj, n'j', n''j'')$ of eq. (127) in the limit (44). First, let us define the following two functions

$$\tilde{H}(\lambda, x) = x^2 \left(\frac{\lambda}{\gamma_\perp} + 2 \right) - \frac{\lambda + \gamma_\parallel}{\gamma_\perp} \left(\frac{\lambda}{\gamma_\parallel} + 1 - x^2 \right), \quad (\text{B.1})$$

$$\tilde{K}(\lambda, \lambda', x) = \left(\frac{\lambda}{\gamma_\parallel} + 1 \right) \left(\frac{\lambda'}{\gamma_\perp} + 2 \right) + \left(\frac{\lambda'}{\gamma_\parallel} + 1 - x^2 \right). \quad (\text{B.2})$$

The explicit expression of the normalization constant \mathcal{N}_{nj} in eq. (122) is

$$\mathcal{N}_{nj} = G(\lambda_{nj}, x) + \frac{2C}{1+x^2} \frac{k}{\gamma_\parallel} \frac{\tilde{H}(\lambda_{nj}, x)}{G(\lambda_{nj}, x)}. \quad (\text{B.3})$$

Furthermore one has:

$$(i) \text{ For } j = j'' = 1, \quad \text{any } j', \quad \Gamma(n1, n'j', n''1)$$

$$= \delta_{n,n'+n''} 2Ck \frac{x}{1+x^2} \frac{\tilde{G}(-i\alpha_n'', x)}{\tilde{G}^2(-i\alpha_n, x)} \tilde{K}(-i\alpha_n, \lambda_{n'j'}^{(0)}, x) + O(T^2). \quad (\text{B.4})$$

$$(ii) \text{ For } j = 1, \quad j'' = 2, 3, \quad \text{any } j',$$

$$\Gamma(n1, n'j', n''2) = O(T^2) \delta_{n,n'+n''}. \quad (\text{B.5})$$

$$(iii) \text{ For } j = 2, 3, \quad j'' = 1, \quad \text{any } j',$$

$$\Gamma(n_3^2, n'j', n''1) = \delta_{n,n'+n''} \gamma_\parallel x \frac{\tilde{G}(-i\alpha_n'', x)}{\tilde{H}(\lambda_{n_3^2}, x)} \tilde{K}(\lambda_{n_3^2}^{(0)}, \lambda_{n'j'}^{(0)}, x) + O(T). \quad (\text{B.6})$$

(iv) For $j = 2, 3, j'' = 2, 3, \text{ any } j'$,

$$\Gamma(n_3^2, n'j', n''j'') = O(T)\delta_{n,n'+n''}. \quad (\text{B.7})$$

In the case $\gamma_{\perp} = \gamma_{\parallel} \equiv \gamma$ that we consider in this chapter the first term in eq. (B.6) vanishes when $j = 3$ and $j' = 2$, or $j = 2$ and $j' = 3$. In fact, in this case, it follows from eq. (83) that

$$\lambda_{n_3^2}^{(0)} = -\gamma \pm i\gamma x. \quad (\text{B.8})$$

By substituting eq. (B.8) into eq. (B.3) one easily verifies that

$$\tilde{K}(\lambda_{n_2}^{(0)}, \lambda_{n_3}^{(0)}, x) = \tilde{K}(\lambda_{n_3}^{(0)}, \lambda_{n_2}^{(0)}, x) = 0. \quad (\text{B.9})$$

Appendix C. Explicit expression for eqs. (142)

Let us consider the nine equations for the amplitudes S_{nj} ($n = 1, 0, -1; j = 1, 2, 3$) with only the terms that survive in the limits (27) and (136). In this limit, one has exactly $\dot{S}_{n2} = \dot{S}_{n3} = 0$. Thus the equations for S_{n2} ($n = 1, 0, -1$) form a closed set of three algebraic equations, whose solution gives the expressions of $\{S_{n2}\}$ as functions of $\{S_{n1}\}$. The same holds for the equations for S_{n3} ($n = 1, 0, -1$).

Next, we define

$$\begin{aligned} \delta(n1, n'j', n''1) &= k^{-1}\Gamma(n1, n'j', n''1), \\ \delta(n2, n'j', n''1) &= \gamma^{-1}\Gamma(n2, n'j', n''1), \end{aligned} \quad (\text{C.1a})$$

and

$$\begin{aligned} \tilde{\lambda}_{n_3^2} &= \gamma^{-1}\lambda_{n_3^2}^{(0)} = -1 \pm ix, & P &= S_{12} \exp(-i\varphi), \\ R &= S_{-12} \exp(i\varphi), & Q &= S_{02}, \end{aligned} \quad (\text{C.1b})$$

and use eq. (141) and the relation $S_{n3} = S_{-n2}^*$. By inserting the expressions for $\{S_{n2}\}$ and $\{S_{n3}\}$ into the time evolution equations for S_{n1} ($n = 1, 2, 3$), we obtain the equations

$$\begin{aligned} \frac{\partial\rho_1}{\partial\tau} &= \text{Re } \lambda_{11}^{(1)}\rho_1 + \text{Re } [\delta(11, 01, 11) + \delta(11, 11, 01)]\rho_1\sigma \\ &\quad + \text{Re } [\delta(11, 02, 11)Q + \delta(11, 03, 11)Q^*]\rho_1 \\ &\quad + \text{Re } [\delta(11, 12, 01)P + \delta(11, 13, 01)R^*]\sigma, \end{aligned} \quad (\text{C.2a})$$

$$\begin{aligned} \frac{\partial \sigma}{\partial \tau} = & \lambda_{01}^{(1)} \sigma + 2 \operatorname{Re} \delta(01, 11, -11) \rho_1^2 \\ & + \delta(01, 01, 01) \sigma^2 + 2 \operatorname{Re} [\delta(01, 12, -11) P] \rho_1 \\ & + 2 \operatorname{Re} [\delta(01, -12, 11) R] \rho_1 + 2 \operatorname{Re} [\delta(01, 02, 01) Q] \sigma, \quad (\text{C.2b}) \end{aligned}$$

where P , Q and R are solutions of the system of linear equations

$$\left\{ \begin{array}{l} A_{11}P + A_{12}Q = -z_1, \\ A_{21}P + A_{22}Q + A_{23}R = -z_2, \\ A_{32}Q + A_{33}R = -z_3, \end{array} \right\} \quad (\text{C.3})$$

where

$$\begin{aligned} A_{11} &= \tilde{\lambda}_{12} + i\tilde{\alpha}_1 + \delta(12, 12, 01)\sigma, \\ A_{12} &= \delta(12, 02, 11)\rho_1, \quad A_{21} = \delta(02, 12, -11)\rho_1, \\ A_{22} &= \tilde{\lambda}_{02} + \delta(02, 02, 01)\sigma, \quad A_{23} = \delta(02, -12, 11)\rho_1, \\ A_{32} &= \delta(-12, 02, -11)\rho_1, \quad A_{33} = \tilde{\lambda}_{-12} - i\tilde{\alpha}_1 + \delta(-12, -12, 01)\sigma, \\ z_1 &= [\delta(12, 11, 01) + \delta(12, 01, 11)]\rho_1\sigma, \\ z_2 &= [\delta(02, 11, -11) + \delta(02, -11, 11)]\rho_1^2 + \delta(02, 01, 01)\sigma^2, \\ z_3 &= [\delta(-12, -11, 01) + \delta(-12, 01, -11)]\rho_1\sigma. \end{aligned} \quad (\text{C.4})$$

Hence, eqs. (C.2) can be written in the form (142) where the functions f and g depend only on the parameters C , x and $\tilde{\alpha}_1$.

Appendix D. Derivation of the Fokker–Planck equation (176)

Let us consider the moments of the generalized Wigner distribution $P_w(\bar{v}, \bar{v}^*, \bar{m}, \beta, \beta^*, t)$:

$$\begin{aligned} &\langle (R^+)^p (R_3)^q (R^-)^r (A^+)^s (A^-)^t \rangle_s(t) \\ &\equiv \int d_2 \bar{v} d\bar{m} d_2 \beta (\bar{v}^*)^p \bar{m}^r \bar{v}^q (\beta^*)^q \beta^r \beta^s P_w(\bar{v}, \bar{v}^*, \bar{m}, \beta, \beta^*, t), \quad (\text{D.1}) \end{aligned}$$

where the suffix “s” means “symmetrized” (see eq. (174)). Using the commutation rules (151) and (156) one derives from the master equation (158),

restricted to the single mode $n = 0$, the hierarchy of time evolution equations for the moments (D.1), which has the structure

$$\begin{aligned} \frac{d}{dt} \langle (R^+)^p (R_3)' (R^-)^q (A^\dagger)^r A^s \rangle_s \\ = \sum_{p' l' q' r' s'} C_{p' l' q' r' s'}^{plqrs} \langle (R^+)^{p'} (R_3)'^{l'} (R^-)^{q'} (A^\dagger)^{r'} A^{s'} \rangle_s, \end{aligned} \quad (\text{D.2})$$

where the coefficients C are suitable constants.

The set of equations (D.2) is equivalent to the partial differential equation for P_w

$$\begin{aligned} \frac{\partial}{\partial t} P_w(\bar{v}, \bar{v}^*, \bar{m}, \beta, \beta^*, t) = & \sum_{\bar{p} \bar{l} \bar{q} \bar{r} \bar{s}} \frac{\partial^n}{\partial (\bar{v}^*)^{\bar{p}} \partial \bar{v}^{\bar{q}} \partial \bar{m}^{\bar{l}} \partial (\beta^*)^{\bar{r}} \partial \beta^{\bar{s}}} \\ & \left(\sum_{p_0 l_0 q_0 r_0 s_0} d_{p_0 l_0 q_0 r_0 s_0}^{\bar{p} \bar{l} \bar{q} \bar{r} \bar{s}} (\bar{v}^*)^{p_0} \bar{m}^{l_0} \bar{v}^{q_0} (\beta^*)^{r_0} \beta^{s_0} \right) \\ & \times P_w(\bar{v}, \bar{v}^*, \bar{m}, \beta, \beta^*, t), \quad n = \bar{p} + \bar{q} + \bar{l} + \bar{r} + \bar{s}, \end{aligned} \quad (\text{D.3})$$

provided the coefficients d are chosen in such a way that eqs. (D.3), with definition (D.1), exactly reproduce eqs. (D.2). The determination of these coefficients can be done in steps, by calculating first the terms with $n = 1$ (drift coefficients), secondly the terms with $n = 2$ (diffusion coefficients), etc. Since we are interested in obtaining a Fokker-Planck equation it is enough to calculate the coefficients d only for $n = 1$ and $n = 2$. On comparing eqs. (D.2) and (D.3) via eq. (D.1) we easily obtain, for $n = 1$

$$d_{p_0 l_0 q_0 r_0 s_0}^{\bar{p} \bar{l} \bar{q} \bar{r} \bar{s}} = - C_{p_0 l_0 q_0 r_0 s_0}^{\bar{p} \bar{l} \bar{q} \bar{r} \bar{s}}, \quad (\text{D.4a})$$

and for $n = 2$

$$\begin{aligned} d_{p_0 l_0 q_0 r_0 s_0}^{\bar{p} \bar{l} \bar{q} \bar{r} \bar{s}} = & \frac{1}{\bar{p}! \bar{l}! \bar{q}! \bar{r}! \bar{s}!} C_{p_0 l_0 q_0 r_0 s_0}^{\bar{p} \bar{l} \bar{q} \bar{r} \bar{s}} \\ & - C_{p_0 - 1 l_0 q_0 r_0 s_0}^{\bar{p} - 1 \bar{l} \bar{q} \bar{r} \bar{s}} - C_{p_0 l_0 - 1 q_0 r_0 s_0}^{\bar{p} \bar{l} - 1 \bar{q} \bar{r} \bar{s}} - C_{p_0 l_0 q_0 - 1 r_0 s_0}^{\bar{p} \bar{l} \bar{q} - 1 \bar{r} \bar{s}} \\ & - C_{p_0 l_0 q_0 r_0 - 1 s_0}^{\bar{p} \bar{l} \bar{q} \bar{r} - 1 \bar{s}} - C_{p_0 l_0 q_0 r_0 s_0 - 1}^{\bar{p} \bar{l} \bar{q} \bar{r} \bar{s} - 1}, \end{aligned} \quad (\text{D.4b})$$

where one must take $C = 0$ when one of its indices is negative. By substituting into eqs. (D.4) the explicit expressions of the coefficients C , and neglecting the terms with derivatives of order higher than the second, eq. (D.3) reduces to a

Fokker-Planck equation for $P_w(\bar{v}, \bar{v}^*, \bar{m}, \beta, \beta^*, t)$. Finally, by transforming to the variables v, v^*, m, x, x^* defined by eq. (175), one obtains eq. (176).

References

- ABRAHAM, E. and S. S. HASSAN, 1980, Opt. Commun. **35**, 291.
- ABRAHAM, E. and S. D. SMITH, 1982a, J. Phys. **E15**, 33.
- ABRAHAM, E. and S. D. SMITH, 1982b, Optical bistability and related devices, Rep. Prog. Phys. **45**, 815.
- ABRAHAM, E., R. K. BULLOUGH and S. S. HASSAN, 1979, Opt. Commun. **29**, 109.
- ABRAHAM, E., S. S. HASSAN and R. K. BULLOUGH, 1980, Opt. Commun. **33**, 93.
- ABRAHAM, E., W. J. FIRTH and E. M. WRIGHT, 1982, Proc. Vth Nat. Quantum Electronics Conf., Hull, England, ed. P. L. Knight (Wiley, New York).
- AGARWAL, G. S., L. M. NARDUCCI, D. H. FENG and R. GILMORE, 1977, Dynamical Approach to Steady state and Fluctuations in Optical Bistable Systems, in: Coherence and Quantum Optics IV, Proc. Fourth Rochester Conf., 1977, eds. L. Mandel and E. Wolf (Plenum, New York, 1978).
- AGARWAL, G. S., L. M. NARDUCCI, R. GILMORE and D. H. FENG, 1978a, Opt. Lett. **2**, 88.
- AGARWAL, G. S., L. M. NARDUCCI, R. GILMORE and D. H. FENG, 1978b, Phys. Rev. **A18**, 620.
- AGARWAL, G. S., L. M. NARDUCCI, R. GILMORE and D. H. FENG, 1979, Phys. Rev. **A20**, 545.
- AGRAWAL, G. P., 1981, Appl. Phys. Lett. **38**, 505.
- AGRAWAL, G. P. and H. J. CARMICHAEL, 1979, Phys. Rev. **A19**, 2074.
- AGRAWAL, G. P. and C. FLYTZANIS, 1980, Phys. Rev. Lett. **44**, 1058.
- AGRAWAL, G. P. and C. FLYTZANIS, 1981, IEEE J. Quantum Electron. **QE-17**, 374.
- ALLEN, L. and J. H. EBERLY, 1975, Optical Resonance and Two-Level Atoms (Wiley, New York).
- ARECCHI, F. T. and R. BONIFACIO, 1965, IEEE J. Quantum Electron. **QE-1**, 169.
- ARECCHI, F. T. and A. POLITI, 1978, Lett. Nuovo Cim. **23**, 65.
- ARECCHI, F. T. and A. POLITI, 1979, Opt. Commun. **29**, 361.
- ARECCHI, F. T., G. GIUSFREDI, E. PETRIELLA and P. SALIERI, 1982, J. Appl. Phys. **29**, 79.
- ARIMONDO, E., A. GOZZINI, L. LOVITCH and E. PISTELLI, 1981, Microwave Dispersive Bistability in a Confocal Fabry-Perot Microwave Cavity, in: BOWDEN *et al.* [1981].
- ASQUINI, M. L. and F. CASAGRANDE, 1981, Z. Phys. **B44**, 233.
- AUSTIN, J. W. and L. G. DESHAZER, 1971, J. Opt. Soc. Am. **61**, 650.
- BACZYNSKI, A., A. KOSSAKOWSKI and T. MARSZAŁEK, 1976, Z. Phys. **B23**, 205.
- BALLAGH, R. I., J. COOPER, M. W. HAMILTON, W. J. SANDLE and D. M. WARRINGTON, 1981, Opt. Commun. **37**, 143.
- BARBARINO, S., A. GOZZINI, I. LONGO, F. MACCARRONE and R. STAMPACCHIA, 1982, Nuovo Cim. **B71**, 183.
- BENZA, V. and L. A. LUGIATO, 1979a, Lett. Nuovo Cim. **26**, 405.
- BENZA, V. and L. A. LUGIATO, 1979b, Z. Phys. **B35**, 383.
- BENZA, V., L. A. LUGIATO and P. MEYSTRE, 1980, Opt. Commun. **33**, 113.
- BENZA, V. and L. A. LUGIATO, 1981, Semiclassical and Quantum Statistical Dressed Mode Description of Optical Bistability, in: BOWDEN *et al.* [1981].
- BENZA, V. and L. A. LUGIATO, 1982, Z. Phys. **47**, 79.
- BJORKHOLM, J. E., P. W. SMITH and W. J. TOMLINSON, 1981, Opt. Lett. **6**, 345.
- BISCHOFBERGER, T. and Y. R. SHEN, 1978, Appl. Phys. Lett. **32**, 156.
- BISCHOFBERGER, T. and Y. R. SHEN, 1979, Phys. Rev. **A19**, 1169.
- BÖSIGER, P., E. BRUN and D. MEIER, 1978, Phys. Rev. **A18**, 671.

- BONIFACIO, R., ed., 1982, Dissipative Systems in Quantum Optics – Resonance Fluorescence, Optical Bistability, Superfluorescence (Springer, Berlin).
- BONIFACIO, R. and L. A. LUGIATO, 1975, Phys. Rev. **A11**, 1507.
- BONIFACIO, R. and L. A. LUGIATO, 1976, Opt. Commun. **19**, 172.
- BONIFACIO, R. and L. A. LUGIATO, 1977, Cooperative Effects in Optical Bistability and Resonance Fluorescence, in: Coherence and Quantum Optics IV, Proc. Fourth Rochester Conf., 1977, eds. L. Mandel and E. Wolf (Plenum, New York).
- BONIFACIO, R. and L. A. LUGIATO, 1978a, Lett. Nuovo Cim. **21**, 505.
- BONIFACIO, R. and L. A. LUGIATO, 1978b, Lett. Nuovo Cim. **21**, 510.
- BONIFACIO, R. and L. A. LUGIATO, 1978c, Lett. Nuovo Cim. **21**, 517.
- BONIFACIO, R. and L. A. LUGIATO, 1978d, Phys. Rev. **A18**, 1129.
- BONIFACIO, R. and L. A. LUGIATO, 1978e, Phys. Rev. Lett. **40**, 1023, 1538.
- BONIFACIO, R. and P. MEYSTRE, 1978, Opt. Commun. **27**, 147.
- BONIFACIO, R. and P. MEYSTRE, 1979, Opt. Commun. **29**, 131.
- BONIFACIO, R., M. GRONCHI and L. A. LUGIATO, 1978, Phys. Rev. **A18**, 2266.
- BONIFACIO, R., L. A. LUGIATO and M. GRONCHI, 1979, Theory of Optical Bistability, in: Laser Spectroscopy IV, Proc. Fourth Int. Conf., Rottach-Egern 1979, eds. H. Walther and K. W. Rothe (Springer, Berlin).
- BONIFACIO, R., M. GRONCHI and L. A. LUGIATO, 1979a, Nuovo Cim. **B53**, 311.
- BONIFACIO, R., M. GRONCHI and L. A. LUGIATO, 1979b, Opt. Commun. **30**, 129.
- BONIFACIO, R., L. A. LUGIATO, J. D. FARINA and L. M. NARDUCCI, 1981, IEEE J. Quantum Electron. **QE-17**, 357.
- BONIFACIO, R., F. CASAGRANDE and L. A. LUGIATO, 1981, Opt. Commun. **36**, 159.
- BORN, M. and E. WOLF, 1970, Principles of Optics, 4th Ed. (Pergamon Press, Elmsford, NY).
- BOWDEN, C. M., 1981, Optical Bistability Based upon Atomic Correlation in a Small Volume, in: BOWDEN *et al.* [1981].
- BOWDEN, C. M. and C. C. SUNG, 1979, Phys. Rev. **A19**, 2392.
- BOWDEN, C. M., M. CIFTAN and H. R. ROBL, eds., 1981, Optical Bistability, Proc. Int. Conf. on Optical Bistability, Asheville, 1980 (Plenum, New York).
- CARMICHAEL, H. J., 1980, Opt. Acta **27**, 147.
- CARMICHAEL, H. J., 1981, Z. Phys. **B42**, 183.
- CARMICHAEL, H. J. and G. P. AGRAWAL, 1980, Opt. Commun. **34**, 293.
- CARMICHAEL, H. J. and J. A. HERMANN, 1980, Z. Phys. **B38**, 365.
- CARMICHAEL, H. J. and D. F. WALLS, 1977, J. Phys. **B10**, L685.
- CARMICHAEL, H. J., R. R. SNAPP and W. C. SCHIEVE, 1982, Phys. Rev. **A26**, 3408.
- CASAGRANDE, F. and L. A. LUGIATO, 1980, Nuovo Cim. **B55**, 173.
- CASAGRANDE, F., L. A. LUGIATO and M. L. ASQUINI, 1980, Opt. Commun. **32**, 492.
- CHOW, W. W., M. O. SCULLY and E. W. VAN STRYLAND, 1975, Opt. Commun. **15**, 6.
- COLLINS, Jr., S. A. and K. C. WASMUNDT, 1980, Opt. Eng. **19**, 478.
- DEGIORGIO, V. and M. O. SCULLY, 1970, Phys. Rev. **A2**, 1170.
- DRUMMOND, P. D., 1981, IEEE J. Quantum Electron. **QE-17**, 301.
- DRUMMOND, P. D., 1982, Opt. Commun. **40**, 224.
- DRUMMOND, P. D. and D. F. WALLS, 1980, J. Phys. **A13**, 725.
- DRUMMOND, P. D. and D. F. WALLS, 1981, Phys. Rev. **A23**, 2563.
- DRUMMOND, P. D., K. J. MCNEIL and D. F. WALLS, 1980a, Opt. Acta **27**, 321.
- DRUMMOND, P. D., K. J. MCNEIL and D. F. WALLS, 1980b, Phys. Rev. **A22**, 1672.
- ENGLUND, J. C., W. C. SCHIEVE, W. ZUREK and R. F. GRAGG, 1981, Fluctuations and Transitions in the Absorptive Optical Bistability, in: BOWDEN *et al.* [1981].
- FARINA, J. D., L. M. NARDUCCI, J. M. YUAN and L. A. LUGIATO, 1980, Opt. Eng. **19**, 469.
- FEIGENBAUM, M. J., 1978, J. Stat. Phys. **19**, 25.

- FEIGENBAUM, M. J., 1979, *J. Stat. Phys.* **21**, 669.
FELBER, F. S. and J. H. MARBURGER, 1976, *Appl. Phys. Lett.* **28**, 731.
FIRTH, W. J., 1981, *Opt. Commun.* **39**, 343.
FIRTH, W. J. and E. M. WRIGHT, 1982, *Opt. Commun.* **40**, 233.
FLECK, J. A., 1968, *Appl. Phys. Lett.* **13**, 365.
GARMIRE, E., J. H. MARBURGER, S. D. ALLEN and H. G. WINFUL, 1979, *Appl. Phys. Lett.* **34**, 374.
GIBBS, H. M., S. L. MCCALL and T. N. C. VENKATESAN, 1976, *Phys. Rev. Lett.* **36**, 113.
GIBBS, H. M., S. L. MCCALL and T. N. C. VENKATESAN, 1979, *Opt. News* **5**, 6.
GIBBS, H. M., S. L. MCCALL, T. N. C. VENKATESAN, A. C. GOSSARD, A. PASSNER and W. WIEGMANN, 1979, *Appl. Phys. Lett.* **35**, 451.
GIBBS, H. M., S. L. MCCALL and T. N. C. VENKATESAN, 1980, *Opt. Eng.* **19**, 463.
GIBBS, H. M., F. A. HOPF, D. L. KAPLAN and R. L. SHOEMAKER, 1981, *Phys. Rev. Lett.* **46**, 474.
GILMORE, R., 1974, *Lie Groups, Lie Algebras and Some of their Applications* (Wiley, New York).
GLAUBER, R. J., 1963a, *Phys. Rev.* **130**, 2529.
GLAUBER, R. J., 1963b, *Phys. Rev.* **131**, 2766.
GOLDSTONE, J. A., P. T. HO and E. GARMIRE, 1981, *Transient Phenomena in Bistable Devices*, in: BOWDEN *et al.* [1981].
GOLL, J. and H. HAKEN, 1980, *Phys. Stat. Sol. (b)* **101**, 489.
GORDON, J. P., 1967, *Phys. Rev.* **161**, 367.
GOZZINI, A., 1982, preprint, Ist Fisica dell'Univ., Pisa.
GOZZINI, A., I. LONGO and F. MACCARRONE, 1982, *Nuovo Cim.* **D1**, 489.
GRAGG, R. F., W. C. SCHIEVE and A. R. BULSARA, 1978, *Phys. Lett.* **68A**, 294.
GRAGG, R. F., W. C. SCHIEVE and A. R. BULSARA, 1979, *Phys. Rev. A* **19**, 2052.
GRAHAM, R. and H. HAKEN, 1968, *Z. Phys.* **213**, 420.
GRAHAM, R. and H. HAKEN, 1970, *Z. Phys.* **237**, 31.
GRAHAM, R. and A. SCHENZLE, 1981, *Phys. Rev. A* **23**, 1302.
GRANT, D. E. and H. J. KIMBLE, 1982, *Opt. Lett.* **7**, 353.
GRANT, D. E. and H. J. KIMBLE, 1983, *Opt. Commun.* **44**, 415.
GRISCHKOWSKI, D., 1978, *J. Opt. Soc. Am.* **68**, 641.
GRONCHI, M. and L. A. LUGIATO, 1978, *Lett. Nuovo Cim.* **23**, 593.
GRONCHI, M. and L. A. LUGIATO, 1980, *Opt. Lett.* **5**, 108.
GRONCHI, M., V. BENZA, L. A. LUGIATO, P. MEYSTRE and M. SARGENT III, 1981, *Phys. Rev. A* **24**, 1419.
GRYNBERG, G., E. GIACOBINO, M. DEVAUD and F. BIRABEN, 1980, *Phys. Rev. Lett.* **45**, 434.
GRYNBERG, G., F. BIRABEN and E. GIACOBINO, 1981, *Appl. Phys.* **B26**, 155.
HAAG, G., M. MUNZ and G. MAROWSKY, 1981, *IEEE J. Quantum Electron.* **QE-17**, 349.
HAKEN, H., 1970, *Laser Theory*, in: *Light and Matter Ic*, ed. L. Genzel, *Handbuch der Physik*, vol. XXV/2c (Springer, Berlin).
HAKEN, H., 1975a, *Z. Phys.* **B21**, 105.
HAKEN, H., 1975b, *Z. Phys.* **B22**, 69.
HAKEN, H., 1977, *Synergetics – An Introduction* (Springer, Berlin).
HAKEN, H. and H. OHNO, 1976a, *Opt. Commun.* **16**, 205.
HAKEN, H. and H. OHNO, 1976b, *Phys. Lett.* **59A**, 261.
HAMILTON, M. W., R. J. BALLAGH and W. J. SANDLE, 1982, *Z. Phys.* **B49**, 263.
HANGGI, P., A. R. BULSARA and R. JANDA, 1980, *Phys. Rev. A* **22**, 671.
HASSAN, S. S., P. D. DRUMMOND and D. F. WALLS, 1978, *Opt. Commun.* **27**, 480.
HEER, C. V. and R. D. GRAFT, 1965, *Phys. Rev. A* **140**, 1088.
HERMANN, J. A., 1980, *Opt. Acta* **27**, 159.

- HERMANN, J. A. and B. V. THOMPSON, 1980, Phys. Lett. **79A**, 153.
- HERMANN, J. A. and B. V. THOMPSON, 1981, Analytic description of multiphoton optical bistability in a ring cavity, in: BOWDEN *et al.* [1981].
- HOPF, F., P. MEYSTRE, P. D. DRUMMOND and D. F. WALLS, 1979, Opt. Commun. **31**, 245.
- IKEDA, K., 1979, Opt. Commun. **30**, 257.
- IKEDA, K. and O. AKIMOTO, 1982, Phys. Rev. Lett. **48**, 617.
- IKEDA, K., H. DAIDO and O. AKIMOTO, 1980, Phys. Rev. Lett. **45**, 709.
- JEWELL, J. L., H. M. GIBBS, S. S. TARNG, A. C. GOSSARD and W. WIEGMANN, 1982, Appl. Phys. Lett. **40**, 291.
- KAPLAN, A. E., 1977, Sov. Phys. JETP **45**, 896.
- KAPLAN, A. E. and P. MEYSTRE, 1982, Opt. Commun. **40**, 229.
- KASANTSEV, A. P., S. G. RAUTIAN and G. I. SURDUTOVICH, 1968, Sov. Phys. JETP **27**, 756.
- KITANO, M., T. YABUZAKI and T. OGAWA, 1981a, Phys. Rev. Lett. **46**, 926.
- KITANO, M., T. YABUZAKI and T. OGAWA, 1981b, Phys. Rev. **A24**, 3156.
- KRAMERS, H. A., 1940, Physica **7**, 284.
- LAMB, W. E., Jr., 1965, Theory of Optical Maser Oscillators, in: Proc. Int. School of Physics "E. Fermi", Course XXI, Varenna 1963, ed. P. A. Miles (Academic, New York).
- LANDAUER, R., 1962, J. Appl. Phys. **33**, 2209.
- LANDAUER, R., 1978, Phys. Today **31**, 23.
- LANDAUER, R. and J. W. F. WOO, 1973, in: Synergetics, ed. H. Haken (Teubner, Stuttgart).
- LAX, M., 1967, Phys. Rev. **157**, 213.
- LUGIATO, L. A., 1978, Lett. Nuovo Cim. **23**, 609.
- LUGIATO, L. A., 1979, Nuovo Cim. **B50**, 89.
- LUGIATO, L. A., 1980a, Opt. Commun. **33**, 108.
- LUGIATO, L. A., 1980b, Lett. Nuovo Cim. **29**, 375.
- LUGIATO, L. A., 1981, Z. Phys. **B41**, 85.
- LUGIATO, L. A. and G. STRINI, 1982a, Opt. Commun. **41**, 67.
- LUGIATO, L. A. and G. STRINI, 1982b, Opt. Commun. **41**, 374.
- LUGIATO, L. A. and G. STRINI, 1982c, Opt. Commun. **41**, 447.
- LUGIATO, L. A., P. MANDEL, S. DEMBINSKI and A. KOSSAKOWSKI, 1978, Phys. Rev. **A18**, 238.
- LUGIATO, L. A., J. D. FARINA and L. M. NARDUCCI, 1980, Phys. Rev. **A22**, 253.
- LUGIATO, L. A., V. BENZA, L. M. NARDUCCI and J. D. FARINA, 1981, Opt. Commun. **39**, 405.
- LUGIATO, L. A., M. MILANI and P. MEYSTRE, 1982, Opt. Commun. **40**, 307.
- LUGIATO, L. A., F. CASAGRANDE and L. PIZZUTO, 1982, Phys. Rev. **A26**, 3438.
- LUGIATO, L. A., M. L. ASQUINI and L. M. NARDUCCI, 1982, Opt. Commun. **41**, 450.
- LUGIATO, L. A., L. M. NARDUCCI, D. K. BANDY and C. A. PENNISE, 1982, Opt. Commun. **43**, 281.
- LUGIATO, L. A., V. BENZA, L. M. NARDUCCI and J. FARINA, 1983, Z. Phys. **B49**, 351.
- LUGOVOI, V. N., 1979, Phys. Stat. Sol. (b) **94**, 79.
- LUGOVOI, V. N., 1981, IEEE J. Quantum Electron. **QE-17**, 384.
- MANDEL, L., R. ROY and S. SINGH, 1981, Optical Bistability Effects in a Dye Ring Laser, in: BOWDEN *et al.* [1981].
- MANDEL, P. and T. ERNEUX, 1982, Opt. Commun. **42**, 362; **44**, 55.
- MARBURGER, J. H. and F. S. FELBER, 1978, Phys. Rev. **A17**, 335.
- MAYR, M., H. RISKEN and H. D. VOLLMER, 1981, Opt. Commun. **36**, 480.
- MC CALL, S. L., 1974, Phys. Rev. **A9**, 1515.
- MC CALL, S. L., 1978, Appl. Phys. Lett. **32**, 284.
- MC CALL, S. L. and H. M. GIBBS, 1978, J. Opt. Soc. Am. **68**, 1378.
- MC CALL, S. L. and H. M. GIBBS, 1980, Opt. Commun. **33**, 335.
- MEIER, D., R. HOLZNER, B. DERIGHETTI and E. BRUN, 1982, Bistability and chaos in NMR

- Systems, in: Proc. Int. Symposium on Synergetics, Schloss Elmau 1982, ed. H. Haken (Springer, Berlin).
- MEYSTRE, P., 1978, Opt. Commun. **26**, 277.
- MEYSTRE, P. and H. HOPF, 1979, Opt. Commun. **29**, 235.
- MEYSTRE, P. and M. O. SCULLY, eds., 1983, Quantum Optics, Experimental Gravitation and Measurement Theory, Proc. NATO ASI, Bad Windsheim, Germany, 1981 (Plenum, New York).
- MILLER, D. A. B., 1981, IEEE J. Quantum Electron. **QE-17**, 306.
- MILLER, D. A. B. and S. D. SMITH, 1979, Opt. Commun. **31**, 101.
- MILLER, D. A. B., S. D. SMITH and A. JOHNSTON, 1979, Appl. Phys. Lett. **35**, 658.
- MILLER, D. A. B., S. D. SMITH and C. T. SEATON, 1981, IEEE J. Quantum Electron. **QE-17**, 312.
- MOLLOW, B. R., 1969, Phys. Rev. **188**, 1969.
- MOLONEY, J. V., M. R. BELIC and H. M. GIBBS, 1982, Opt. Commun. **41**, 379.
- NICOLIS, G. and R. LEFEVER, 1977, Phys. Lett. **62A**, 469.
- NICOLIS, G. and I. PRIGOGINE, 1977, Self-organization in Non-Equilibrium Systems – From Dissipative Structures to Order Through Fluctuations (Wiley, New York).
- OKADA, M. and K. TAKIZAWA, 1981, IEEE J. Quantum Electron. **QE-17**, 2135.
- POWELL, H. T. and G. J. WOLGA, 1971, IEEE J. Quantum Electron. **QE-7**, 213.
- RISKEN, H. and K. NUMMEDAL, 1968, J. Appl. Phys. **49**, 4662.
- ROHART, F. and B. MACKE, 1980, J. Physique **41**, 837.
- ROSANOV, N. N. and V. E. SEMENOV, 1981, Opt. Commun. **38**, 435.
- ROY, R. and M. S. ZUBAIRY, 1980a, Phys. Rev. **A21**, 274.
- ROY, R. and M. S. ZUBAIRY, 1980b, Opt. Commun. **32**, 163.
- RUSHIN, S. and S. H. BAUER, 1979, Chem. Phys. Lett. **66**, 100.
- SALOMAA, R. and S. STENHOLM, 1973, Phys. Rev. **A8**, 2695.
- SANDLE, W. J. and A. GALLAGHER, 1981, Phys. Rev. **A24**, 2017.
- SANDLE, W. J., R. J. BALLAGH and A. GALLAGHER, 1981, Optical Bistability Experiments and Mean-Field Theories, in: BOWDEN *et al.* [1981].
- SARGENT III, M., 1978, Phys. Rep. **43**, 223.
- SARGENT III, M., 1980, Sov. J. Quantum Electron. **10**, 1247.
- SARGENT III, M., W. E. LAMB, Jr. and R. L. FORK, 1967, Phys. Rev. **164**, 450.
- SARGENT III, M., M. O. SCULLY and W. E. LAMB, Jr., 1974, Laser Physics (Addison-Wesley, Reading, MA).
- SARID, D., 1981, Opt. Lett. **6**, 552.
- SCHAEFER, R. B. and C. R. WILLIS, 1976, Phys. Rev. **A13**, 1874.
- SCHENZLE, A. and H. BRAND, 1978, Opt. Commun. **27**, 85.
- SCHENZLE, A. and H. BRAND, 1979, Opt. Commun. **31**, 401.
- SCHWENDIMANN, P., 1979, J. Phys. **A12**, L39.
- SCOTT, J. F., M. SARGENT III and C. CANTRELL, 1975, Opt. Commun. **15**, 13.
- SEIDEL, H., 1971, U.S. Patent 3, 610, 731.
- SMITH, P. W., ed., 1981, Special Issue on Optical Bistability, IEEE J. Quantum Electron. **QE-17**, N3.
- SMITH, P. W. and E. H. TURNER, 1977, Appl. Phys. Lett. **30**, 280.
- SMITH, P. W., W. J. TOMLINSON, P. J. MALONEY and J. P. HERMANN, 1981, IEEE J. Quantum Electron. **QE-17**, 340.
- SNAPP, R. R., H. J. CARMICHAEL and W. C. SCHIEVE, 1981, Opt. Commun. **40**, 68.
- SPENCER, M. B. and W. E. LAMB, Jr., 1972, Phys. Rev. **A5**, 884.
- SPILLER, E., 1972, J. Appl. Phys. **43**, 1673.
- STAUPENDAHL, G. and K. A. SCHINDLER, 1982, Opt. Quantum Electron. **14**, 157.
- STEYN-ROSS, M. L. and C. W. GARDINER, 1983, Phys. Rev. **A27**, 310.

- STRATONOVICH, R. L., 1963, Topics in the Theory of Random Noise (Gordon and Breach, New York).
- SZÖKE, A., V. DANEU, J. GOLDHAR and N. A. KURNIT, 1969, Appl. Phys. Lett. **15**, 376.
- TEWARI, S. P., 1979, Opt. Acta **26**, 145.
- VENKATESAN, T. N. C. and S. L. MCCALL, 1977, Appl. Phys. Lett. **30**, 282.
- WALLS, D. F., P. ZOLLER and M. L. STEYN-ROSS, 1981, IEEE J. Quantum Electron. **QE-17**, 380.
- WEIDLICH, W. and F. HAAKE, 1965a, Z. Phys. **185**, 30.
- WEIDLICH, W. and F. HAAKE, 1965b, Z. Phys. **186**, 203.
- WEYER, K. G., H. WIEDENMANN, M. RATEIKE, W. R. MCGILLIVRAY, P. MEYSTRE and H. WALTHER, 1981, Opt. Commun. **37**, 426.
- WIGNER, E. P., 1932, Phys. Rev. **40**, 749.
- WILLIS, C. R., 1978, Opt. Commun. **26**, 62.
- WILLIS, C. R., 1981, Complex Order Parameters in Quantum Optics. First-Order Phase Transitions Analogies, in: BOWDEN *et al.* [1981].
- WILLIS, C. R. and J. DAY, 1979, Opt. Commun. **28**, 137.
- WINFUL, H. G. and G. D. COOPERMAN, 1982, Appl. Phys. Lett. **40**, 298.
- WOO, J. W. F. and R. LANDAUER, 1971, IEEE J. Quantum Electron. **QE-7**, 435.
- YUEN, H. P., 1976, Phys. Rev. A**13**, 2226.
- ZARDECKI, A., 1980, Phys. Rev. A**22**, 1664.